Research on Removal of Arsenic and Manganese from Water using Polymer Gel

(高分子ゲルを使用した水からのヒ素とマンガンの除去に関する研究)

2022 年 3 月

広島大学大学院工学研究科

Syed Ragib Safi

Research on Removal of Arsenic and Manganese from Water using Polymer Gel

(高分子ゲルを使用した水からのヒ素とマンガンの除去に関する研究)

Syed Ragib Safi

In partial fulfillment of the requirements for the degree of Doctor of Engineering

Hiroshima University

Graduate School of Engineering

1-4-1 Kagamiyama Higashihiroshima Hiroshima 739-8527 Japan

March, 2022

Abstract

Due to a shortage of surface water supplies, a considerable population in many regions of the world already uses groundwater as a source of drinking water. Unfortunately, unwanted compounds are present in groundwater sources because of anthropogenic causes and the geological makeup of aquifers, and these compounds limit the use of shallow aquifers. Arsenic-contaminated groundwater is a significant health problem across the world. The research gaps in removing arsenic are selectivity, regeneration and effective removal rate at neutral pH levels.

To improve the removal rate of arsenic through adsorption, I developed an adsorbent, which is a cationic gel composite of *N,N*-dimethylamino propylacrylamide, methyl chloride quaternary (DMAPAAQ) and Iron(III) Hydroxide (FeOOH) particles. FeOOH is reported to increase the adsorption performance of the adsorbent for both forms of arsenic. The preparation of the gel is different from the other polymer gels used for adsorption of arsenic and other metals, and it ensures that the gel contains 62.05% FeOOH particles. It should also provide good selectivity, be simple to use and be cost-effective in terms of reusability. The study showed that the gel selectively adsorbed arsenic effectively at neutral pH levels. The results demonstrate that the maximum amount of As(V) adsorption was 123.4 mg/g, which is higher than the other adsorbents. In addition, the gel adsorbed As(V) selectively in the presence of Sulphate. Also, regeneration of the gel was performed for eight consecutive days with 87.6% effectiveness. Additionally, the adsorption mechanism of this gel composite and time required for reaching the equilibrium adsorption is discussed in this dissertation.

The iron contents in the gel were detected and its maximum impregnation was ensured. We found that the gel contains 62.05% FeOOH components. In addition, the Mössbauer spectroscopy was used to examine the type of impregnated iron in the gel composite and found that it was γ-FeOOH. Finally, Fourier transform infrared spectroscopy (FTIR) was used to examine the surface functional groups present in the gel and the differences in those groups before and after iron impregnation. Similarly, the differences of the surface functional groups in the gel, before and after the adsorption of both forms of arsenic, was also investigated.

The most predominant arsenic species in groundwater is As(III), which has a toxicity of 25–60 times that of As(V). It was discovered that the gel could adsorb highest quantity of As(III) at neutral pH levels. The DMAPAAQ+FeOOH arsenic adsorption isotherm resembled the Langmuir isotherm very well. At neutral pH levels, the maximum adsorption capacity of the DMAPAAQ+FeOOH gel composite (27.68 mg/g) was computed. As(III) was converted to As(V) through oxidation and was then adsorbed on the gel surface by both the amino group and FeOOH particles. In addition, the results indicated that in the presence of Sulphate and Chloride ion, the DMAPAAQ+FeOOH gel composite preferentially adsorbs As(III). Furthermore, because the gel composite can be renewed, it is both cost-effective and environmentally beneficial. The regeneration experiment was carried out for eight days in a row with an efficiency of 48.7 percent. Finally, unlike other techniques now in use, DMAPAAQ+FeOOH does not require any extra separation steps, resulting in easy gel handling and a straightforward adsorption procedure.

The groundwater in approximately 50% of the Bangladesh landmass contains Mn concentrations greater than the limit prescribed by the WHO drinking water guidelines. Although studies have suggested that γ-FeOOH can effectively remove Mn from water, its practicability has not been investigated, considering that the additional processes required to separate the adsorbents and precipitates are not environment-friendly. To improve the efficiency of adsorptive Mn-removal under natural conditions, DMAPAAQ+FeOOH gel composite, and a non-ionic polymer gel composite, *N,N'*-Dimethylacrylamide (DMAA) loaded with iron hydroxide (DMAA + FeOOH), was employed. The results suggest that the higher efficiency of the cationic gel composite is owed to the higher γ-FeOOH content in its gel structure. The maximum adsorption of Mn by DMAPAAQ + FeOOH was 39.02 mg/g. Furthermore, the presence of As did not influence the adsorption of Mn on the DMAPAAQ + FeOOH gel composite and vice versa. DMAPAAQ adsorbed As and the γ-FeOOH particles simultaneously adsorbed Mn.

Acknowledgement

At first, I thank the Almighty God for all the privileges, respect, opportunities and making me who I am.

I thank my family for their endless support, sacrifices and strong faith in me. My parents, Mr. Syed Rabiul Alam and Mrs. Safina Alam, always believed that I am the most special person of the world. Hence, their faith, hope and strength is the biggest motivating factor in my life. They always remind me the responsibility I have towards the wellbeing of the human being and the society. My beloved wife, Ms. Robya Bintay Matin, sacrificed her prosperous career for my education. She worked extremely hard and supported me financially with all her earnings, also single handedly fulfilled all the responsibilities. I believe she is an exceptionally matured, kind hearted and strong personality, who gave me the strength to face "life". Without her help, I would not even survive. My naughty little daughter, Syeda Safi Rushda, had such a strong effect in my life. She ended up becoming my biggest strength and the strongest motivation. Lastly, I would like to thank my parents-in-law, Dr. Md. Abdul matin and Mrs. Dilruba Begum for supporting me and having high hopes from me.

I would like to have the honor to thank my supervisor, Assistant Professor Takehiko Goto for believing in me, motivating me and supporting me through everything. I also thank Professor Wataru Nishijima and Professor Toshinori Tsuru for their judgement on this dissertation. I thank each member of Polymer Technology laboratory for being very helpful, supportive and kind to me all the time. It would not be possible to reach this success without the help of everyone in my lab.

In addition, I must express my thankfulness to the Bangladesh community in Hiroshima. Each member in this community helped me whenever I needed their cooperation. They provided me a sense of security, togetherness, unity, and comfort.

Lastly, I express my gratitude to the Japan Society for the Promotion of Science (JSPS) for hiring me as research fellow DC1, and also providing me Kakenhi research grant (grant number 19J22780).

Syed Ragib Safi

March, 2022

List of Contents

List of Figures

List of Tables

Chapter 1: Introduction

With the expanding population and global industrialization, surface water supplies are becoming increasingly insufficient. Humans have to develop new water sources due to a lack of surface water. Groundwater is a freshwater option that can meet human need for drinking water as well as industrial needs. Furthermore, due to a shortage of surface water supplies, a considerable population in many regions of the world already uses groundwater as a source of drinking water (Goren et al., 2020). Unfortunately, unwanted compounds are present in groundwater sources as a result of anthropogenic causes and the geological makeup of aquifers, and these compounds limit the use of shallow aquifers (Kumar et al., 2017). Among the common groundwater pollutants (fluoride, pesticides, fertilizers, lead etc.), the arsenic (As) contamination has attracted worldwide attention due to its serious danger to human health and ecological life (Fendorf et al., 2010). It has been published that about 140 million people in worldwide are expose to the excessive levels of As via groundwater consumption. In addition, besides As, Manganese (Mn) also contaminates groundwater in different parts of the world. In this chapter, the reason behind I chose As and Mn over other contaminants to remove from water was discussed. Also, I explained the previously used technologies to remove As and Mn. Finally, I explained the chapter wise specific objectives of this thesis.

1.1. Contamination of arsenic

Arsenic contamination of groundwater is a threat concerning millions of people around the world. Arsenic is one of the common global environmental pollutants (Bhattacharya et al., 2007; Hu et al., 2015a), it is ubiquitous in the earth's crust (Sarkar and Paul, 2016). Among the common groundwater pollutants (fluoride, pesticides, fertilizers, lead etc.), the arsenic (As) contamination has attracted worldwide attention due to its serious danger to human health and ecological life (Fendorf et al., 2010). It has been published that about 140 million people in worldwide are expose to the excessive levels of As via groundwater consumption. **Figure 1.1** shows the world map depicting areas where arsenic contamination in aquifers, mining sites and geothermal water has been reported.

In Bangladesh alone, it has been estimated that more than 125 million people are exposed to naturally occurring arsenic in drinking water at levels exceeding the World Health Organization guideline of 10 μg/L. According to survey data from 2000 to 2010, an estimated 35 to 77 million people in the country have been chronically exposed to arsenic in their drinking water in what has been described as the largest mass poisoning in history. In rural areas, 97% of the population relies on tube wells installed since the 1970s to reduce disease from ingestion of pathogen-laden surface waters. Unfortunately, this has resulted in a population highly exposed to arsenic but with limited means or incentives for seeking safe water alternatives (Flanagan et al., 2012).

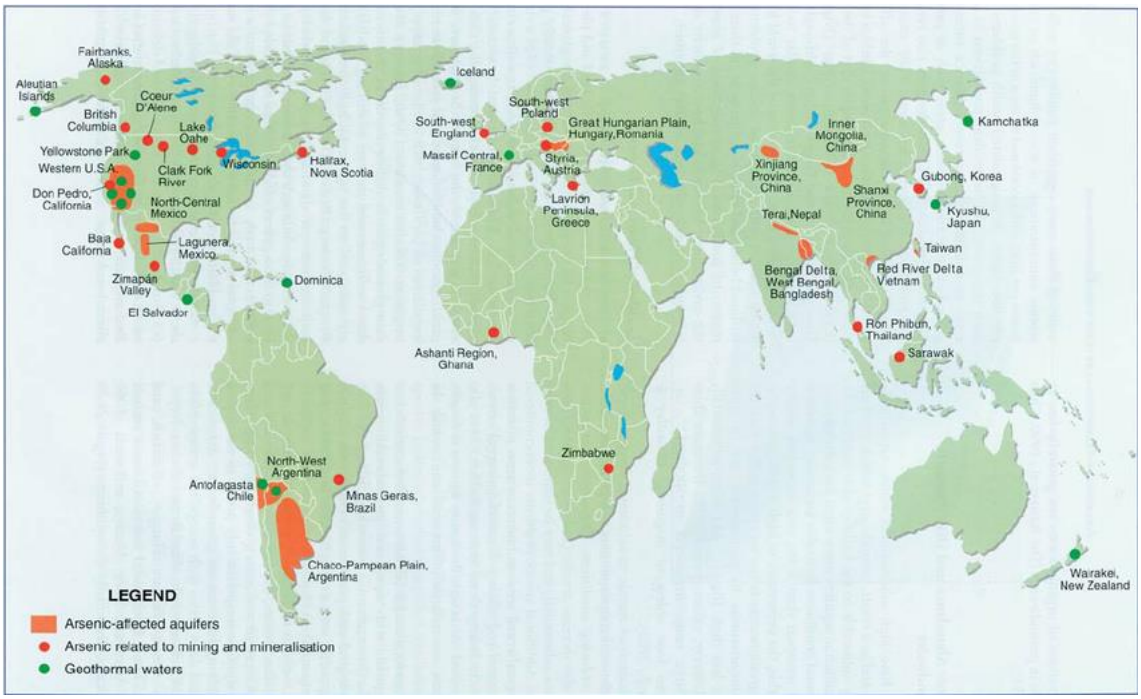

Figure 1.1. A world map depicting areas where arsenic contamination in groundwater has been reported (Centeno et al., 2007).

1.2. Arsenic contamination in Bangladesh

The relation between total number of tubewell samples and different concentration of arsenic in the discricts of Bangladesh is shown in **Figure 1.2**. From the results of Figure 1.2, 52,202 hand tube-well water analyses for As in all 64 districts of Bangladesh, Bangladesh was categorized into five zones: highly affected, moderately affected, mildly affected, very mildly affected and unaffected/As safe. The groundwater of four districts (Rangamati, Khagrachari, Bandarban and Cox's Bazar) is unaffected or As safe (As<10 µg/l) for drinking. Ten districts (Dinajpur, Joypurhat, Kurigram, Lalmonirhat, Naogaon, Nilphamari, Panchagarh, Barguna, Bhola and Patuakhali) are considered as very mildly affected (As levels were between 10 and 50 µg/l) and district Natore is termed as mildly affected (As concentrations were within >50-<100 µg/l). Nine districts (Sirajganj, Thakurgaon, Habiganj, Moulavibazar, Sylhet, Sherpur, Tangail, Brahmanbaria and Chittagong) are regarded as moderately affected (As were between 100-300 µg/l). The others 40 districts (Bogra, Gaibandha, Nawabganj, Pabna, Rajshahi, Rangpur, Bagherhat, Chuadanga, Jessore, Jhenaidaha, Khulna, Kushtia, Meherpur, Magura, Narail, Sathkhira, Barisal, Jhalakathi, Pirojpur, Sunamganj, Dhaka, Faridpur, Gazipur, Gopalganj, Jamalpur, Kishoreganj, Madaripur, Manikganj, Munshiganj, Mymensingh, Narayanganj, Narshingdi, Netrokona, Rajbari, Shariatpur, Chandpur, Comilla, Feni, Lakshmipur and Noakhali) where As above 300 µg/l was detected in tube-well water samples are considered as highly affected.

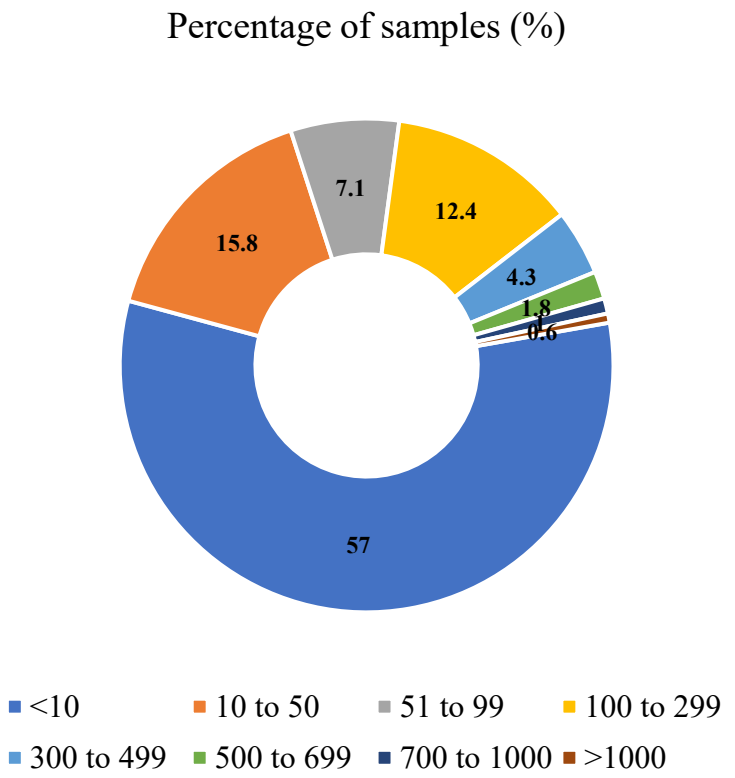

Figure 1.2. Samples with different concentrations of As (µg/L) in the districts of Bangladesh (Chakraborti et al., 2010).

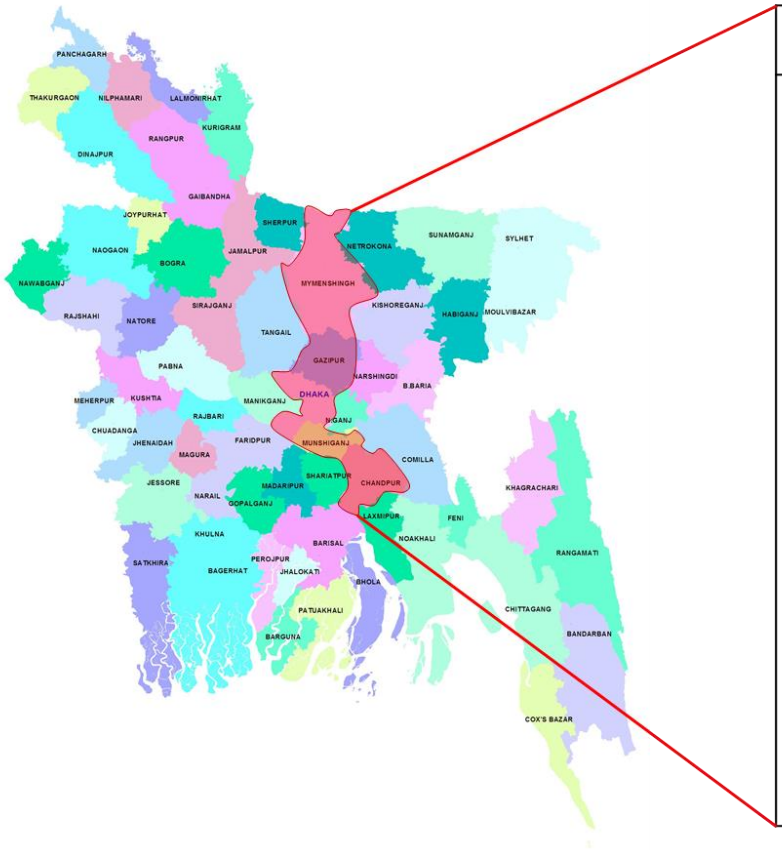

Concentration (mg/L)	Area name
0.62	Chadpur 1
0.11	Chadpur 2
0.25	Chadpur 3
0.11	Chadpur 4
0.32	Chadpur 5
0.2	Chadpur 6
0.26	Chadpur 7
0.2	Chadpur 8
0.29	Chadpur 9
0.5	Chadpur 10
0.17	Matlab
0.04	Dhaka Dokkinkhan
0.05	Dhaka Mirpur
0.05	Mymensingh Central
0.02	Mymensingh South
0	Gaffargaon
0.04	Churkhai
0.14	Kalirbazar I
0.009	Kalirbajar J
0.12	Gouripur

Figure 1.3. Examination of samples from different parts of Bangladesh, the sample zone is marked in red. (The red colored values are the ones that exceeded the WHO standard value of As contamination).

In addition, in 2018, I collected groundwater samples from different parts of Bangladesh as shown in the red marked zone in Figure 1.3. The figure also shows that out of the 20 samples collected, the concentration of As exceeded the permissible As limit in water by WHO in 13 samples.

A total of 30,959 hand tubewells in 64 Bangladeshi districts were surveyed for depth information. In each depth quartile, the proportion of wells that surpass 10 µg/l, 50 µg/l, and

300 µg/l of As is shown in **Figure 1.4**. As concentrations in the studied wells peaked between 15 and 25 meters and then gradually decreased as depth was increased. Despite this, almost 24% of tubewells in the deepest quartile (median tubewell depth of 55 m) had As levels higher above the current WHO recommendation threshold (Chakraborti et al., 2010).

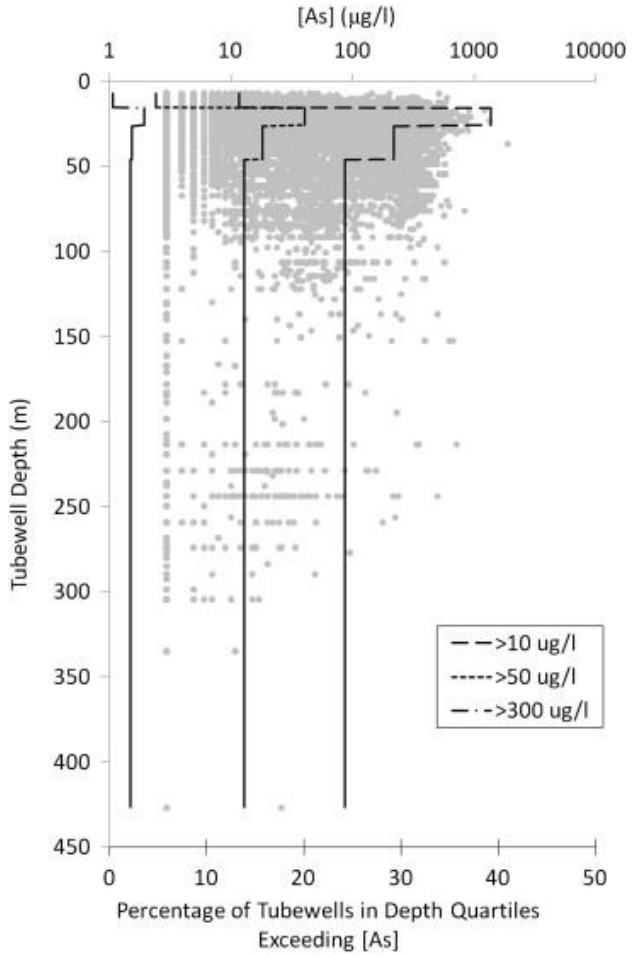

Figure 1.4. Arsenic content in sampled tubewells (log scale) vs. depth (m). The percentage of wells that surpassed 10 μ g/l, 50 μ g/l, and 300 μ g/l in each depth quartile is also displayed versus tubewell depth (Chakraborti et al., 2010).

1.2.1 Effect of arsenic on human health

Arsenic (As) is a toxic element (Sarkar and Paul, 2016), and if consumed in drinking water, it can cause various chronic diseases (Basu et al., 2014; Hu et al., 2015a; Jomova et al., 2011) such as pneumonia (George et al., 2015), diabetes, hypertension, cancer, skin lesions, and severely damages the digestive, circulatory, neurological and respiratory system (Boddu et al., 2008; Murugesan et al., 2006; Praveen et al., 2017; Siddiqui and Chaudhry, 2017; Wang et al., 2001). Almost 200 million people in 105 countries are exposed to chronic diseases caused by long term exposure and consumption of water that is polluted by arsenic (Shakoor et al., 2018). Long term exposure may also result in loss of life.

Numerous studies suggest that arsenic compounds are inimical to human health (Basu et al., 2014; Hu et al., 2015a; Jomova et al., 2011). Further, it has been recognized as a group 1 carcinogen by the International Agency for Research on Cancer (IARC) (Hu et al., 2015a; Jomova et al., 2011). Usually, arsenic enters the human body through drinking water and contaminated food (Praveen et al., 2017). The greatest threat to public health is arsenic poisoning and is most commonly consumed in drinking water. Arsenic contaminated water is acutely toxic and can cause various health problems such as cancer of the skin, lungs, liver, kidney, and bladder, disturbances of the cardiovascular and nervous system functions and may eventually lead to death (Boddu et al., 2008).

1.2.2 Sources of arsenic

Among the many sources of arsenic in the environment, arsenic can be found in the atmosphere, soils, rocks, natural waters and organisms (Matschullat, 2000; Safi et al., 2019a). In water, two types of inorganic oxyanions of arsenic are dominant, As(III) and As(V) (Deng et al., 2018). Human beings are exposed to high levels of arsenic through the consumption of groundwater (Lenoble et al., 2005). Natural processes such as weathering reactions, anthropogenic and biological activities, and volcanic emissions mobilize arsenic in the environment (Smedley and Kinniburgh, 2002). Although, natural conditions are the major causes of arsenic pollution, humans continue to cause additional environmental impact through the following activities:

- Mining wastes and combustion of fossil fuels (Davis et al., 1996; Johnson and Thornton, 1987);
- The use of pesticides containing arsenic (Mariner et al., 1996);
- The use of Arsenic as an additive to livestock feed (Smedley and Kinniburgh, 2002).

Arsenic (As) is a result of both natural and anthropogenic activities (Boddu et al., 2008; Naidu et al., 2006), such as forest fires, the arsenical pesticides in farming, mining and the processing of ores (He et al., 2018a; Meharg and Hartley-Whitaker, 2002; Sheng et al., 2012). Additionally, industrial wastewater, use of arsenical pesticides/herbicides and power generation from coal or geothermal sources also contribute to arsenic contamination (Krishna et al., 2001). However, natural sources of arsenic have led to the largest incidence of poisoning (Naidu et al., 2006).

The World Health Organization (WHO) has set the maximum limit of arsenic contamination in drinking water at less than 0.01mg/L(WHO, 2003; Zhu et al., 2016). However, this limit is exceeded in the groundwater in almost twenty-one countries including USA, China, Chile, Taiwan, Mexico, Argentina, Poland, Canada, Hungary, Japan and others. Among these countries, Bangladesh and India have the highest levels of arsenic contamination in groundwater (Deschamps et al., 2005; Mohan and Pittman, 2007).

Inorganic arsenic has high solubility and mobility in acidic, neutral and alkaline water (Hu et al., 2015a). Inorganic arsenic can occur in the environment in several forms. In natural waters, and thus in drinking water, it is mostly found in trivalent (arsenic (III) (As (III))) or pentavalent (arsenic (V) (As(V))) states. Oxyanions of As(V) are dominant under oxidizing conditions, while oxyanions of As(III) prevail in reducing environments (Lemonte et al., 2017; Niazi et al., 2018, 2015; Niazi and Burton, 2016; Oremland and Stolz, 2003; Shakoor et al., 2018; Sridharan and Nathan, 2018). As(III) is harder to remove than As(V) (Deng et al., 2018), because at neutral pH levels, adsorption processes are not effective on uncharged forms of As(III) (Zhu et al., 2016). First detected in well water in the early 1990s, arsenic is released from sediment by biogeochemical processes that promote reducing environments. The tubewells, affordably priced at about 100 United States dollars (US$), draw the arsenic-containing groundwater from a shallow depth of 10–70 m. Groundwater from depths > 150 m usually contains less arsenic and can be a sustainable drinking water source (Flanagan et al., 2012).

1.2.3 Methods to prevent arsenic

Various treatment techniques were used by the researchers for the removal of arsenic from water (Oremland and Stolz, 2003). Previously, researchers and scientists have developed different arsenic removal methods (Oremland and Stolz, 2003) including coagulation, precipitation(Jia et al., 2006), ion-exchange(Hering et al., 2017; Kim and Benjamin, 2004; Nidheesh and Singh, 2017; Smith et al., 2017), adsorption, reverse osmosis, ultrafiltration, electrochemical treatments(Nidheesh and Singh, 2017), combinations of adsorption and membrane technology(Linlin et al., 2018) and others(Ali, 2012; Crittenden et al., 2012; Gupta et al., 2012; Pendergast and Hoek, 2011). Many researchers agree that adsorption is one of the best techniques because of its user friendliness, cost efficiency and overall effectiveness(Babel and Kurniawan, 2003; Bibi et al., 2016; He et al., 2018b; Hu et al., 2017; Li et al., 2016; Mohan and Pittman, 2007; Niazi et al., 2018; Shaheen et al., 2013; Shakoor et al., 2016; Vithanage et al., 2017). Activated carbons are one of the most frequently used adsorbents. However, they only function at very narrow pH ranges and also the amount of adsorption of both As(III) and As(V) is low(Hu et al., 2017) as well.

1.2.4 Adsorption

Among the adsorbents, iron oxyhydroxide powders are considered to be one of the most efficient adsorbents for arsenic in aqueous solutions (Hu et al., 2015a; Saharan et al., 2014). However, these adsorbents may saturate early in the performing process and need

some synthetic precursor for their preparation which leads to the toxicity of iron oxide. In addition, these adsorbents harms the water quality in the long term (Siddiqui and Chaudhry, 2017). Separation of the iron oxyhydroxides particles after the adsorption process requires sedimentation or filtration, which results in additional cost and low mechanical resistance (Hu et al., 2015a; Tuna et al., 2013).

Recently, a combination of adsorption and membrane technology is also studied and applied on Songhua river water, in China, but the removal rate was ineffective (Linlin et al., 2018). Several other adsorbents such as fly ash, Fe oxides-based nano adsorbents, Fe sulfides have been used to remove arsenic from water (Bibi et al., 2016, 2017; Cope et al., 2014; Irem et al., 2017; Lata and Samadder, 2016a; Niazi et al., 2018; Niazi and Burton, 2016; Shaheen et al., 2013; Shakoor et al., 2016; Vithanage et al., 2017). However, the majority of these adsorbents have some disadvantages, including low adsorption capacity and reusability, low stability, high operational and maintenance costs and use of hazardous chemicals in synthesis of some adsorbents (Niazi et al., 2018).

1.3. Polymer gel as adsorbents

Polymers that were previously utilized for arsenic adsorption Are poly(3-acrylamidopropyl)trimethylammonium chloride (p(APTMACl)) (Barakat and Sahiner, 2008), poly(methyl acrylate), poly(vinyl acetate), poly(acrylic acid) (Malana et al., 2011), poly(vinyl alcohol) (Santos et al., 2012), quaternized poly(4-vinylpyridine) (Sahiner et al., 2011), and poly(acrylonitril-co-acrylamidopropyl-trimethyl ammonium chloride) (Dudu et al., 2015). Among these polymers, cationic p(APTMACl) has attracted great interest due to its simple formation in aqueous solution (Imyim et al., 2016).

p(APTMACl), which is a cationic cryogel was prepared and a 96% of removal rate was achieved (Sahiner et al., 2015). Iron oxyhydroxide powders are also contemplated as effective adsorbents (Hu et al., 2015b; Saharan et al., 2014). Recently, researchers utilized several types of polymer gels for instance cryogels, microgels, cationic hydrogels, etc., to adsorb arsenic. These gels exhibited competent adsorption properties. For example, the cationic cryogel, poly(3-acrylamidopropyl) trimethyl ammonium chloride [p(APTMACl)] achieved an arsenic removal rate of 96% (Sahiner et al., 2015). Additionally, at pH 9, approximately 99.7% removal efficiency was achieved by this cationic hydrogel (Barakat and Sahiner, 2008). A microgel, tris(2-aminoethyl) amine (TAEA) and glyceroldiglycidyl ether (GDE), p(TAEA-co-GDE) achieved 98.72 mg/g of maximum arsenic adsorption capacity was achieved by the microgel at pH 4 (Rehman et al., 2017). Although these gels have high adsorption capabilities, their selectivity in all studied environments was low and they failed to effectively remove arsenic from water at neutral pH levels(Safi et al., 2019a). A maximum adsorption capacity of 227 μg/g of was measured when Fe(III)-Sn(IV) mixed

binary oxide-coated sand was used at a temperature of 313 K and a pH of 7(Chaudhry et al., 2016). Alternatively, Fe-Zr binary oxide-coated sand (IZBOCS) has also been used to remove arsenic and achieved a maximum adsorption capacity of 84.75 mg/g at 318 K and a pH of 7 (Chaudhry et al., 2017). The core shell $Fe@Fe_2O_3$ nanobunches (NBZI) removed arsenic from acidic wastewater by adsorption and co-precipitation. But, since this technique produces sediments, additional separation processes are required(Tang et al., 2017).

Because of their amazing capacity to detect particular ions, certain ion-imprinting polymers have been developed and deployed in recent years (Ashraf et al., 2011; Chang et al., 2011). Ion-imprinting allows cross-linking functional monomers to self-assemble around templated ions, resulting in recognition sites with the selectivity of a specific target ion. Surface imprinting technique enables the presence of recognition sites on the surface of supporting material, ensuring complete removal of templated ions and easy access to target ions (Liu et al., 2011). As a result, the surface imprinting process may be utilized to establish a huge number of binding sites on nanosized support materials (Chi et al., 2021).

Ion imprinted polymers (IIPs) have an unrivaled advantage in selective adsorption and recovery of heavy metals due to their unique cavity structure and specific adsorption sites that are complimentary to the target ions (Fu et al., 2015; Rao et al., 2006). As a result, IIPs have the ability to revolutionize production of novel adsorbents that can be chemically recreated and reused, thus cutting treatment costs. Heavy metal cations have been selectively removed using several types of imprinted polymer adsorbents, such as Cu (Hoai et al., 2010), Cd (Zhu et al., 2017), Ni (Saraji and Yousefi, 2009), and Pb (Liu et al., 2011). In natural

waters, however, arsenic species are mainly found as oxyanions rather than metal cations. The charge-to-radius ratio of metal anions is smaller than that of metal cations, which reduces the electrostatic interaction with functional monomers or ligands by 3–5 times (Alizadeh et al., 2016). As a result, it is more difficult for them to establish their own well-known websites. Second, with the nonpolar imprinting chemicals often used, anions are difficult to dissolve (Vilar, 2008). For the two reasons described above, metal anions are rarely utilized as templates in ion imprinting (Fang et al., 2018).

Other reported adsorbents exhibited low adsorption performances, lack of recyclability, low stability, high operational and maintenance costs, and the use of hazardous chemicals in the synthesis process (Niazi et al., 2018). Therefore, researchers need to develop a technology that can remove arsenic efficiently at neutral pH levels, provide selectivity, cost effectiveness and can be reused.

1.4. Composite of Polymer gel and Iron hydroxide

To improve this situation, researchers need to establish arsenic removal processes that are highly effective in terms of the adsorption abilities, selectivity and cost-benefits. To increase the amount of arsenic adsorption, I developed an adsorbent which is a cationic gel composite of *N,N*-dimethylamino propylacrylamide, methyl chloride quaternary (DMAPAAQ) (**Figure 1.5**) and Iron(III) Hydroxide (FeOOH) (**Figure 1.6**) particles. FeOOH is reported to increase the adsorption performance of the adsorbent for both forms of arsenic (Lin et al., 2018). In this study, we prepared the gel composite in a unique way. The gel composite is non-porous and also, FeOOH was impregnated during the preparation of the gel composite. This gel functions when it is put into water and its surface area increases to adsorb arsenic. Inside the gel, a cationic charge (quaternary amino group) adsorbs arsenic and the iron hydroxide found in this gel improves selective adsorption. This procedure is explored further in the next chapter and also in Safi et al.'s study (Safi et al., 2019b).

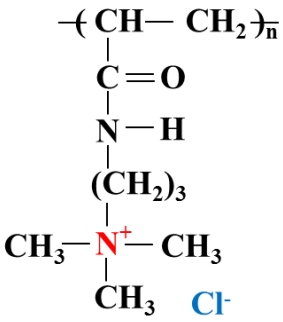

Figure 1.5. Polymer structure of DMAPAAQ gel.

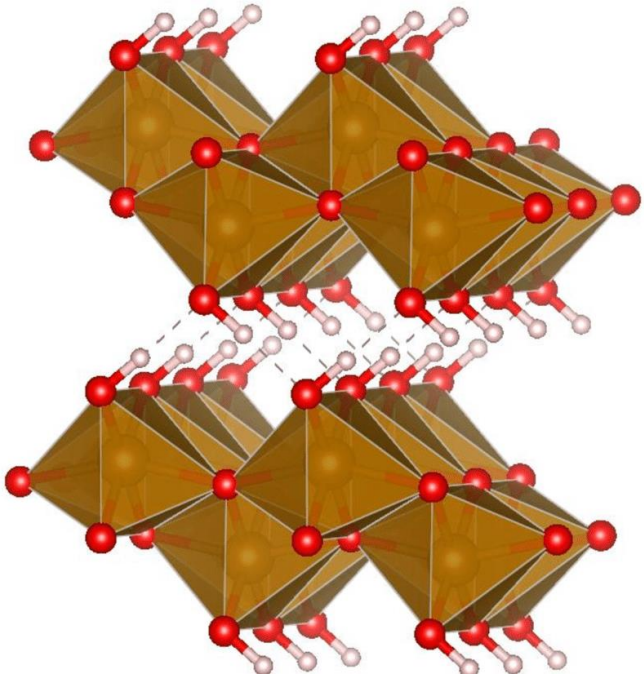

Figure 1.6. Structure of γ -FeOOH: iron centers are hidden in octahedra, oxygen centers are in red, hydrogen centers are in white (Shubin et al., 2018).

1.5. Removal of As(III) using polymer gels

The most ubiquitous arsenic species in groundwater is As(III), which is 25–60 times more hazardous than As (V) (Korte and Fernando, 1991). In natural waterways, arsenic species are generally found as oxyanions ($H_2AsO_3^-$, $HAsO_3^{2-}$) rather than metal cations. The charge-to-radius ratios of metal anions are 3–5 times lower than those of metal cations (Alizadeh et al., 2016), With functional monomers or ligands, this lowers the electrostatic impact, making it harder to generate particular recognition sites. As(III) adsorption is typically less than As(V) adsorption. In solution, As(III) exists primarily as H_3AsO_3 and, to a marginal extent, as $H_2AsO_3^-$ (Sharma and Sohn, 2009). Therefore, the adsorption of As(III) is weak. (Imyim et al., 2016). Diverse processes have been developed for As(III) oxidation, such as chemical oxidants (chlorine, permanganate, etc.) (Sorlini and Gialdini, 2010) and advanced oxidation processes (AOPs) (UV/H_2O_2) (Sorlini et al., 2010), Fenton reaction (Hug and Leupin, 2003), UV/nitrite (Kim et al., 2014), UV/peroxydisulfate (Neppolian et al., 2008), and PMS (Wang et al., 2014). For typical chemical oxidants, the potential production of toxic byproducts such as trihalomethane, nitrosoamine, and bromate is a severe concern (chlorine, chloramine, and ozone) (Sharma and Sohn, 2009). The employment of specific response devices is required for UV-based AOPs. The Fenton method has a number of disadvantages, including a high pH dependence and the generation of sludge. In contrast, PMS is a very benign oxidant since its end products (SO_4^{2-}) are often nonpolluting and inert. Solid PMS is also more convenient to handle than liquid or gaseous oxidants. On the other hand, the direct oxidation of As(III) by PMS is limited and time-consuming. In addition, further treatments are required to eradicate the As(V) and residual As (III). A heterogeneous

catalytic method that combines oxidation and adsorption will simplify the overall elimination operation (Kim et al., 2015; Önnby et al., 2014; Voegelin and Hug, 2003). Metal oxides are one of the most common types of catalysts used in heterogeneous oxidation (Lei et al., 2015). In the meanwhile, they can serve as effective arsenic adsorbents (Lata and Samadder, 2016b; Wei et al., 2019). Therefore, in this thesis the adsorption of As(III) with DMAPAAQ+FeOOH is examined.

1.6. Contamination of Mn

Manganese (Mn) is a known mutagen whose accumulation may cause hepatic encephalopathy. Consumption of Mn through drinking water may cause neurological damage. The WHO has set a limit of 0.5 mg/L for Mn in drinking water because of its neurotoxicity and other detrimental effects in humans and other animals in Japan and Greece (Frisbie et al., 2002).

Table 1.1. Risk-based drinking water criteria and the percentage of area exceeding these criteria (Frisbie et al., 2002).

Element	Drinking water criterial by WHO (mg/L)	Percentage of Bangladesh's area exceeding criteria by WHO (%)
As	0.01	49
Mn	0.5	50
Pb	0.01	3
Ni	0.02	<1
Cr	0.05	<1

Following arsenic (As), Mn is one of the most commonly-found contaminants in most rivers and groundwater in Bangladesh (Sarkar et al., 2019). **Table 1.1** describes that approximately 50% of the area of Bangladesh contains groundwater having Mn concentrations greater than suggested by the World Health Organization (WHO) health-based drinking water guidelines. The maximum concentration of Mn in groundwaters in

Bangladesh was found to be 2.0 mg/L, whereas the WHO approves a maximum of 0.5 mg/L of Mn in drinking water. In over 35% of the samples collected by Frisbie et al., the WHO drinking water guidelines were exceeded for As and Mn (Frisbie et al., 2002). Besides, as explained in **Table 1.2**, the maximum concentration of Mn in industrial wastewater in Bangladesh was found to be as high as 5.0 mg/L (Department of Environment, 2008; Hasan et al., 2019). In addition, As and Mn are among the most critical pollutants of drinking water in the South African region (Verlicchi and Grillini, 2019). The coexistence of As and Mn in groundwater has been reported earlier (Bora et al., 2017). Therefore, the simultaneous removal of As and Mn needs to be studied.

1.7. Technologies to remove As and Mn simultaneously

Many studies have been conducted on the removal of As and a few have focused on the removal of Mn. However, studies on simultaneous removal of As and Mn are rare because it is difficult to remove anionic and cationic components using a single adsorbent. Although As and Mn have been removed separately or exclusively (Budinova et al., 2009; Pires et al., 2015), their simultaneous adsorption has not been conducted to date. Two previous studies have reported the removal of As, Mn, and Fe (Bora et al., 2017; Yang et al., 2014) and one study developed a treatment system using coagulation and filtration for the simultaneous removal of As and Mn (Waste, 2010). Although these three studies claimed to remove As, they removed only one oxidation state of arsenic, arsenite (As(III)). In these studies, As(III) was oxidised by the coexisting MnO_2, resulting in the removal of As(III) and Mn from the initial solution. Furthermore, the influence of the precipitate formed due to the coexistence of As(III) and Mn on the removal efficiencies of the methods has not been investigated using response surface methodology (RSM), microorganisms in a biofilter and the sedimentation-filtration treatment process (Waste, 2010). Furthermore, in solutions containing arsenate (As(V)) and As(III), the extent of simultaneous removal of As and Mn would differ, because As(V) is not oxidised by MnO_2. Furthermore, no studies were found on the simultaneous removal of Mn and total As. Finally, the changes in the surface functional groups were not investigated using Fourier transform infrared (FTIR) spectroscopy, and the adsorption mechanisms were not confirmed in the aforementioned works. Therefore, in this thesis, I tried to address these research gaps by simultaneously adsorbing As(III), As(V) and Mn with a single adsorbent under natural water conditions as illustrated in **Figure 1.7**.

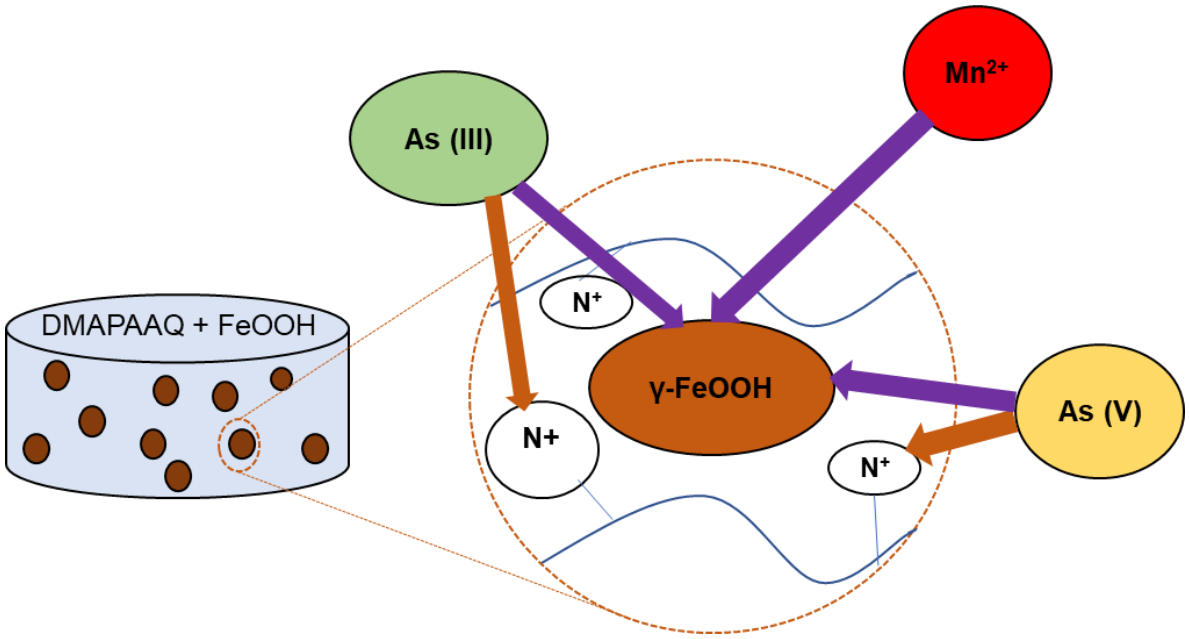

Figure 1.7. Simultaneous adsorption of arsenic and manganese by DMAPAAQ+FeOOH gel composite.

Table 1.2. Mn concentration in surface water and groundwater in Bangladesh (Hasan et al., 2019).

Sample	Concentration of Mn (mg/L)
WHO Standards	0.5
Bangladesh Standards (Drinking water)	0.1
Bangladesh Standards (Industrial effluents)	5
Deep Tubewells of Cox's Bazar paleobeach area	1.37
Shallow Tubewells of Cox's Bazar paleobeach area	1.87
Tube wells of Singair, Manikgonj	2.08
Buriganga River, Dhaka	0.157
Airport Lake, Dhaka	0.1085

1.8. Objectives

This dissertation is divided into the following chapters. The objectives of each chapter is outlined:

In the first chapter, **chapter 1**, my objective was to discuss about why As and Mn were removed in this dissertation and also the technologies that were involved in the removal process.

In the second chapter, **chapter 2**, my objective is to first prepare a new adsorbent which will adsorb arsenic effectively. The gel should also provide selectivity and simplify

production processes. The purpose of the unique preparation of the gel differently than the previous polymer gels used for arsenic and other metals adsorption was to assure that the gel contains maximum FeOOH particles in it's structure. At neutral pH levels, the gel should efficiently adsorbed arsenic. In addition, the gel should be reusable for several cycles in a row with efficiency.

Then in the following chapter, **chapter 3**, I examined the causes behind the high adsorption amount of arsenic and other results provided because of using the gel composite, which is selective in adsorption and regeneration. In this chapter, I evaluated the characteristics that contribute to the high adsorption performances of the gel composite and discussed the details. It was also examined that whether maximum FeOOH particles was impregnated, which was one of the objectives of Chapter 2. In addition, my goal was to find the type of FeOOH and the changes of surface functional groups due to arsenic adsorption in the gel.

In **chapter 4**, the objective was to examine the effectiveness of DMAPAAQ+FeOOH in removing As(III), which is harder to remove than As(V). Other objectives were to investigate the pH dependency, regeneration efficiency after continuous eight cycles, surface functional changes due to As(III) adsorption and selective adsorption of As(III).

Then, in the **chapter 5**, my objective was to investigate the adsorptive removal of Mn using my previously-developed gel, DMAPAAQ+FeOOH. Additionally, I examined the Mn removal efficiency of DMAPAAQ+FeOOH gel to that of the non-ionic gel, *N,N'*-

Dimethylacrylamide (DMAA) (**Figure 1.8**) and non-ionic gel composite (DMAA + FeOOH). The broad objective was to examine the simultaneously adsorb As and Mn.

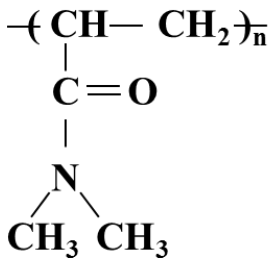

Figure 1.8. Polymer structure of DMAA gel.

Lastly, **chapter 6** summarizes the results of this study.

References

Ali, I., 2012. New Generation Adsorbents for Water Treatment. Chemical Reviews 112, 5073–5091. https://doi.org/10.1021/cr300133d

Alizadeh, T., Sabzi, R.E., Alizadeh, H., 2016. Synthesis of nano-sized cyanide ion-imprinted polymer via non-covalent approach and its use for the fabrication of a CN−-selective carbon nanotube impregnated carbon paste electrode. Talanta 147, 90–97. https://doi.org/10.1016/j.talanta.2015.09.043

Babel, S., Kurniawan, T.A., 2003. Low-cost adsorbents for heavy metals uptake from contaminated water: a review. Journal of Hazardous Materials 97, 219–243. https://doi.org/10.1016/S0304-3894(02)00263-7

Barakat, M.A.A., Sahiner, N., 2008. Cationic hydrogels for toxic arsenate removal from aqueous environment. Journal of Environmental Management 88, 955–961. https://doi.org/10.1016/j.jenvman.2007.05.003

Basu, A., Saha, D., Saha, R., Ghosh, T., Saha, B., 2014. A review on sources, toxicity and remediation technologies for removing arsenic from drinking water. Research on Chemical Intermediates 40, 447–485. https://doi.org/10.1007/s11164-012-1000-4

Bhattacharya, P., Welch, A.H., Stollenwerk, K.G., McLaughlin, M.J., Bundschuh, J., Panaullah, G., 2007. Arsenic in the environment: Biology and Chemistry. Science of the Total Environment 379, 109–120. https://doi.org/10.1016/j.scitotenv.2007.02.037

Bibi, I., Icenhower, J., Niazi, N.K., Naz, T., Shahid, M., Bashir, S., 2016. Chapter 21 - Clay Minerals: Structure, Chemistry, and Significance in Contaminated Environments and Geological {CO2} Sequestration, in: Prasad, M.N. V, Shih, K. (Eds.), Environmental Materials and Waste. Academic Press, pp. 543–567. https://doi.org/10.1016/B978-0-12-803837-6.00021-4

Bibi, S., Farooqi, A., Yasmin, A., Kamran, M.A., Niazi, N.K., 2017. Arsenic and fluoride removal by potato peel and rice husk (PPRH) ash in aqueous environments. International Journal of Phytoremediation 19, 1029–1036. https://doi.org/10.1080/15226514.2017.1319329

Boddu, V.M., Abburi, K., Talbott, J.L., Smith, E.D., Haasch, R., 2008. Removal of arsenic (III) and arsenic (V) from aqueous medium using chitosan-coated biosorbent. Water Research 42, 633–642. https://doi.org/10.1016/j.watres.2007.08.014

Bora, A.J., Mohan, R., Dutta, R.K., 2017. Simultaneous removal of arsenic, iron and manganese from groundwater by oxidation-coagulation-adsorption at optimized pH. Water Supply 18, 60–70. https://doi.org/10.2166/ws.2017.092

Budinova, T., Savova, D., B.Tsyntsarski, Ania, C.O., Cabal, B., Parra, J.B., Petrov, N., 2009. Biomass waste-derived activated carbon for the removal of arsenic and manganese ions from aqueous solutions. Applied Surface Science 255, 4650–4657. https://doi.org/10.1016/j.apsusc.2008.12.013

Centeno, J.A., Tseng, C.-H., Voet, G.B.V. der, Finkelman, R.B., 2007. Global Impacts Of Geogenic Arsenic: A Medical Geology Research Case. ambi 36, 78–81. https://doi.org/10.1579/0044-7447(2007)36[78:GIOGAA]2.0.CO;2

Chakraborti, D., Rahman, M.M., Das, B., Murrill, M., Dey, S., Chandra Mukherjee, S., Dhar, R.K., Biswas, B.K., Chowdhury, U.K., Roy, S., Sorif, S., Selim, M., Rahman, M., Quamruzzaman, Q., 2010. Status of groundwater arsenic contamination in Bangladesh: A 14-year study report. Water Research, Groundwater Arsenic: From Genesis to Sustainable Remediation 44, 5789–5802. https://doi.org/10.1016/j.watres.2010.06.051

Chaudhry, S.A., Ahmed, M., Siddiqui, S.I., Ahmed, S., 2016. Fe(III)–Sn(IV) mixed binary oxide-coated sand preparation and its use for the removal of As(III) and As(V) from water: Application of isotherm, kinetic and thermodynamics. Journal of Molecular Liquids 224, 431–441. https://doi.org/10.1016/J.MOLLIQ.2016.08.116

Chaudhry, S.A., Zaidi, Z., Siddiqui, S.I., 2017. Isotherm, kinetic and thermodynamics of arsenic adsorption onto Iron-Zirconium Binary Oxide-Coated Sand (IZBOCS): Modelling and process optimization. Journal of Molecular Liquids 229, 230–240. https://doi.org/10.1016/J.MOLLIQ.2016.12.048

Cope, C.O., Webster, D.S., Sabatini, D.A., 2014. Arsenate adsorption onto iron oxide amended rice husk char. Science of the Total Environment 488–489, 554–561. https://doi.org/10.1016/j.scitotenv.2013.12.120

Crittenden, J., Trussell, R., Hand, D., Howe, K., Tchobanoglous, G., 2012. Advanced Oxidation, in: MWH's Water Treatment: Principles and Design, Third Edition. Wiley-Blackwell, pp. 1415–1484. https://doi.org/10.1002/9781118131473.ch18

Davis, A., Ruby, M. V., Bloom, M., Schoof, R., Freeman, G., Bergstrom, P.D., 1996. Mineralogic constraints on the bioavailability of arsenic in smelter-impacted soils. Environmental Science and Technology 30, 392–399. https://doi.org/10.1021/es9407857

Deng, Y., Li, Y., Li, X., Sun, Y., Ma, J., Lei, M., Weng, L., 2018. Influence of calcium and phosphate on pH dependency of arsenite and arsenate adsorption to goethite. Chemosphere 199, 617–624. https://doi.org/10.1016/j.chemosphere.2018.02.018

Department of Environment, M. of E. and F., Bangladesh, 2008. Guide for Assessment of Effluent Treatment Plants [WWW Document]. URL http://old.doe.gov.bd/publication_images/15_etp_assessment_guide.pdf (accessed 4.12.21).

Deschamps, E., Ciminelli, V.S.T., Höll, W.H., 2005. Removal of As(III) and As(V) from water using a natural Fe and Mn enriched sample. Water Research 39, 5212–5220. https://doi.org/10.1016/j.watres.2005.10.007

Dudu, T.E., Sahiner, M., Alpaslan, D., Demirci, S., Aktas, N., 2015. Removal of As(V), Cr(III) and Cr(VI) from aqueous environments by poly(acrylonitril-co-acrylamidopropyl-trimethyl ammonium chloride)-based hydrogels. Journal of Environmental Management 161, 243–251. https://doi.org/10.1016/j.jenvman.2015.07.015

Fendorf, S., Michael, H.A., van Geen, A., 2010. Spatial and Temporal Variations of Groundwater Arsenic in South and Southeast Asia. Science 328, 1123–1127. https://doi.org/10.1126/science.1172974

Flanagan, S. V, Johnston, R.B., Zheng, Y., 2012. Arsenic in tube well water in Bangladesh: health and economic impacts and implications for arsenic mitigation. Bulletin of the World Health Organization 90, 839–46. https://doi.org/10.2471/BLT.11.101253

Frisbie, S.H., Ortega, R., Maynard, D.M., Sarkar, B., 2002. The concentrations of arsenic and other toxic elements in Bangladesh's drinking water. Environ Health Perspect 110, 1147–1153.

George, C.M., Brooks, W.A., Graziano, J.H., Nonyane, B.A.S., Hossain, L., Goswami, D., Zaman, K., Yunus, M., Khan, A.F., Jahan, Y., Ahmed, D., Slavkovich, V., Higdon, M., Deloria-Knoll, M., O' Brien, K.L., 2015. Arsenic exposure is associated with pediatric pneumonia in rural Bangladesh: a case control study. Environmental Health 14, 83. https://doi.org/10.1186/s12940-015-0069-9

Goren, A.Y., Kobya, M., Oncel, M.S., 2020. Arsenite removal from groundwater by aerated electrocoagulation reactor with Al ball electrodes: Human health risk assessment. Chemosphere 251, 126363. https://doi.org/10.1016/j.chemosphere.2020.126363

Gupta, V.K., Ali, I., Saleh, T.A., Nayak, A., Agarwal, S., 2012. Chemical treatment technologies for waste-water recycling-an overview. RSC Adv. 2, 6380–6388. https://doi.org/10.1039/C2RA20340E

Hasan, Md.K., Shahriar, A., Jim, K.U., 2019. Water pollution in Bangladesh and its impact on public health. Heliyon 5, e02145. https://doi.org/10.1016/j.heliyon.2019.e02145

He, R., Peng, Z., Lyu, H., Huang, H., Nan, Q., Tang, J., 2018a. Synthesis and characterization of an iron-impregnated biochar for aqueous arsenic removal. Science of the Total Environment 612, 1177–1186. https://doi.org/10.1016/j.scitotenv.2017.09.016

He, R., Peng, Z., Lyu, H., Huang, H., Nan, Q., Tang, J., 2018b. Synthesis and characterization of an iron-impregnated biochar for aqueous arsenic removal. Science of the Total Environment 612, 1177–1186. https://doi.org/10.1016/j.scitotenv.2017.09.016

Hering, J.G., Katsoyiannis, I.A., Theoduloz, G.A., Berg, M., Hug, S.J., 2017. Arsenic Removal from Drinking Water: Experiences with Technologies and Constraints in Practice. Journal of Environmental Engineering 143, 03117002. https://doi.org/10.1061/(ASCE)EE.1943-7870.0001225

Hu, Q., Liu, Y., Gu, X., Zhao, Y., 2017. Adsorption behavior and mechanism of different arsenic species on mesoporous MnFe2O4 magnetic nanoparticles. Chemosphere 181, 328–336. https://doi.org/10.1016/J.CHEMOSPHERE.2017.04.049

Hu, X., Ding, Z., Zimmerman, A.R., Wang, S., Gao, B., 2015a. Batch and column sorption of arsenic onto iron-impregnated biochar synthesized through hydrolysis. Water Research 68, 206–216. https://doi.org/10.1016/j.watres.2014.10.009

Hu, X., Ding, Z., Zimmerman, A.R., Wang, S., Gao, B., 2015b. Batch and column sorption of arsenic onto iron-impregnated biochar synthesized through hydrolysis. Water Research 68, 206–216. https://doi.org/10.1016/j.watres.2014.10.009

Hug, S.J., Leupin, O., 2003. Iron-Catalyzed Oxidation of Arsenic(III) by Oxygen and by Hydrogen Peroxide: pH-Dependent Formation of Oxidants in the Fenton Reaction. Environ. Sci. Technol. 37, 2734–2742. https://doi.org/10.1021/es026208x

Imyim, A., Sirithaweesit, T., Ruangpornvisuti, V., 2016. Arsenite and arsenate removal from wastewater using cationic polymer-modified waste tyre rubber. Journal of Environmental Management 166, 574–578. https://doi.org/10.1016/j.jenvman.2015.11.005

Irem, S., Islam, E., Mahmood Khan, Q., Anwar ul Haq, M., Jamal Hashmat, A., 2017. Adsorption of arsenic from drinking water using natural orange waste: kinetics and fluidized bed column studies. Water Science and Technology: Water Supply.

Jia, Y., Xu, L., Fang, Z., Demopoulos, G.P., 2006. Observation of surface precipitation of arsenate on ferrihydrite. Environmental Science and Technology 40, 3248–3253. https://doi.org/10.1021/es051872+

Johnson, C.A., Thornton, I., 1987. Hydrological and chemical factors controlling the concentrations of Fe, Cu, Zn and As in a river system contaminated by acid mine drainage. Water Research 21, 359–365. https://doi.org/10.1016/0043-1354(87)90216-8

Jomova, K., Jenisova, Z., Feszterova, M., Baros, S., Liska, J., Hudecova, D., Rhodes, C.J., Valko, M., 2011. Arsenic: Toxicity, oxidative stress and human disease. Journal of Applied Toxicology 31, 95–107. https://doi.org/10.1002/jat.1649

Kim, D., Bokare, A.D., Koo, M. suk, Choi, W., 2015. Heterogeneous Catalytic Oxidation of As(III) on Nonferrous Metal Oxides in the Presence of H2O2. Environ. Sci. Technol. 49, 3506–3513. https://doi.org/10.1021/es5056897

Kim, D., Lee, J., Ryu, J., Kim, K., Choi, W., 2014. Arsenite Oxidation Initiated by the UV Photolysis of Nitrite and Nitrate. Environ. Sci. Technol. 48, 4030–4037. https://doi.org/10.1021/es500001q

Kim, J., Benjamin, M.M., 2004. Modeling a novel ion exchange process for arsenic and nitrate removal. Water Research 38, 2053–2062. https://doi.org/10.1016/j.watres.2004.01.012

Korte, N.E., Fernando, Q., 1991. A review of arsenic (III) in groundwater. Critical Reviews in Environmental Control 21, 1–39. https://doi.org/10.1080/10643389109388408

Krishna, M.V.B., Chandrasekaran, K., Karunasagar, D., Arunachalam, J., 2001. A combined treatment approach using Fenton ' s reagent and zero valent iron for the removal of arsenic from drinking water 84, 229–240.

Kumar, P., Singh, C.K., Saraswat, C., Mishra, B., Sharma, T., 2017. Evaluation of aqueous geochemistry of fluoride enriched groundwater: A case study of the Patan district, Gujarat, Western India. Water Science 31, 215–229. https://doi.org/10.1016/j.wsj.2017.05.002

Lata, S., Samadder, S.R., 2016a. Removal of arsenic from water using nano adsorbents and challenges: A review. Journal of Environmental Management 166, 387–406. https://doi.org/10.1016/j.jenvman.2015.10.039

Lata, S., Samadder, S.R., 2016b. Removal of arsenic from water using nano adsorbents and challenges: A review. Journal of Environmental Management 166, 387–406. https://doi.org/10.1016/j.jenvman.2015.10.039

Lei, Y., Chen, C.-S., Tu, Y.-J., Huang, Y.-H., Zhang, H., 2015. Heterogeneous Degradation of Organic Pollutants by Persulfate Activated by CuO-Fe3O4: Mechanism, Stability, and Effects of pH and Bicarbonate Ions. Environ. Sci. Technol. 49, 6838–6845. https://doi.org/10.1021/acs.est.5b00623

Lemonte, J.J., Stuckey, J.W., Sanchez, J.Z., Tappero, R., Rinklebe, J., Sparks, D.L., 2017. Sea Level Rise Induced Arsenic Release from Historically Contaminated Coastal Soils. Environmental Science and Technology 51, 5913–5922. https://doi.org/10.1021/acs.est.6b06152

Lenoble, V., Laclautre, C., Deluchat, V., Serpaud, B., Bollinger, J.C., 2005. Arsenic removal by adsorption on iron(III) phosphate. Journal of Hazardous Materials 123, 262–268. https://doi.org/10.1016/j.jhazmat.2005.04.005

Li, W., Chen, D., Xia, F., Tan, J.Z.Y., Huang, P.P., Song, W.G., Nursam, N.M., Caruso, R.A., 2016. Extremely high arsenic removal capacity for mesoporous aluminium magnesium oxide composites. Environmental Science: Nano 3, 94–106. https://doi.org/10.1039/c5en00171d

Lin, S., Yang, H., Na, Z., Lin, K., 2018. A novel biodegradable arsenic adsorbent by immobilization of iron oxyhydroxide (FeOOH) on the root powder of long-root Eichhornia crassipes. Chemosphere 192, 258–266. https://doi.org/10.1016/j.chemosphere.2017.10.163

Linlin, H., Wang, N., Wang, C., Li, G., 2018. Arsenic removal from water and river water by the combined adsorption - UF membrane process. Chemosphere 202, 768–776. https://doi.org/10.1016/j.chemosphere.2018.03.159

Malana, M.A., Qureshi, R.B., Ashiq, M.N., 2011. Adsorption studies of arsenic on nano aluminium doped manganese copper ferrite polymer (MA, VA, AA) composite: Kinetics and mechanism. Chemical Engineering Journal 172, 721–727. https://doi.org/10.1016/j.cej.2011.06.041

Mariner, P.E., Holzmer, F.J., Jackson, R.E., Meinardus, H.W., Wolf, F.G., 1996. Effects of high pH on arsenic mobility in a shallow sandy aquifer and on aquifer permeability along the adjacent shoreline, commencement bay superfund site, Tacoma, Washington. Environmental Science and Technology 30, 1645–1651. https://doi.org/10.1021/es9506420

Matschullat, J., 2000. Arsenic in the geosphere - A review. Science of the Total Environment 249, 297–312. https://doi.org/10.1016/S0048-9697(99)00524-0

Meharg, A.A., Hartley-Whitaker, J., 2002. Arsenic uptake and metabolism in arsenic resistant and nonresistant plant species. New Phytologist 154, 29–43. https://doi.org/10.1046/j.1469-8137.2002.00363.x

Mohan, D., Pittman, C.U., 2007. Arsenic removal from water/wastewater using adsorbents-A critical review. Journal of Hazardous Materials 142, 1–53. https://doi.org/10.1016/j.jhazmat.2007.01.006

Murugesan, G.S., Sathishkumar, M., Swaminathan, K., 2006. Arsenic removal from groundwater by pretreated waste tea fungal biomass. Bioresource Technology 97, 483–487. https://doi.org/10.1016/j.biortech.2005.03.008

Naidu, R., Naidu, R., Smith, E., Owens, G., Bhattacharya, P., Nadebaum, P., 2006. Managing Arsenic in the Environment From Soil to Human Health Managing Arsenic in the Environment From Soil to Human Health. CSIRO Publishing, Australia.

Neppolian, B., Celik, E., Choi, H., 2008. Photochemical Oxidation of Arsenic(III) to Arsenic(V) using Peroxydisulfate Ions as an Oxidizing Agent. Environ. Sci. Technol. 42, 6179–6184. https://doi.org/10.1021/es800180f

Niazi, N.K., Bibi, I., Shahid, M., Ok, Y.S., Shaheen, S.M., Rinklebe, J., Wang, H., Murtaza, B., Islam, E., Farrakh Nawaz, M., Lüttge, A., 2018. Arsenic removal by Japanese oak wood biochar in aqueous solutions and well water: Investigating arsenic fate using integrated spectroscopic and microscopic techniques. Science of the Total Environment 621, 1642–1651. https://doi.org/10.1016/j.scitotenv.2017.10.063

Niazi, N.K., Burton, E.D., 2016. Arsenic sorption to nanoparticulate mackinawite (FeS): An examination of phosphate competition *. Environmental Pollution 218, 111–117. https://doi.org/10.1016/j.envpol.2016.08.031

Niazi, N.K., Singh, B., Minasny, B., 2015. Mid-infrared spectroscopy and partial least-squares regression to estimate soil arsenic at a highly variable arsenic-contaminated site. International Journal of Environmental Science and Technology 12, 1965–1974. https://doi.org/10.1007/s13762-014-0580-5

Nidheesh, P. V., Singh, T.S.A., 2017. Arsenic removal by electrocoagulation process: Recent trends and removal mechanism. Chemosphere 181, 418–432. https://doi.org/10.1016/j.chemosphere.2017.04.082

Önnby, L., Kumar, P.S., Sigfridsson, K.G.V., Wendt, O.F., Carlson, S., Kirsebom, H., 2014. Improved arsenic(III) adsorption by Al2O3 nanoparticles and H2O2: Evidence of oxidation to arsenic(V) from X-ray absorption spectroscopy. Chemosphere 113, 151–157. https://doi.org/10.1016/j.chemosphere.2014.04.097

Oremland, R.S., Stolz, J.F., 2003. The Ecology of Arsenic. Science 300, 939–944. https://doi.org/10.1126/science.1081903

Pendergast, M.M., Hoek, E.M. V, 2011. A review of water treatment membrane nanotechnologies. Energy Environ. Sci. 4, 1946–1971. https://doi.org/10.1039/C0EE00541J

Pires, V.G.R., Lima, D.R.S., Aquino, S.F., Libânio, M., Pires, V.G.R., Lima, D.R.S., Aquino, S.F., Libânio, M., 2015. EVALUATING ARSENIC AND MANGANESE REMOVAL FROM WATER BY CHLORINE OXIDATION FOLLOWED BY CLARIFICATION. Brazilian Journal of Chemical Engineering 32, 409–419. https://doi.org/10.1590/0104-6632.20150322s00003564

Praveen, A., Mehrotra, S., Singh, N., 2017. Rice planted along with accumulators in arsenic amended plots reduced arsenic uptake in grains and shoots. Chemosphere 184, 1327–1333. https://doi.org/10.1016/j.chemosphere.2017.06.107

Rehman, S. ur, Khan, A.R., Sahiner, M., Sengel, S.B., Aktas, N., Siddiq, M., Sahiner, N., 2017. Removal of arsenate and dichromate ions from different aqueous media by amine based p(TAEA-co-GDE) microgels. Journal of Environmental Management 197, 631–641. https://doi.org/10.1016/j.jenvman.2017.04.053

Safi, S.R., Gotoh, T., Iizawa, T., Nakai, S., 2019a. Development and regeneration of composite of cationic gel and iron hydroxide for adsorbing arsenic from ground water. Chemosphere 217, 808–815. https://doi.org/10.1016/j.chemosphere.2018.11.050

Safi, S.R., Gotoh, T., Iizawa, T., Nakai, S., 2019b. Removal of Arsenic Using a Cationic Polymer Gel Impregnated with Iron Hydroxide. Journal of Visualized Experiments e59728. https://doi.org/10.3791/59728

Saharan, P., Chaudhary, G.R., Mehta, S.K., Umar, A., 2014. Removal of Water Contaminants by Iron Oxide Nanomaterials. Journal of Nanoscience and Nanotechnology 14, 627–643. https://doi.org/10.1166/jnn.2014.9053

Sahiner, N., Demirci, S., Sahiner, M., Yilmaz, S., Al-Lohedan, H., 2015. The use of superporous p(3-acrylamidopropyl)trimethyl ammonium chloride cryogels for removal of toxic arsenate anions. Journal of Environmental Management 152, 66–74. https://doi.org/10.1016/j.jenvman.2015.01.023

Sahiner, N., Ozay, O., Aktas, N., Blake, D.A., John, V.T., 2011. Arsenic (V) removal with modifiable bulk and nano p(4-vinylpyridine)-based hydrogels: The effect of hydrogel sizes and quarternization agents. Desalination 279, 344–352. https://doi.org/10.1016/j.desal.2011.06.028

Santos, A., de Oliveira, F.W.F., Silva, F.H.A., Maria, D.A., Ardisson, J.D., Macêdo, W.A. de A., Palmieri, H.E.L., Franco, M.B., 2012. Synthesis and characterization of iron-PVA hydrogel microspheres and their use in the arsenic (V) removal from aqueous solution. Chemical Engineering Journal 210, 432–443. https://doi.org/10.1016/j.cej.2012.08.078

Sarkar, A., Paul, B., 2016. The global menace of arsenic and its conventional remediation-A critical review. Chemosphere 158, 37–49. https://doi.org/10.1016/j.chemosphere.2016.05.043

Sarkar, A.M., Rahman, A.K.M.L., Samad, A., Bhowmick, A.C., Islam, J.B., 2019. Surface and Ground Water Pollution in Bangladesh: A Review. 1 6, 47–69. https://doi.org/10.20448/journal.506.2019.61.47.69

Shaheen, S.M., Eissa, F.I., Ghanem, K.M., Gamal El-Din, H.M., Al Anany, F.S., 2013. Heavy metals removal from aqueous solutions and wastewaters by using various byproducts. Journal of Environmental Management 128, 514–521. https://doi.org/10.1016/j.jenvman.2013.05.061

Shakoor, M.B., Bibi, I., Niazi, N.K., Shahid, M., Nawaz, M.F., Farooqi, A., Naidu, R., Rahman, M.M., Murtaza, G., Lüttge, A., 2018. The evaluation of arsenic contamination potential, speciation and hydrogeochemical behaviour in aquifers of Punjab, Pakistan. Chemosphere 199, 737–746. https://doi.org/10.1016/j.chemosphere.2018.02.002

Shakoor, M.B., Niazi, N.K., Bibi, I., Murtaza, G., Kunhikrishnan, A., Seshadri, B., Shahid, M., Ali, S., Bolan, N.S., Ok, Y.S., Abid, M., Ali, F., 2016. Remediation of arsenic-contaminated water using agricultural wastes as biosorbents. Critical Reviews in Environmental Science and Technology 46, 467–499. https://doi.org/10.1080/10643389.2015.1109910

Sharma, V.K., Sohn, M., 2009. Aquatic arsenic: Toxicity, speciation, transformations, and remediation. Environment International 35, 743–759. https://doi.org/10.1016/j.envint.2009.01.005

Sheng, G., Li, Y., Yang, X., Ren, X., Yang, S., Hu, J., Wang, X., 2012. Efficient removal of arsenate by versatile magnetic graphene oxide composites. RSC Advances 2, 12400. https://doi.org/10.1039/c2ra21623j

Shubin, A., Kovalskii, V., Ruzankin, S., Zilberberg, I., Parmon, V., 2018. Water oxidation versus hydroxylation by the terminal oxo center of the Fe(III)-hydroxide: DFT predictions.

Siddiqui, S.I., Chaudhry, S.A., 2017. Iron oxide and its modified forms as an adsorbent for arsenic removal: A comprehensive recent advancement. Process Safety and Environmental Protection 111, 592–626. https://doi.org/10.1016/j.psep.2017.08.009

Smedley, P.L., Kinniburgh, D.G., 2002. A review of the source, behaviour and distribution of arsenic in natural waters. Applied Geochemistry 17, 517–568. https://doi.org/10.1016/S0883-2927(02)00018-5

Smith, K., Li, Zhenyu, Chen, B., Liang, H., Zhang, X., Xu, R., Li, Zhilin, Dai, H., Wei, C., Liu, S., 2017. Corrigendum to "Comparison of sand-based water filters for point-of-use arsenic removal in China" [Chemosphere 168 (2017) 155–162](S0045653516314047)(10.1016/j.chemosphere.2016.10.021). Chemosphere 173, 632. https://doi.org/10.1016/j.chemosphere.2017.01.051

Sorlini, S., Gialdini, F., 2010. Conventional oxidation treatments for the removal of arsenic with chlorine dioxide, hypochlorite, potassium permanganate and monochloramine. Water Research, Groundwater Arsenic: From Genesis to Sustainable Remediation 44, 5653–5659. https://doi.org/10.1016/j.watres.2010.06.032

Sorlini, S., Gialdini, F., Stefan, M., 2010. Arsenic oxidation by UV radiation combined with hydrogen peroxide. Water Science and Technology 61, 339–344. https://doi.org/10.2166/wst.2010.799

Sridharan, M., Nathan, D.S., 2018. Chemometric Tool to Study the Mechanism of Arsenic Contamination in Groundwater of Puducherry Region, South East Coast of India. Chemosphere. https://doi.org/10.1016/j.chemosphere.2018.05.083

Tang, L., Feng, H., Tang, J., Zeng, G., Deng, Y., Wang, J., Liu, Y., Zhou, Y., 2017. Treatment of arsenic in acid wastewater and river sediment by Fe@Fe2O3 nanobunches: The effect of environmental conditions and reaction mechanism. Water Research 117, 175–186. https://doi.org/10.1016/j.watres.2017.03.059

Tuna, A.Ö.A., özdemir, E., şimşek, E.B., Beker, U., 2013. Removal of As(V) from aqueous solution by activated carbon-based hybrid adsorbents: Impact of experimental conditions. Chemical Engineering Journal 223, 116–128. https://doi.org/10.1016/j.cej.2013.02.096

Verlicchi, P., Grillini, V., 2019. Surface and Groundwater Quality in South African Area—Analysis of the Most Critical Pollutants for Drinking Purposes. Proceedings 48, 3. https://doi.org/10.3390/ECWS-4-06430

Vithanage, M., Herath, I., Joseph, S., Bundschuh, J., Bolan, N., Ok, Y.S., Kirkham, M.B., Rinklebe, J., 2017. Interaction of arsenic with biochar in soil and water: A critical review. Carbon 113, 219–230. https://doi.org/10.1016/j.carbon.2016.11.032

Voegelin, A., Hug, S.J., 2003. Catalyzed Oxidation of Arsenic(III) by Hydrogen Peroxide on the Surface of Ferrihydrite: An in Situ ATR-FTIR Study. Environ. Sci. Technol. 37, 972–978. https://doi.org/10.1021/es025845k

Wang, W., Yang, L., Hou, S., Tan, J., Li, H., 2001. Prevention of endemic arsenism with selenium. Current Science 81, 1215–1218.

Wang, Z., Bush, R.T., Sullivan, L.A., Chen, C., Liu, J., 2014. Selective Oxidation of Arsenite by Peroxymonosulfate with High Utilization Efficiency of Oxidant. Environ. Sci. Technol. 48, 3978–3985. https://doi.org/10.1021/es405143u

Waste, T.O.C. of the 14th I.C. on T. and M., 2010. Tailings and Mine Waste 2010. CRC Press.

Wei, Y., Liu, H., Liu, C., Luo, S., Liu, Y., Yu, X., Ma, J., Yin, K., Feng, H., 2019. Fast and efficient removal of As(III) from water by CuFe2O4 with peroxymonosulfate: Effects of oxidation and adsorption. Water Research 150, 182–190. https://doi.org/10.1016/j.watres.2018.11.069

WHO, W.H.Organization., 2003. Arsenic in Drinking-water. Background document for preparation of WHO Guidelines for drinking-water quality. World Health Organization Geneva 1–18.

Yang, L., Li, X., Chu, Z., Ren, Y., Zhang, J., 2014. Distribution and genetic diversity of the microorganisms in the biofilter for the simultaneous removal of arsenic, iron and manganese from simulated groundwater. Bioresource Technology 156, 384–388. https://doi.org/10.1016/j.biortech.2014.01.067

Zhu, N., Yan, T., Qiao, J., Cao, H., 2016. Adsorption of arsenic, phosphorus and chromium by bismuth impregnated biochar: Adsorption mechanism and depleted adsorbent utilization. Chemosphere 164, 32–40. https://doi.org/10.1016/j.chemosphere.2016.08.036

Chapter 2: Generation and Replication of a Cationic Gel and Iron Hydroxide Composite for As (V) Adsorption from Ground Water

2.1. Introduction

Arsenic-contaminated groundwater is a significant health problem across the world. Various techniques for removing arsenic have been explored in previous investigations. However, the majority of them are unable to selectively remove and regenerate arsenic. To improve this situation, researchers need to establish arsenic removal processes that are highly effective in terms of the removal efficiency, selectivity and cost-benefits. Adsorption procedures are the most promising options among them because of their great efficiency, simplicity of operation, and low cost (Bibi et al., 2016; He et al., 2018; Niazi et al., 2018; Shaheen et al., 2013; Shakoor et al., 2016; Vithanage et al., 2017). Nevertheless, the adsorbents may saturate early in the process and require a synthetic precursor for production. Furthermore, the adsorbents have a long-term negative impact on water quality (Siddiqui and Chaudhry, 2017). After the adsorption process, sedimentation or filtering is required to separate the iron oxyhydroxides particles, which adds to the cost and reduces mechanical resistance (Hu et al., 2015; Tuna et al., 2013). Lastly, the majority of the adsorbents have drawbacks, such as limited adsorption capacity and reusability, low stability, high operating and maintenance costs, and the usage of toxic chemicals in some adsorbents' production (Niazi et al., 2018).

To improve the amount of arsenic adsorption, I developed an adsorbent, which is a cationic gel composite of *N,N*-dimethylamino propylacrylamide, methyl chloride quaternary

(DMAPAAQ) and Iron(III) Hydroxide (FeOOH) particles. FeOOH is reported to increase the adsorption performance of the adsorbent for both forms of arsenic (Lin et al., 2018).

In this chapter, I created an adsorbent, a cationic polymer gel loaded with iron hydroxide, that is more efficient than previous adsorbents at removing arsenic from groundwater. The cationic polymer gel is made up of *N,N*-dimethylamino propylacrylamide and quaternary methyl chloride (DMAPAAQ). My gel composite is non-porous and also, FeOOH was impregnated during the preparation of the gel composite and is explored further in the next chapter. For both types of arsenic, FeOOH is said to improve the adsorption efficiency of the adsorbent (Lin et al., 2018).

The purpose of the unique preparation of the gel differently than the previous polymer gels used for arsenic and other metals adsorption was to assure that the gel contains maximum FeOOH particles in it's structure. Also, it should also have good selectivity, be simple to use. At neutral pH levels, the gel should efficiently absorbed arsenic. In addition, the gel should be reusable for several cycles in a row with efficiency. This chapter also discusses the adsorption process of this gel composite as well as the time necessary to attain equilibrium adsorption.

2.2. Experimental

2.2.1 Materials

The monomer, *N,N'*-dimethylamino propylacrylamide, methyl chloride quaternary (DMAPAAQ) (75% in H_2O) was supplied by KJ Chemicals Corporation, Japan. The crosslinker, *N,N'*-Methylene bisacrylamide (MBAA) and the arsenic (III) source, arsenic(III) oxide was purchased from Sigma-Aldrich, USA. The accelerator sodium sulfite (Na_2SO_3), the arsenic(V) source, di-sodium hydrogenarsenate heptahydrate ($Na_2HAsO_4.7H_20$) and ferric chloride ($FeCl_3$) was purchased from Nacalai Tesque, Inc., Japan. Sodium hydroxide (NaOH) was purchased from Kishida Chemicals Corporation, Japan. *N,N'*- dimethyl acrylamide (DMAA) and the initiator, ammonium peroxodisulfate (APS) was purchased from Kanto Chemical Co. Inc., Japan.

2.2.2 Preparation of the gel composite

N,N-dimethylamino propylacrylamide, methyl chloride quaternary (DMAPAAQ) was used as a monomer, *N,N'*-Methylene bisacrylamide (MBAA) as a crosslinker, sodium sulfite as an accelerator, and ammonium peroxodisulfate (APS) as an initiator to make the Cationic gel composite. The monomer and crosslinker are included in the "monomer solution." The initiator and $FeCl_3$ make up the "initiator solution." In addition, sodium hydroxide and ferric chloride were added to the monomer and initiator solutions, respectively, to allow the following reaction to occur during the formation of the gel, which is a unique feature of the gel composite preparation technique.

$$FeCl_3+3NaOH \rightarrow Fe(OH)_3+3NaCl.$$

This process entailed the polymerization of monomers in order to create a hydrogel iron hydroxide composite and to increase the amount of FeOOH in the gel.

The detailed composition of the gel is shown in **Table 2.1**. The solutions were produced by N_2 for 10 minutes before being mixed with the monomer and initiator solutions. After then, the two answers were combined. The reaction lasted 4 hours at 10 degrees Celsius. After the hydrogel iron hydroxide composite has been produced, it is sliced into 5mm long cubic forms. The gels were then rinsed for 24 hours in distilled water to eliminate any unreacted compounds. Finally, they were dried in a 50°C oven for 24 hours. For comparison, a non-ionic gel composite was made utilizing monomer, *N,N′*-dimethyl acrylamide (DMAA), and FeOOH to assess the arsenic adsorption property using the procedure described above.

Table 2.1. Composition of gel composite.

	Chemical	**Quantity (mol/m^3)**
Monomer	DMAPAAQ, DMAA	500
Crosslinker	MBAA	50
Accelerator	Sodium Sulfite	80
	Sodium Hydroxide (NaOH)	2100
Initiator	Ammonium peroxodisulfate (APS)	30
	Ferric Chloride ($FeCl_3$)	700

2.2.3 Measurement of arsenic adsorption properties by the gel composite

To perform the arsenic adsorption experiment, 20 mg of dried gel composite (DMAPAAQ+FeOOH, DMAA+FeOOH and DMAPAAQ) was added in 40 mL of $Na_2HAsO_4.7H_2O$ solution in a small beaker and was kept in the stirrer at 120 rpm rotation, at 20°C for 24 hours. Following this, 5 ml sample was collected using a syringe. The remaining amount of arsenic present in the solution was measured by High Profile Liquid Chromatography (HPLC) Dionex 1100 ICX by Thermo Fisher Scientific Inc., MA, USA. The amount of adsorption of arsenic was measured by the following equation:

$$Q = \frac{(C_0 - C)V}{m}$$

Where, Q : Amount of adsorption [mol/g], C_0 : Initial concentration [mol/L], C : Equilibrium concentration [mol/L], V : Quantity of solution [L], m : Mass of the Adsorbent [g].

Water used in all experiments was prepared in a water purification system. The pH values of the solutions were measured using pH/ORP meter D-72, (Horiba Scientific, Japan).

2.2.4 pH sensitivity of DMAPAAQ+FeOOH gel composite

To perform the pH sensitivity experiment, 20 mg of dried DMAPAAQ+FeOOH gel composite was added in 40 mL of $Na_2HAsO_4.7H_2O$ solution. Additionally, HCL and NaOH were added to the solution to obtain different pH values (2.04, 6.82, 7.86, 9.92, 11.77, 12.86).

The solution was then placed in a small beaker and was kept in the stirrer at 120 rpm rotation, at 20°C for 24 hours. Following this, 5 ml sample was collected using a syringe. The remaining amount of arsenic present in the solution was measured by High Profile Liquid Chromatography (HPLC) Dionex 1100 ICX by Thermo Fisher Scientific Inc., MA, USA.

2.2.5 Arsenic adsorption kinetic experiment

As(V) adsorption kinetics were carried out on the selected adsorbents (DMAPAAQ, DMAPAAQ+FeOOH, DMAA+FeOOH gel composites) using the same conditions and procedures as described above. Briefly, 20 mg of each adsorbent was added to 40 mL of 0.2mmol/L As(V) solution on a stirrer at 120 rpm rotation at 20°C. At each sampling time (0.5, 1, 3, 5, 7, 11, 24, and 48 hours), 5 mL samples were collected using a syringe and the remaining amount of arsenic in the solution was analyzed using HPLC for measuring As(V) concentration.

2.2.6 Regeneration of DMAPAAQ+FeOOH gel composite for arsenic adsorption

To test the regeneration of the DMAPAAQ+FeOOH gel composite, the adsorption-desorption experiment was conducted repeatedly for eight days. The adsorption experiment was conducted using 0.2 mmol arsenic solution. The details of the adsorption operation are the same which were described in the section “Measurement of arsenic adsorption properties by the gel composite”. After the adsorption experiment, samples were collected for measuring the remaining arsenic in the water. The gels were separated and washed with

deionized water five times so as to remove external arsenic from the gel surface. Following this, the gel was added to 0.5 M 40 mL NaCl solution to perform the desorption experiment under the same conditions as the adsorption experiment. Samples were collected in the same way as previously mentioned to measure desorbed arsenic in the NaCl solution. This adsorption-desorption cycle was performed for eight days.

2.2.7 Selectivity of arsenic adsorption

To evaluate the selective adsorption of arsenic by the gel composites, the adsorption experiment was conducted using 20mg dried adsorbent. The adsorbent was added to a 40 mL solution of 0.2 mM arsenic and different concentrations of Na_2SO_4. The solution was then magnetically stirred for 24 hours at 20°C and 120 rpm. The samples were collected using a syringe and the remaining amount of arsenic was measured using HPLC. Following the same procedure to measure the adsorption of Sulphate (SO_4^{2-}), the remaining amount of SO_4^{2-} was also measured using HPLC.

2.3. Results And Discussion

2.3.1 pH sensitivity of DMAPAAQ+FeOOH gel composite

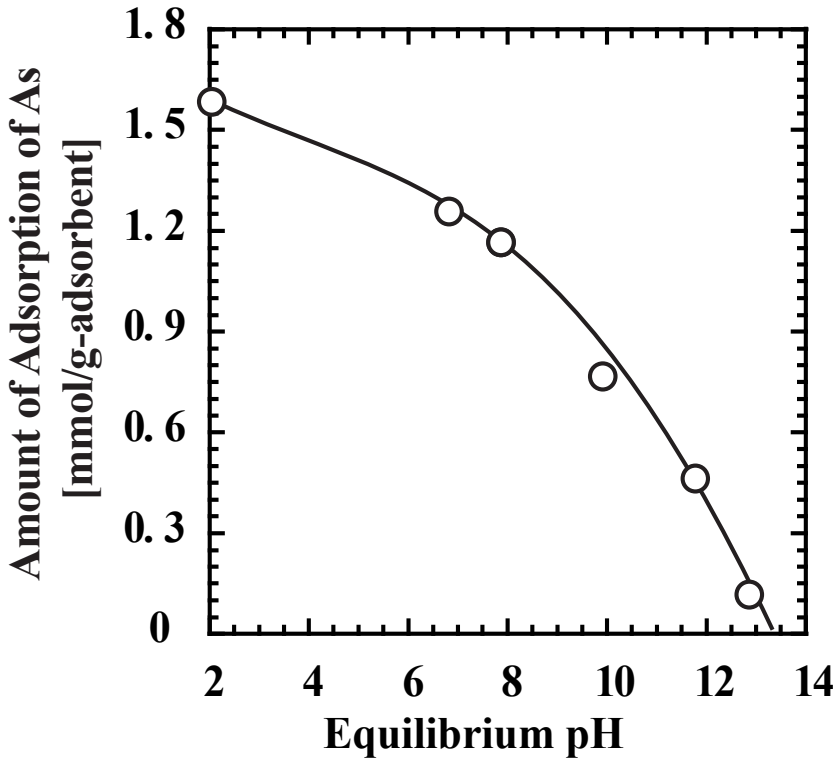

Figure 2.1. pH Sensitivity of DMAPAAQ+FeOOH gel composite.

The DMAPAAQ+FeOOH gel composite's pH sensitivity was investigated. The arsenic solution used in the experiment was 2mmol/L. To determine arsenic adsorption levels at different pH values, different concentrations of HCL and NaOH were added to the arsenic solution. The quantity of adsorption is larger at low pH values, but decreased at high pH levels, as seen in **Fig. 2.1**. The maximum quantity of arsenic adsorption was seen at pH 2.04, according to the findings. The quantity of arsenic adsorption reduced as the pH values steadily rose. The change in As(V) adsorption was detected when the pH was changed.

Because pH affects the surface charge of adsorbents, it can influence the adsorption of charged ions, as As (V) is a charged species (Martinson and Reddy, 2009). The gel structure became less adsorption-friendly as the pH increased. When the pH level rose, arsenic ions formed compounds with hydroxyl ions. The FeOOH particles in the gel were not able to connect with the arsenic complex ions because they were already strongly charged with hydroxyl ions. As a result, at higher pH levels, adsorption did not occur. However, under real-world settings, when the pH of the water is neutral (about 7), DMAPAAQ+FeOOH has a high adsorption capacity. It's a noteworthy result since, as previously stated in the "introduction" section, most polymer gels and other adsorbents fail to efficiently adsorb As(V) at neutral pH. As a result, the remaining studies were carried out with neutral pH values, taking into account the real-world circumstances of arsenic-affected water.

2.3.2 Adsorption Reaction Kinetics

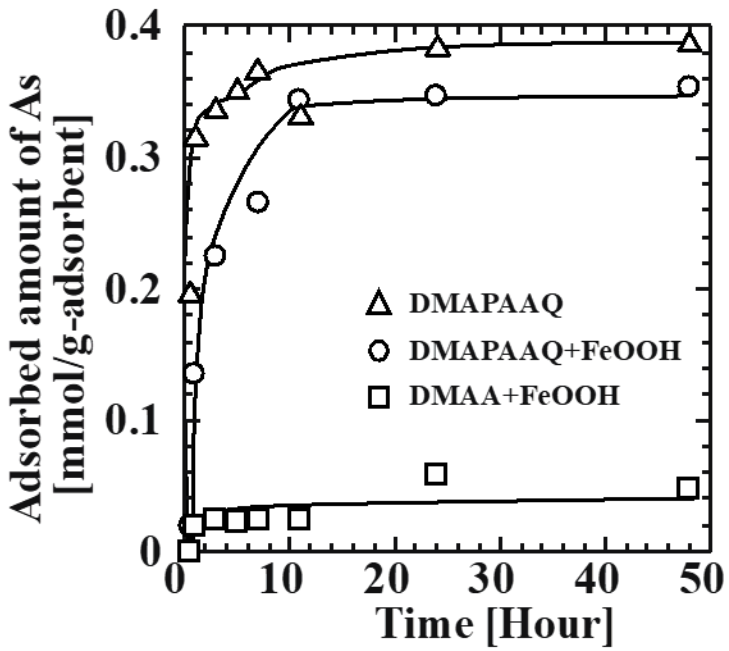

Figure 2.2. Arsenic adsorption kinetics of DMAPAAQ, DMAPAAQ+FeOOH and DMAA+FeOOH gels.

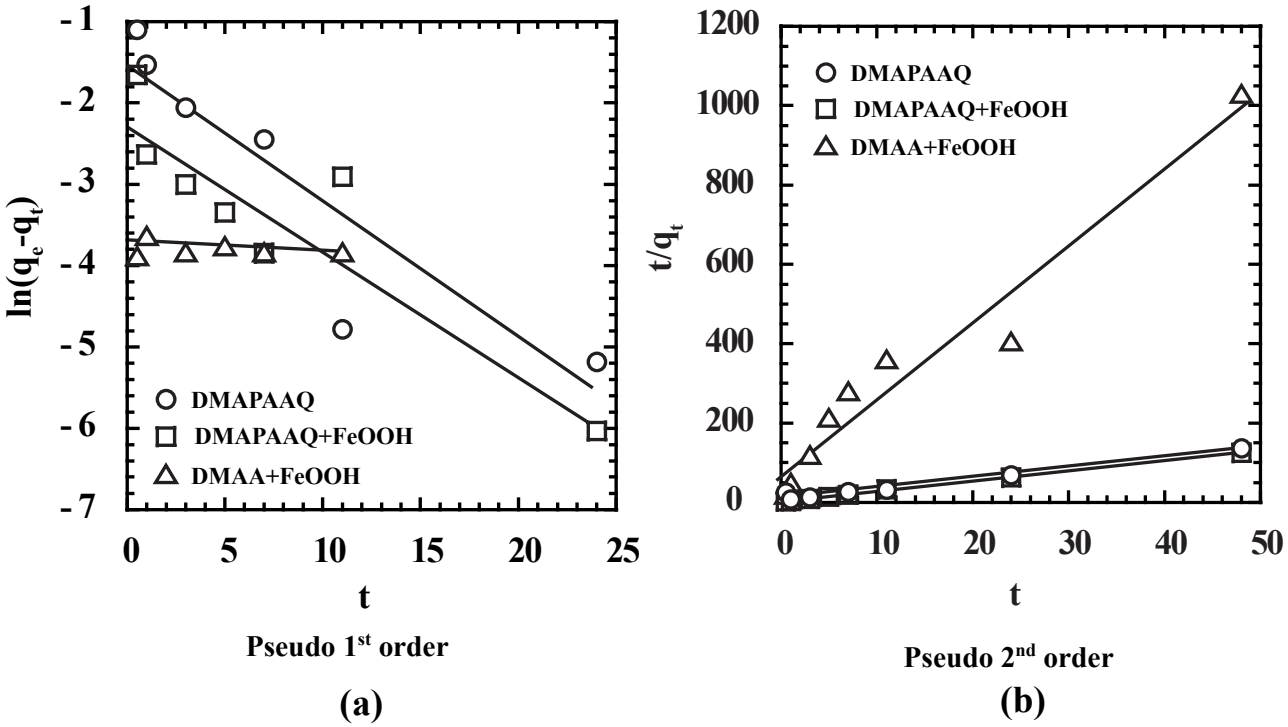

Figure 2.3. (a) Pseudo first order kinetic model and **(b)** Pseudo second order kinetic model for adsorption of arsenic.

DMAPAAQ gel, DMAPAAQ+FeOOH gel composite, and DMAA+FeOOH gel composite adsorption reaction kinetics were investigated, and the time necessary to achieve equilibrium is presented in **Fig. 2.2**. The DMAA+FeOOH gel composite had the quickest equilibrium adsorption time, barely 1 hour. The adsorption equilibrium was reached in 10 hours for the DMAPAAQ+FeOOH gel composite and 24 hours for the DMAPAAQ gel. Two kinetic models, pseudo 1st order and pseudo 2nd order, were used to examine the rate of adsorption of the three gels. The similarity between the experimental and the calculated values were denoted by the correlation coefficients (R^2) as shown in **Table 2.2**. The higher R^2 value defines the respective kinetic model. The pseudo 1st order and 2nd order kinetic

models are shown in **Fig. 2.3 (a)** and **Fig. 2.3 (b)** respectively. In the figure, the value of R^2 is higher for all three gels for pseudo 2nd order kinetics and also, their adsorption matched well with the 2nd order kinetics. As a result, the chemisorption between DMAPAAQ+FeOOH gel composite and arsenic solution was the rate limiting step of the adsorption process (Allen et al., 2005).

Table 2.2. Parameters of pseudo 1st and pseudo 2nd order for adsorption of arsenic.

Gel Composite	$q_{e,exp}$	**Pseudo 1st order**			**Pseudo 2nd order**		
	[mmol/g]	$q_{e,cal}$ **[mmol/g]**	K_1 **[h^{-1}]**	R^2	$q_{e,cal}$ **[mmol/g]**	K_2 **[h^{-1}]**	R^2
DMAPAAQ	0.3526	0.205	0.171	0.764	0.389	0.693	0.974
DMAPAAQ+FeOOH	0.3856	0.107	0.1571	0.866	0.387	4.04	0.999
DMAA+FeOOH	0.0466	0.023	0.0074	0.079	0.051	5.568	0.95

2.3.3 Amount of arsenic adsorption

Fig. 2.4 shows the arsenic adsorption isotherms for DMAPAAQ, DMAPAAQ+FeOOH, and DMAA+FeOOH, as well as a comparison of the quantity of arsenic adsorption. Furthermore, the experimental result is compared to the predicted value using Langmuir's adsorption isotherm equation. The maximal capacity of arsenic adsorption, Q_{max}, was also determined using the Langmuir adsorption isotherm. When the data is compared to the experimental values, the DMAPAAQ+FeOOH, DMAA+FeOOH, and

DMAPAAQ gels all match well. As a result of the ionic interaction with the amino group (DMAPAAQ) and adsorption with iron hydroxide (DMAPAAQ+FeOOH), arsenic adsorption is chemisorption (**Fig. 2.3 (b)**). The maximum adsorption capacity, or Q_{max}, is an essential metric in determining the adsorbents' usefulness. As a result, at neutral pH values, the Q_{max} values of As (V) adsorption by various adsorbents were compared and reported in **Table 2.3**. 2.09 mmol/g, 1.63 mmol/g, and 1.22 mmol/g, respectively, are the Q_{max} values of DMAPAAQ, DMAPAAQ+FeOOH, and DMAA+FeOOH. DMAPAAQ gel adsorbs arsenic better than non-cationic gel composite DMAA+FeOOH and DMAPAAQ+FeOOH gel composite. Because the amino group of the DMAPAAQ gel binds to the arsenic ion and releases chloride ions in the case of the DMAPAAQ gel. However, arsenic ions are shared by the amino group and the FeOOH particles in the DMAPAAQ+ FeOOH. As a result, the amount of adsorption in the gel and the gel composite vary. However, because the DMAA gel is non-ionic and lacks charges, it cannot form binding with the arsenic ions, DMAA+FeOOH had a lower amount of arsenic adsorption.

When DMAPAAQ+FeOOH was compared to the highest As(V) adsorption capacity of other adsorbents created by the researchers at neutral pH, I discovered that DMAPAAQ+FeOOH has a stronger ability to adsorb As(V) than the other previously researched adsorbents because it provides favorable adsorption sites to the arsenic ion (details in the following section). Even though DMAPAAQ has a higher Q_{max} value, the DMAPAAQ+FeOOH gel composite is the most appropriate adsorbent because it can adsorb high levels of arsenic in affected water at natural pH levels and because it can adsorb high levels of arsenic in affected water at low pH levels. Despite the fact that DMAPAAQ has a

higher Q_{max} value, the DMAPAAQ+FeOOH gel composite is the best adsorbent because it can adsorb high levels of arsenic in affected water at natural water conditions, has good selectivity in the presence of other ions, and has regeneration properties, which will be discussed in the following sections.

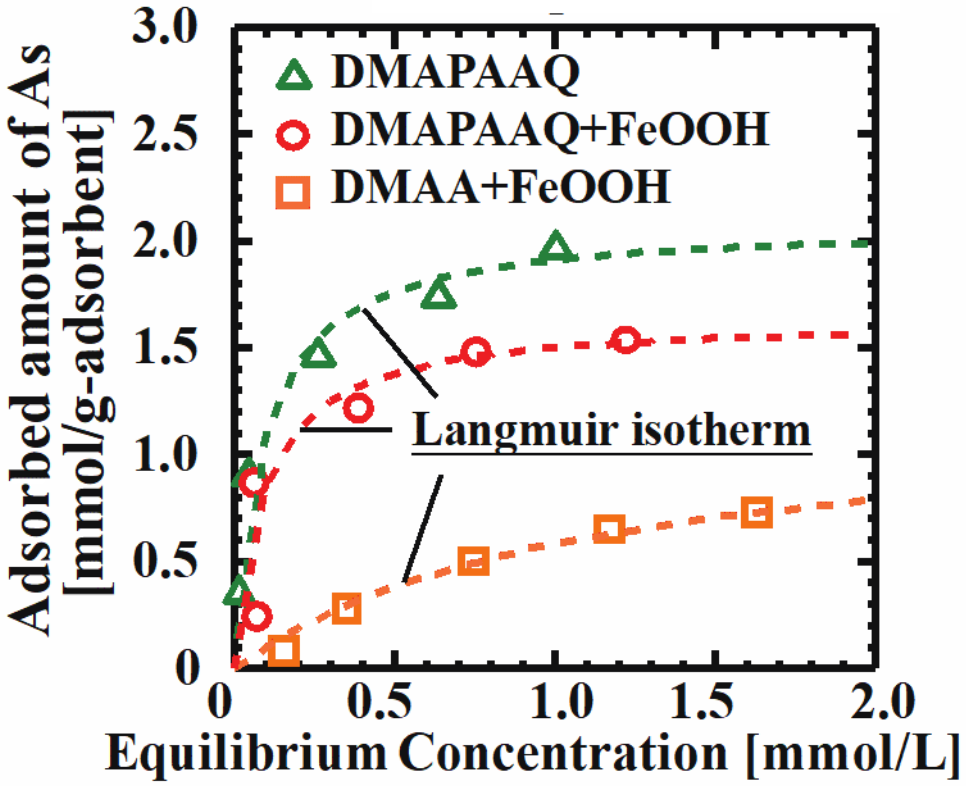

Figure 2.4. Arsenic adsorption isotherm of DMAPAAQ, DMAPAAQ+FeOOH and DMAA+FeOOH.

Table 2.3. Maximum adsorption of arsenic by Langmuir adsorption isotherm equation.

Adsorbent	**Q_{max} [mmol/g] ([mg/g])**	**R^2**	**Reference**
DMAPAAQ+FeOOH	1.63(123.4)	0.997	This work
DMAPAAQ	2.09(156.4)	0.996	This work
DMAA+FeOOH	1.22(91.3)	0.990	This work
Iron Hydroxide	0.74(56.8)		(Yanagita et al., 2013)
Magnetite (Fe_3O_4)	1.02(76)		(Yean et al., 2005)
Magnetite-GO	0.51(38)		(Yoon et al., 2009)
GNP/Fe-Mg Oxide	1.39(103.9)		(La et al., 2017)
Coconut Coir Pith	0.18(13.57)		(Anirudhan and Unnithan, 2007)
Tea Fungal Biomass	0.004(0.31)		(Murugesan et al., 2006)
Chitosan Red Scoria	0.009(0.72)		(Asere et al., 2017)
Chitosan Pumice Blends	0.009(0.71)		(Asere et al., 2017)
amid-IDPN-p(VBC)	1.17(88)		(Ajmal et al., 2016)
p(4-VP)-2-BEA-HCL	0.31(23.26)		(Sahiner et al., 2011)
P(4-VP)-HCL	0.30(22.6)		(Sahiner et al., 2011)
High iron-containing fly ash	0.26(19.46)		(Li et al., 2009)

p(AN-co-APTMACl)	0.12(8.88)	(Dudu et al., 2015)
Amid-p(AN-co-APTMACl)	0.29(21.83)	(Dudu et al., 2015)
P(APTMACl)	0.29(22.39)	(Dudu et al., 2015)

2.3.4 Arsenic adsorption mechanism of DMAPAAQ+FeOOH gel composite

Relating to the quantity of arsenic adsorption, it was discovered that the DMAPAAQ+FeOOH composite's adsorption was chemisorption. Cl^- counters ion with the amino group of DMAPAAQ when DMAPAAQ gel is introduced to the arsenic solution. The Cl^- is subsequently released into the solution, and the arsenic is adsorbed by the DMAPAAQ gel's amino group (**Fig. 2.5 (a)**). In the instance of DMAPAAQ+FeOOH, FeOOH absorbed arsenic in addition to Cl^- (**Fig. 2.5 (b)**). As a consequence, the amount of Cl^- released into solution is lower than when DMAPAAQ is used.

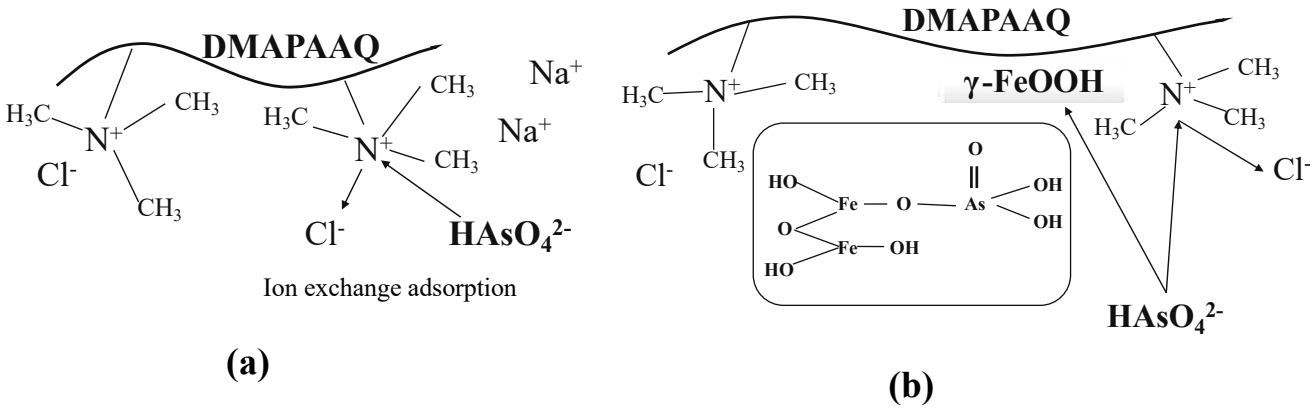

Figure 2.5. Mechanism of arsenic adsorption in (a) DMAPAAQ gel and **(b)** DMAPAAQ+FeOOH gel composite.

I computed the ratio of arsenic adsorbed by the amino group of DMAPAAQ and FeOOH particles in the DMAPAAQ+FeOOH gel to better understand the arsenic adsorption

process by DMAPAAQ and DMAPAAQ+FeOOH gel composite as shown in **Fig. 2.5 (a)** and **2.5 (b)**. The maximum quantity of arsenic adsorption by DMAPAAQ+FeOOH and DMAPAAQ is 1.63 mmol/g and 2.09 mmol/g, respectively, as mentioned in the preceding section "Arsenic adsorption isotherm." The amino group of DMAPAAQ and FeOOH particles absorbed the most arsenic, 0.58 mmol/g and 1.05 mmol/g, respectively.

According to the computations, FeOOH particles adsorb 64.4 percent of arsenic, while the amino group of DMAPAAQ adsorbs 35.6 percent. Using the Langmuir adsorption isotherm, I determined that the maximum amount of Cl^- desorption by DMAPAAQ+FeOOH and DMAPAAQ was 0.78 mmol/g and 2.83 mmol/g, respectively. The product of the maximum amount of desorption of Cl^- (0.78 mmol/g) and the ratio of the maximum amount of adsorption of arsenic (2.09 mmol/g) and the maximum amount of desorption of Cl^- (2.83 mmol/g) by DMAPAAQ gel was used to calculate the maximum amount of arsenic adsorption by the amino group of DMAPAAQ in DMAPAAQ+FeOOH gel. Furthermore, I also found the connection between the quantity of arsenic adsorption and the amount of Cl^- desorption. The average valence of arsenic in DMAPAAQ gel was -1.35, according to the aforementioned information. Because arsenic may vary its valence up to -3, it's assumed that the -1 and -2 valences were combined at neutral pH levels in this experiment. As a result, the exact mechanism of arsenic adsorption and desorption, as well as the connection between the two, are described in this section. This discovery is significant since the processes of the previously described adsorbents and techniques are not addressed in such depth stoichiometrically.

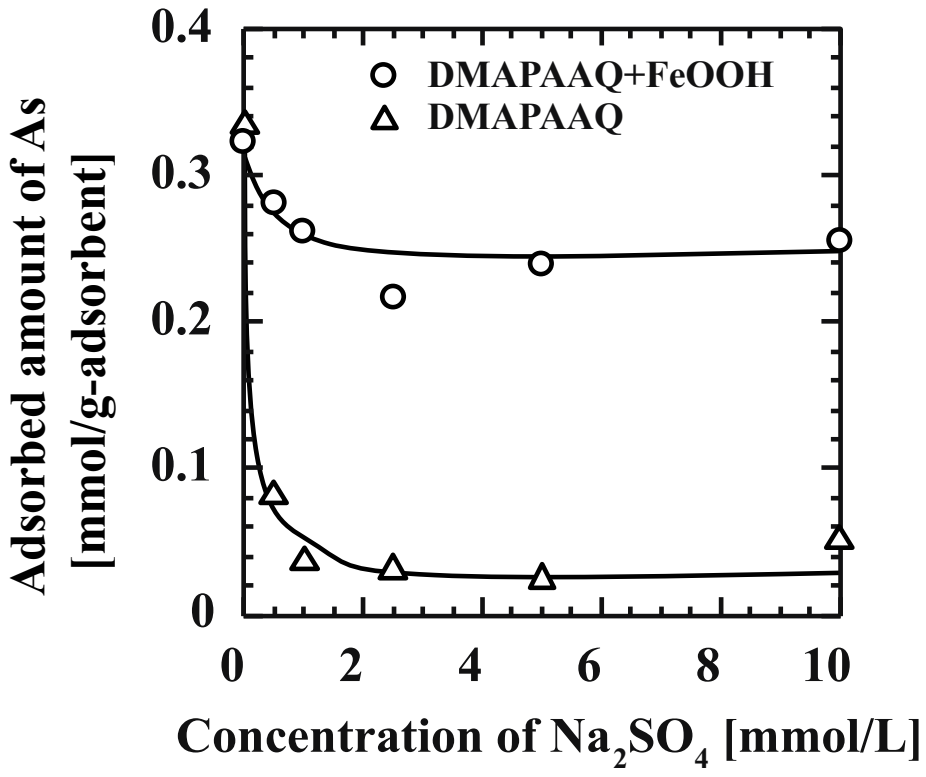

Figure 2.6. Selectivity of arsenic adsorption in the presence of Sulphate ion.

2.3.5 Selectivity of Arsenic Adsorption

In the presence of Sulphate ion, the selectivity of Arsenic adsorption was investigated. In addition to arsenic, groundwater includes ions such as CO_3^{2-}, HCO_3^{-}, H_2CO_3, Cl^{-}, SO_4^{2-}, SO_3^{2-}, HS^{-} (Chaplin et al., 2006). The ratio of oscillator strengths from the methyl symmetric stretch and the methylene symmetric stretch of Sulphate ion (SO_4^{2-}) was greatest, according to the Hofmeister series. As a result, the sulphate ion (SO_4^{2-}) has the potential to infiltrate the monolayer's headgroup area and disturb the hydrocarbon packing (Zhang and Cremer, 2006). Sulphate concentrations in groundwater can reach 230 mg/L (Fawell et al., 2004). As a result,

I chose the $SO4^{2-}$ ion to test the selectivity of arsenic adsorption by my gel composite, because if DMAPAAQ + FeOOH can effectively adsorb As(V) from a solution containing a mixture of As(V) and Na_2SO_4, then the presence of other ions will not affect the adsorbent's ability to adsorb arsenic. This experiment is significant because water in real life contains not just As(V), but also a variety of other ions.

Figure 2.6 depicts the impact of SO_4^{2-} concentration on arsenic adsorption by DMAPAAQ and DMAPAAQ+FeOOH. According to my findings, the quantity of As adsorption by DMAPAAQ and DMAPAAQ+FeOOH at 10 mmol/L SO_4^{2-} is 0.05 mmol/g and 0.26 mmol/g, respectively. In a solution of Na_2SO_4 and $Na_2HAsO_4.7H_20$, I discovered that the selectivity of arsenic adsorption of DMAPAAQ+FeOOH is about twenty-five times greater than that of DMAPAAQ. As a consequence, even when a high concentration of Sulphate is present, the DMAPAAQ+FeOOH gel composite may adsorb large quantities of arsenic. As a result, DMAPAAQ+FeOOH has a higher selectivity for arsenic adsorption than DMAPAAQ. Arsenic is absorbed by the gel in the case of DMAPAAQ due to an ionic contact with the amino group. As a consequence, even when a high concentration of Sulphate is present, the DMAPAAQ+FeOOH gel composite may adsorb large quantities of arsenic. As a result, DMAPAAQ+FeOOH has a higher selectivity for arsenic adsorption than DMAPAAQ. Arsenic is absorbed by the gel in the case of DMAPAAQ due to an ionic contact with the amino group. When the initial sulfate ion concentration is raised, the sulfate ion functions as an anion, inhibiting arsenic adsorption and resulting in a reduction in arsenic adsorption. However, when employing DMAPAAQ+FeOOH, the quantity of arsenic adsorption decreased somewhat at initially, but then stayed almost constant. This is due to

the iron hydroxide's ability to preferentially bind arsenic through complicated adsorption. As a result, DMAPAAQ+FeOOH gel composite is a superior adsorbent than DMAPAAQ gel at selectively adsorbing As(V) from water.

The quantity of sulfate adsorption by DMAPAAQ and DMAPAAQ+FeOOH gel composite was also evaluated in order to fully clarify the process of selective adsorption. The quantity of sulfate adsorption by DMAPAAQ gel (1.12 mmol/g) is larger than that of DMAPAAQ+FeOOH gel composite (0.35 mmol/g), as shown in the figure. DMAPAAQ+FeOOH adsorbs significant levels of arsenic and low amounts of sulphate due to the presence of FeOOH particles in the gel composite. This result also demonstrates that the DMAPAAQ+FeOOH gel composite may selectively adsorb arsenic.

2.3.6 Regeneration of DMAPAAQ+FeOOH gel composite

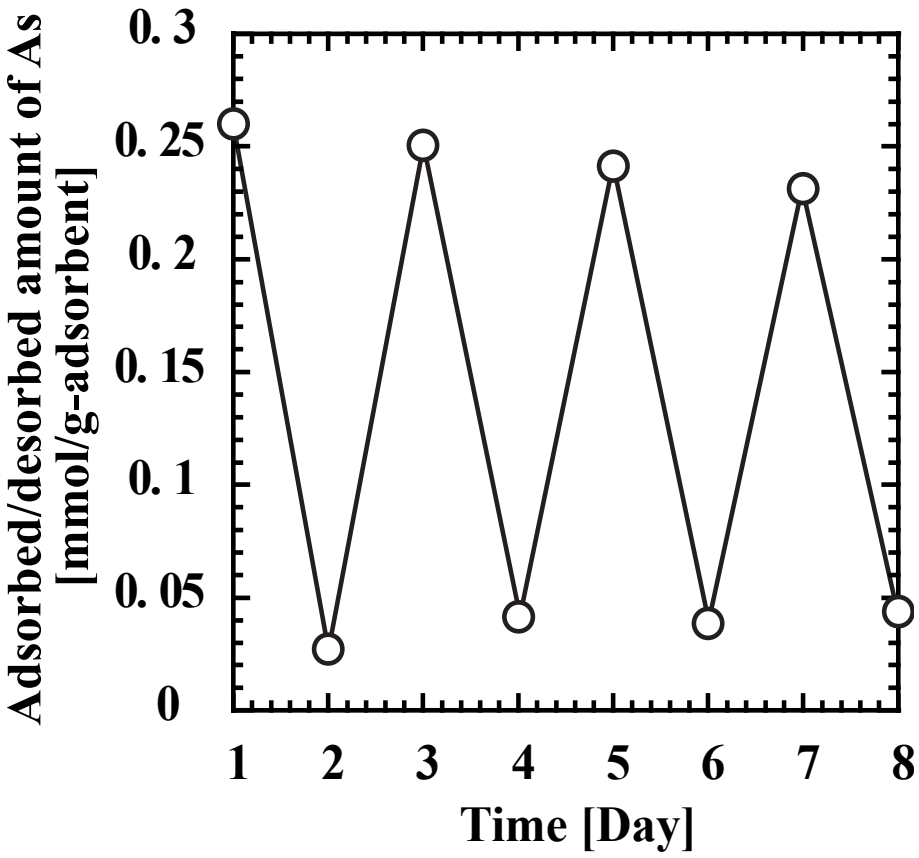

Figure 2.7. Regeneration of DMAPAAQ+FeOOH gel composite.

Recycling is an essential feature of an adsorbent since it helps to decrease costs, enhance usability, make the adsorbent environmentally friendly, and make it easier to handle (Rehman et al., 2016). As a result, industrial adsorbent production is conceivable. **Fig. 2.7** shows the regeneration of DMAPAAQ + FeOOH gel composite. Arsenic adsorption is performed in 0.2 mmol/L $Na_2HAsO_4.7H_2O$ solution and arsenic desorption is performed in 0.5 mol/L NaCl solution. The adsorption-desorption cycle was repeated for eight days in a row. The quantity of arsenic adsorption by the DMAPAAQ + FeOOH gel composite on day

1 and day 7 were used to calculate the effectiveness of the regeneration process. I discovered that the regeneration process is 87.6 percent efficient. The loss of adsorption sites is to blame for the decreased effectiveness of the regeneration process. During the desorption process, certain amino groups of DMAPAAQ, as well as the FeOOH in the DMAPAAQ+FeOOH gel composite, were unable to efficiently desorb the adsorbed arsenic ions in the NaCl solution. When As(V) was adsorbing on biochar, a similar pattern was found (He et al., 2018).

Although NaOH is the most commonly used desorption solvent, I tested the desorption process with NaCl instead of NaOH due to its toxicity. When the adsorption-desorption research was conducted for eight days, the gel composite was effectively regenerated, as illustrated in **Fig. 2.7**.

2.4. Conclusions

To increase the amount of FeOOH in the gel composite, I used an unusual preparation technique to create a composite of cationic gel and FeOOH in this study. The pH sensitivity of the gel composite was investigated, and it was discovered that the gel can adsorb a large quantity of As(V) at neutral pH levels. According to the adsorption reaction kinetics, the gel may achieve equilibrium adsorption in 24 hours. The pseudo 2^{nd} order kinetic model matches the reaction rate of adsorption by the DMAPAAQ+FeOOH gel composite.

The DMAPAAQ+FeOOH arsenic adsorption isotherm resembles the Langmuir isotherm very well. At neutral pH levels, the maximum adsorption capacity of the DMAPAAQ+FeOOH gel composite (1.63mmol/g) was computed and compared to the other previously investigated adsorbents, and my gel composite demonstrated superior arsenic adsorption capacity than the other adsorbents.

The DMAPAAQ+FeOOH gel composite's adsorption mechanism was also investigated and described. Both the amino group of DMAPAAQ and FeOOH particles inside the DMAPAAQ+FeOOH gel composite absorb As(V), with their respective arsenic adsorption ratios of 35.6 percent and 64.4 percent. In addition, the results indicated that in the presence of Sulphate ion, the DMAPAAQ+FeOOH gel composite preferentially adsorbs arsenic. As a result, even if other ions are present, the gel composite may preferentially adsorb As(V) from groundwater. Arsenic selectivity is provided by the FeOOH in the DMAPAAQ+FeOOH gel composite.

Furthermore, because the gel composite can be renewed, it is both cost-effective and environmentally beneficial. The regeneration experiment was carried out for eight days in a row with an efficiency of 87.6 percent. I investigated the regeneration process in a different way, using NaCl instead of the potentially hazardous NaOH for As desorption (V). Finally, unlike other techniques now in use, DMAPAAQ+FeOOH does not require any extra separation steps, resulting in easy gel handling and a straightforward adsorption procedure.

In the next chapter, FTIR was used to determine the change in the surface functional groups and energy level of the DMAPAAQ+FeOOH gel composite. All of the discussions in this chapter demonstrate that my gel composite, DMAPAAQ+FeOOH, may solve the problem of arsenic pollution in groundwater not only because of its high adsorption capacity, but also because of its excellent selectivity, regeneration, and process simplification.

References

Ajmal, M., Demirci, S., Uzun, Y., Siddiq, M., Aktas, N., Sahiner, N., 2016. Introduction of double amidoxime group by double post surface modification on poly (vinylbenzyl chloride) beads for higher amounts of organic dyes , As (V) and Cr (VI) removal. JOURNAL OF COLLOID AND INTERFACE SCIENCE 470, 39–46. https://doi.org/10.1016/j.jcis.2016.02.040

Allen, S.J., Gan, Q., Matthews, R., Johnson, P.A., 2005. Kinetic modeling of the adsorption of basic dyes by kudzu 286, 101–109. https://doi.org/10.1016/j.jcis.2004.12.043

Anirudhan, T.S., Unnithan, M.R., 2007. Arsenic(V) removal from aqueous solutions using an anion exchanger derived from coconut coir pith and its recovery. Chemosphere 66, 60–66. https://doi.org/10.1016/j.chemosphere.2006.05.031

Asere, T.G., Mincke, S., De Clercq, J., Verbeken, K., Tessema, D.A., Fufa, F., Stevens, C. V, Du Laing, G., 2017. Removal of Arsenic (V) from Aqueous Solutions Using Chitosan–Red Scoria and Chitosan–Pumice Blends. International Journal of Environmental Research and Public Health 14.

Bibi, I., Icenhower, J., Niazi, N.K., Naz, T., Shahid, M., Bashir, S., 2016. Chapter 21 - Clay Minerals: Structure, Chemistry, and Significance in Contaminated Environments and Geological {CO2} Sequestration, in: Prasad, M.N. V, Shih, K. (Eds.), Environmental Materials and Waste. Academic Press, pp. 543–567. https://doi.org/10.1016/B978-0-12-803837-6.00021-4

Chaplin, B.P., Roundy, E., Guy, K.A., Shapley, J.R., Werth, C.I., 2006. Effects of natural water ions and humic acid on catalytic nitrate reduction kinetics using an alumina supported Pd-Cu catalyst. Environmental Science and Technology 40, 3075–3081. https://doi.org/10.1021/es0525298

Dudu, T.E., Sahiner, M., Alpaslan, D., Demirci, S., Aktas, N., 2015. Removal of As(V), Cr(III) and Cr(VI) from aqueous environments by poly(acrylonitril-co-acrylamidopropyl-trimethyl ammonium chloride)-based hydrogels. Journal of Environmental Management 161, 243–251. https://doi.org/10.1016/j.jenvman.2015.07.015

Fawell, J.K., Ohanian, E., Giddings, M., Toft, P., Magara, Y., Jackson, P., 2004. Sulfate in Drinking-water Background document for development of WHO Guidelines for Drinking-water Quality. World Health Organization 8.

He, R., Peng, Z., Lyu, H., Huang, H., Nan, Q., Tang, J., 2018. Synthesis and characterization of an iron-impregnated biochar for aqueous arsenic removal. Science of the Total Environment 612, 1177–1186. https://doi.org/10.1016/j.scitotenv.2017.09.016

Hu, X., Ding, Z., Zimmerman, A.R., Wang, S., Gao, B., 2015. Batch and column sorption of arsenic onto iron-impregnated biochar synthesized through hydrolysis. Water Research 68, 206–216. https://doi.org/10.1016/j.watres.2014.10.009

La, D.D., Patwari, J.M., Jones, L.A., Antolasic, F., Bhosale, S. V., 2017. Fabrication of a GNP/Fe-Mg Binary Oxide Composite for Effective Removal of Arsenic from Aqueous Solution. ACS Omega 2, 218–226. https://doi.org/10.1021/acsomega.6b00304

Li, Y., Zhang, F., Xiu, F., 2009. Science of the Total Environment Arsenic (V) removal from aqueous system using adsorbent developed from a high iron-containing fl y ash. Science of the Total Environment, The 407, 5780–5786. https://doi.org/10.1016/j.scitotenv.2009.07.017

Lin, S., Yang, H., Na, Z., Lin, K., 2018. A novel biodegradable arsenic adsorbent by immobilization of iron oxyhydroxide (FeOOH) on the root powder of long-root Eichhornia crassipes. Chemosphere 192, 258–266. https://doi.org/10.1016/j.chemosphere.2017.10.163

Martinson, C.A., Reddy, K.J., 2009. Adsorption of arsenic(III) and arsenic(V) by cupric oxide nanoparticles. Journal of Colloid and Interface Science 336, 406–411. https://doi.org/10.1016/j.jcis.2009.04.075

Murugesan, G.S., Sathishkumar, M., Swaminathan, K., 2006. Arsenic removal from groundwater by pretreated waste tea fungal biomass. Bioresource Technology 97, 483–487. https://doi.org/10.1016/j.biortech.2005.03.008

Niazi, N.K., Bibi, I., Shahid, M., Ok, Y.S., Shaheen, S.M., Rinklebe, J., Wang, H., Murtaza, B., Islam, E., Farrakh Nawaz, M., Lüttge, A., 2018. Arsenic removal by Japanese oak wood biochar in aqueous solutions and well water: Investigating arsenic fate using integrated spectroscopic and microscopic

techniques. Science of the Total Environment 621, 1642–1651. https://doi.org/10.1016/j.scitotenv.2017.10.063

Rehman, S. ur, Siddiq, M., Al-Lohedan, H., Aktas, N., Sahiner, M., Demirci, S., Sahiner, N., 2016. Fast removal of high quantities of toxic arsenate via cationic p(APTMACl) microgels. Journal of Environmental Management 166, 217–226. https://doi.org/10.1016/j.jenvman.2015.10.026

Sahiner, N., Ozay, O., Aktas, N., Blake, D.A., John, V.T., 2011. Arsenic (V) removal with modi fi able bulk and nano p (4-vinylpyridine) -based hydrogels : The effect of hydrogel sizes and quarternization agents. DES 279, 344–352. https://doi.org/10.1016/j.desal.2011.06.028

Shaheen, S.M., Eissa, F.I., Ghanem, K.M., Gamal El-Din, H.M., Al Anany, F.S., 2013. Heavy metals removal from aqueous solutions and wastewaters by using various byproducts. Journal of Environmental Management 128, 514–521. https://doi.org/10.1016/j.jenvman.2013.05.061

Shakoor, M.B., Niazi, N.K., Bibi, I., Murtaza, G., Kunhikrishnan, A., Seshadri, B., Shahid, M., Ali, S., Bolan, N.S., Ok, Y.S., Abid, M., Ali, F., 2016. Remediation of arsenic-contaminated water using agricultural wastes as biosorbents. Critical Reviews in Environmental Science and Technology 46, 467–499. https://doi.org/10.1080/10643389.2015.1109910

Siddiqui, S.I., Chaudhry, S.A., 2017. Iron oxide and its modified forms as an adsorbent for arsenic removal: A comprehensive recent advancement. Process Safety and Environmental Protection 111, 592–626. https://doi.org/10.1016/j.psep.2017.08.009

Tuna, A.Ö.A., özdemir, E., şimşek, E.B., Beker, U., 2013. Removal of As(V) from aqueous solution by activated carbon-based hybrid adsorbents: Impact of experimental conditions. Chemical Engineering Journal 223, 116–128. https://doi.org/10.1016/j.cej.2013.02.096

Vithanage, M., Herath, I., Joseph, S., Bundschuh, J., Bolan, N., Ok, Y.S., Kirkham, M.B., Rinklebe, J., 2017. Interaction of arsenic with biochar in soil and water: A critical review. Carbon 113, 219–230. https://doi.org/10.1016/j.carbon.2016.11.032

Yanagita, T., Jiang, Y., Nakamura, M., 2013. Arsenic adsorption properties of new iron hydroxide. Journal of Japan Society on Water Environment 36, 149–155. https://doi.org/10.2965/jswe.36.149

Yean, S., Cong, L., Yavuz, C.T., Mayo, J.T., Yu, W.W., Kan, A.T., Colvin, V.L., Tomson, M.B., 2005. Effect of magnetite particle size on adsorption and desorption of arsenite and arsenate. Journal of Materials Research 20, 3255–3264. https://doi.org/10.1557/jmr.2005.0403

Yoon, J., Amy, G., Chung, J., Sohn, J., Yoon, Y., 2009. Removal of toxic ions (chromate, arsenate, and perchlorate) using reverse osmosis, nanofiltration, and ultrafiltration membranes. Chemosphere 77, 228–235. https://doi.org/10.1016/J.CHEMOSPHERE.2009.07.028

Zhang, Y., Cremer, P.S., 2006. Interactions between macromolecules and ions: the Hofmeister series. Current Opinion in Chemical Biology 10, 658–663. https://doi.org/10.1016/J.CBPA.2006.09.020

Chapter 3: The effect of γ-FeOOH on enhancing arsenic adsorption from groundwater with DMAPAAQ + FeOOH gel composite

3.1. Introduction

The goal of this chapter is to investigate the factors that cause the gel composite, which is made up of N,N-dimethylamino propylacrylamide, methyl chloride quaternary (DMAPAAQ), and Iron(III) Hydroxide (FeOOH) particles, to adsorb more arsenic than other adsorbents or removal techniques and to provide better selectivity and reusability when compared to other adsorbents or removal techniques.As discussed in the previous chapter, this gel can effectively adsorb arsenic at neutral pH levels, something most of the previous researches could not attain. The gel follows pseudo 2^{nd} order reaction kinetics, which suggests that the adsorption type was chemisorption. The maximum arsenic adsorption capacity of the gel was 123.4 mg/g, at neutral pH levels. The adsorption amount of As(V) by DMAPAAQ + FeOOH gel composite was higher than the other researches at neutral pH levels(Safi et al., 2019a). This gel functions when it is put into water and its surface area increases to adsorb arsenic. Inside the gel, a cationic charge (quaternary amino group) adsorbs arsenic and the iron hydroxide found in this gel improves selective adsorption and also helped to provide recyclability. (Safi et al., 2019a, 2019b).

Recently, researchers utilized several types of polymer gels for instance cryogels, microgels, cationic hydrogels, etc., to adsorb arsenic. These gels exhibited competent adsorption properties. For example, the cationic cryogel, poly(3-acrylamidopropyl) trimethyl

ammonium chloride [p(APTMACl)] achieved an arsenic removal rate of 96%(Sahiner et al., 2015). Additionally, at pH 9, approximately 99.7% removal efficiency was achieved by this cationic hydrogel(Barakat and Sahiner, 2008). A microgel, tris(2-aminoethyl) amine (TAEA) and glyceroldiglycidyl ether (GDE), p(TAEA-co-GDE) achieved 98.72 mg/g of maximum arsenic adsorption capacity was achieved by the microgel at pH 4 (Rehman et al., 2017). Although these gels have high adsorption capabilities, their selectivity in all studied environments was low and they failed to effectively remove arsenic from water at neutral pH levels(Safi et al., 2019a).

A maximum adsorption capacity of 227 μg/g of was measured when Fe(III)-Sn(IV) mixed binary oxide-coated sand was used at a temperature of 313 K and a pH of 7(Chaudhry et al., 2016). Alternatively, Fe-Zr binary oxide-coated sand (IZBOCS) has also been used to remove arsenic and achieved a maximum adsorption capacity of 84.75 mg/g at 318 K and a pH of 7(Chaudhry et al., 2017). The core shell $Fe@Fe_2O_3$ nanobunches (NBZI) removed arsenic from acidic wastewater by adsorption and co-precipitation. But, since this technique produces sediments, additional separation processes are required(Tang et al., 2017).

Other reported adsorbents exhibited low adsorption performances, lack of recyclability, low stability, high operational and maintenance costs, and the use of hazardous chemicals in the synthesis process(Niazi et al., 2018). Therefore, researchers need to develop a technology that can remove arsenic efficiently at neutral pH levels, provide selectivity, cost effectiveness and can be reused.

A transmission electron microscope (TEM) and thermogravimetric analyser (TGA) was used to detect the iron contents in the gel and ensure its maximum impregnation. In addition, the Mössbauer spectroscopy was utilized to examine the type of impregnated iron in the gel composite and found that it was γ-FeOOH. Finally, Fourier transform infrared spectroscopy (FTIR) was used to examine the surface functional groups present in the gel and the differences in those groups before and after iron impregnation. Similarly, the differences of the surface functional groups in the gel, before and after the adsorption of both forms of arsenic was also experimented. To summarize, this chapter described the characteristics of the gel composite, which is selective in adsorption and cost effective. Also, in this chapter, I evaluated the characteristics that contribute to the high adsorption performances of the gel composite and discussed the details in the later sections.

3.2. Methods

3.2.1 Materials

The monomer, *N,N'*-dimethylamino propylacrylamide, methyl chloride quaternary (DMAPAAQ) (75% in H_2O) was supplied by KJ Chemicals Corporation, Japan. The crosslinker, *N,N'*-Methylene bisacrylamide (MBAA) and the arsenic (III) sources, arsenic(III) oxide and sodium (meta) arsenite were purchased from Sigma-Aldrich, USA. The accelerator sodium sulfite (Na_2SO_3), the arsenic(V) source, disodium hydrogenarsenate heptahydrate ($Na_2HAsO_4.7H_20$) and ferric chloride($FeCl_3$) was purchased from Nacalai Tesque, Inc., Japan. Sodium hydroxide (NaOH) was purchased from Kishida Chemicals Corporation, Japan. *N,N'*- dimethyl acrylamide (DMAA) and the initiator, ammonium peroxodisulfate (APS) was purchased from Kanto Chemical Co. Inc., Japan.

3.2.2 Preparation of the gel composite

The gel was prepared using the strategy meticulously described in Safi et al. 2019(Safi et al., 2019a, 2019b). I used *N,N*-dimethylamino propylacrylamide, methyl chloride quaternary (DMAPAAQ) as a monomer, *N,N'*-Methylene bisacrylamide (MBAA) as a crosslinker, sodium sulfite as an accelerator and ammonium peroxodisulfate (APS) as an initiator. Firstly, the monomer, DMAPAAQ and the crosslinker, MBAA, and the accelerator, sodium Sulfite and NaOH were composed and named as “monomer solution”. On the other hand, the initiator, APS and $FeCl_3$ were mixed and named as “initiator solution”. The amount of NaOH and $FeCl_3$ were taken on 3:1 proportion. The monomer and initiator

solutions were first synthesized by N_2 for 10 minutes at 10 °C. The solutions were then mixed, and the reaction went for 4 hours at the same temperature (10 °C). The detailed composition of the gel composite is shown in **Table 3.1**. After the gel is formed, the block was first collected and washed with deionized water. Following this, the gel block was cut to obtain uniform square shaped pieces of gel composite of 5mm in length. Finally, they were washed again with deionized water for 24 hours and dried in the oven for 24 hours at 50°C. The purpose of adding NaOH and $FeCl_3$ was to initiate the following reaction as well as to ensure the maximum content $Fe(OH)_3$ in the structure of the gel composite.

$$FeCl_3+3NaOH \rightarrow Fe(OH)_3+3NaCl \qquad (3.1)$$

To evaluate the difference in terms of the characteristics of the cationic and non-cationic gel composite, *N,N'*-dimethyl acrylamide (DMAA) and FeOOH was prepared in the same way as DMAPAAQ+FeOOH gel composite.

Table 3.1. Preparation condition of gel composite.

	Chemical	**Quantity (mol/m^3)**
Monomer	DMAPAAQ, DMAA	500
Crosslinker	MBAA	50
Accelerator	Sodium Sulfite	80
	Sodium Hydroxide (NaOH)	2100

Initiator	Ammonium peroxodisulfate (APS)	30
	Ferric Chloride ($FeCl_3$)	700

3.2.3 Transmission Electron Microscope (TEM) Analysis

The TEM images of the gel composite of DMAPAAQ and FeOOH and the gel composite of DMAA and FeOOH were analysed by Transmission Electron Microscope (TEM-2010, JEOL Ltd., Japan) to find the presence of FeOOH components in the gel structure. I grinded 0.2 mg of DMAPAAQ+FeOOH gel to create fine powder, which was then immersed in 20 mL Isopropyl alcohol solution for 30 minutes. Following this, I collected 5 mL solution as a sample.

3.2.4 Thermogravimetric (TG) Analysis

The examination of content of FeOOH in the DMAPAAQ+FeOOH and DMAA+FeOOH gel composite was carried out using a thermogravimetric analyser (TGA-50, Thermogravimetric Analyzer, Shimadzu, Japan) to evaluate the content of FeOOH in the gel composite. I took a piece of dry gel and cut it into a small piece to weigh 5 mg, with a stainless steel cutter. The small piece of gel was then placed in the titanium sample holder and the experiment was conducted at a heating rate of 5°C/min from 50°C to 600°C in

atmosphere. After testing each sample, the titanium holder was cleaned thoroughly using a clean cotton bud. I held the titanium holder with forceps to avoid heat.

3.2.5 Mössbauer Spectroscopy

The experimentation of the type of FeOOH was conducted using Mössbauer spectrometer (Wissel MB-500, Germany) to examine the type of FeOOH in the gel composite, with the help of Natural Science Centre for Basic Research and Development, Hiroshima University.

3.2.6 Fourier Transform Infrared Spectroscopy (FTIR) Analysis

To examine the changes in the surface functional groups of DMAPAAQ gel after the FeOOH impregnation, I used the Fourier transform infrared spectroscopy (FTIR) (IR-Prestige 21, Shimadzu, Japan). In addition, I evaluated the changes in the surface functional groups of DMAPAAQ+FeOOH gel composite after the impregnation of As(III) and As(V). The concentration of As (III) and As(V) solutions were 0.2 mM. The solutions were prepared using distilled water as solvent. To adsorb arsenic, 20 mg of dried DMAPAAQ + FeOOH gel was immersed in 0.2 mM As (III) and As(V) solutions respectively for 24 hours at 25 °C. FTIR spectra of the DMAPAAQ gel, DMAPAAQ+FeOOH gel composite, DMAA+FeOOH gel composite and the As (III) and As (V) loaded DMAPAAQ+FeOOH samples were recorded. The wavelength range was from 400cm^{-1} to 4000cm^{-1}. The samples were milled

with potassium bromide (KBr) to form a very fine powder and then compressed into a thin pellet for analysis.

3.2.7 X-Ray Diffraction (XRD) Analysis

The XRD analysis was conducted using MiniFlex 600 by Rigaku Corporation, Japan. I grinded 0.2 mg of DMAPAAQ + FeOOH gel into fine powder and placed the powder into glass film designated for XRD experiment. The purpose was to examine the polymer structure of the gel.

3.2.8 X-Ray Photoelectron Spectroscopy (XPS) Analysis

The XPS analysis was conducted using an ESCA 3400 Electron spectrometer by Kratos Analytical Ltd., UK to investigate the adsorption mechanism. I grinded 0.2 mg of DMAPAAQ + FeOOH gel into fine powder and placed the powder into glass film designated for XRD experiment. About 20 mg of dried DMAPAAQ + FeOOH gel pieces were immersed in 50 mg/L $Na_2HAsO_4.7H_20$ and sodium (meta) arsenite solutions respectively. The solutions were then placed in a shaker for almost 9 hours at 25°C and 120 rpm. The gels were then collected and dried in the oven at 70°C for 12 hours. After drying, the gels were grinded with a mortar into fine powder, which was used for the experiment.

3.3. Results and Discussion

3.3.1 The presence of FeOOH particles in the gel composites

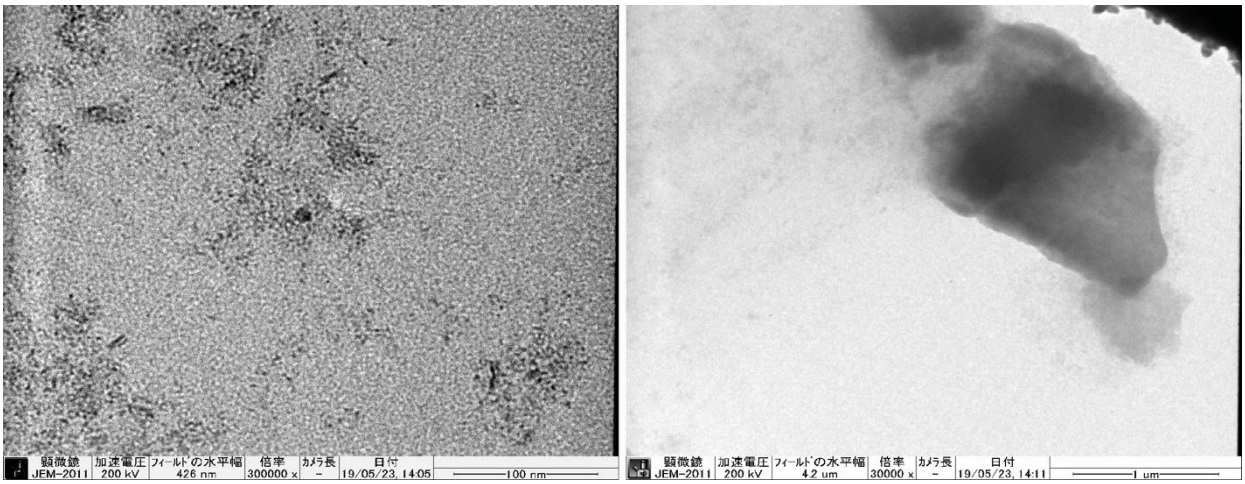

Figure 3.1. TEM images of DMAPAAQ+ FeOOH gel composite（Scale bar length：left 100 nm, right 1 μm）.

After preparing the gel composite, I analysed whether the gel contained iron particles. The diameter of the FeOOH particles of DMAPAAQ+FeOOH and DMAA+FeOOH composites were evaluated using a Transmission Electron Microscope (TEM-2010, JEOL Ltd., Japan). I found the presence of FeOOH particles in DMAPAAQ + FeOOH and DMAA + FeOOH gel composites after examination. TEM images of DMAPAAQ + FeOOH are shown in **Fig. 3.1**. In Fig. 3.1, the nano sized particles were clearly visible. In the right image of Fig. 3.1, conglomerated FeOOH particles in the structure of DMAPAAQ gel was visible. When the image was further magnified, the presence of the FeOOH particles of about 6-13 nm could be confirmed (from the left image of Fig. 3.1).

These results validate the preparation method described in the previous chapter(Safi et al., 2019a, 2019b) and confirm that FeOOH components are successfully impregnated. The impregnation of the polymer gel structure with FeOOH is important because it increases the adsorption efficiency of the adsorbents for both As(III) and As(V)(Lin et al., 2018). Since, both the FeOOH particles and the polymer gel structure can adsorb arsenic, it can be shown that the presence of the FeOOH particles helps to increase the capability of adsorption of arsenic.

Therefore, it is considered that arsenic is likely to be incorporated in the FeOOH particles and also in the polymer structure of DMAPAAQ gel. This shows that high adsorption ability can be achieved by combining two adsorbents in one gel composite.

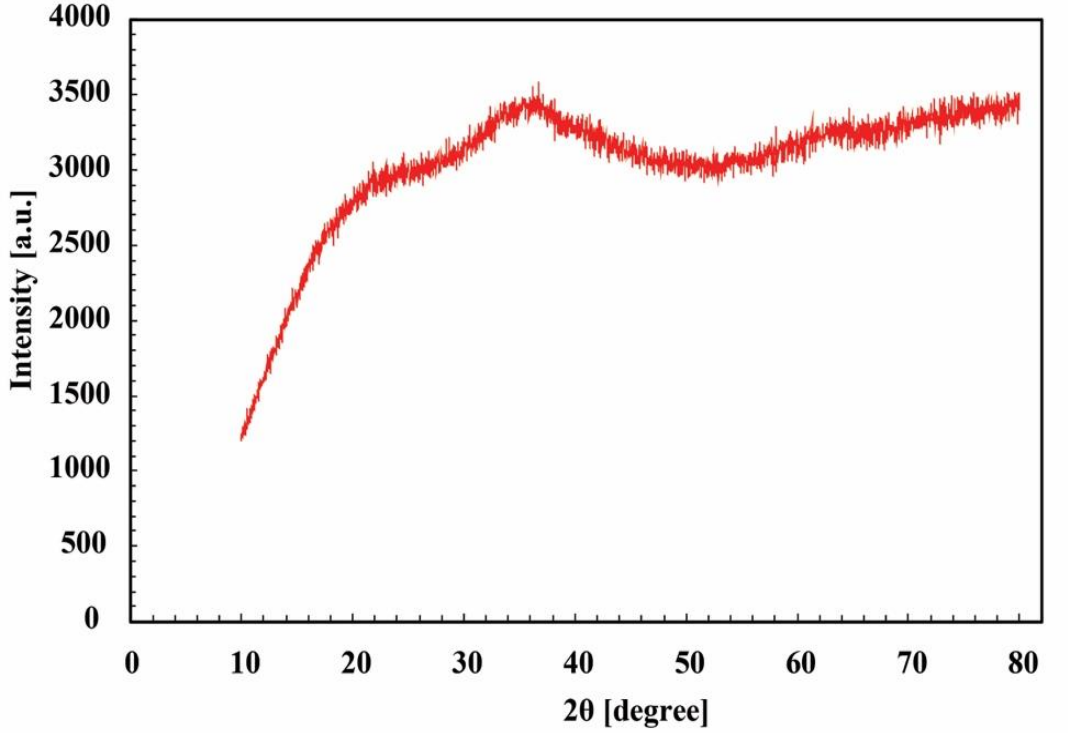

Figure 3.2. XRD analysis of DMAPAAQ+FeOOH gel composite.

I also analyzed the polymer structure of the DMAPAAQ + FeOOH gel composite by conducting an X-ray diffraction system. The result of the XRD analysis is shown in **Fig. 3.2.** The figure suggest that the diffractograms of DMAPAAQ + FeOOH samples show that the crystalline phase of DMAPAAQ + FeOOH was not developed. Hence, it suggests that the polymer structure of the gel is amorphous and it shows no crystallinity in the structure(Michler, 2008). The TEM images also showed no sign of crystallinity of the particles or polymer in the gel structure. The polymer structure of DMAPAAQ + FeOOH is highly crosslinked between the DMAPAAQ gel and FeOOH particles.

3.3.2 Content of FeOOH in the gel composite

The volume of FeOOH in the gel composite may affect the ability of the gel composite to adsorb arsenic. Moreover, the higher the volume of FeOOH in the gel composite, the higher the selectivity of arsenic adsorption. In addition, maximum adsorption of arsenic can be obtained. As described in the 'Methods' section, to achieve the highest content of FeOOH inside of the gel composite, $FeCl_3$ and NaOH concentrations were varied to a ratio of 1:3 during the preparation of the gel. One of the novelties of this unique preparation method is that $FeCl_3$ was added in the initiator solution and NaOH was added with the monomer solution so that when the two solutions are mixed, FeOOH is produced by the reaction between $FeCl_3$ and NaOH, at the preparation stage. Hence, this method will ensure that the gel contains the highest volume of FeOOH. DMAPAAQ + FeOOH gel was prepared with different concentrations of $FeCl_3$ (400, 450, 550, 600 and 700 mM/L).

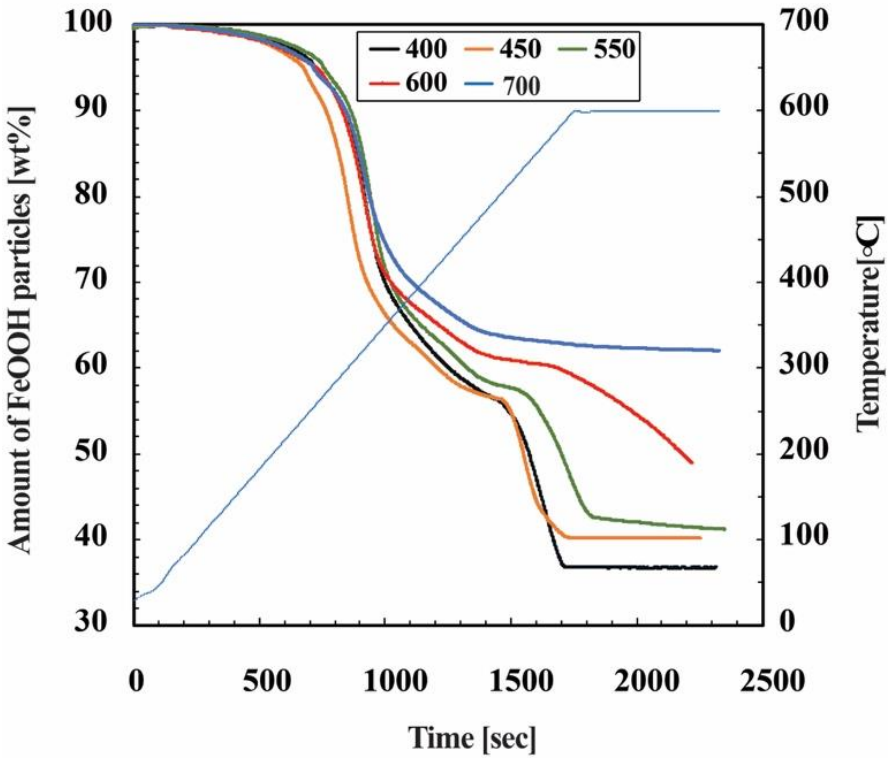

Figure 3.3. Thermogravimetric analysis curves to analyse the Content of FeOOH in DMAPAAQ+FeOOH gel composite.

Similarly, a non-cationic gel composite, DMAA + FeOOH gel was developed with different concentrations of $FeCl_3$ (450, 550, 650 and 700 mM/L), for comparison purpose. The content of the FeOOH particles in the gel composites of DMAPAAQ + FeOOH and DMAA + FeOOH at different $FeCl_3$ concentrations was measured by Thermogravimetric Analyzer (TGA-50, Shimadzu Co., Japan). It is suspected that most of the Fe ions have formed iron hydroxide inside of the gel. **Fig. 3.3** shows that when the $FeCl_3$ concentration was 700 mM / L, the content of the particles was highest (62.05 wt%). The result was confirmed by the TGA curves shown in Fig. 3.3, where the TGA curves were shown for the

different concentrations of $FeCl_3$ (400, 450, 550, 600 and 700 mM/L), in the structure of DMAPAAQ + FeOOH gel.

On the other hand, when the concentration of $FeCl_3$ was set to more than 700 mM/L, formation of the DMAPAAQ + FeOOH gel composite became difficult. The reason for this difficulty is that when the concentration of NaOH was high, DMAPAAQ was hydrolysed and the formation of radicals by the initiator, ammonium peroxodisulfate (APS) was inhibited. As the maximum content of FeOOH was found at $FeCl_3$ concentration of 700 mM/L, I chose this concentration to prepare the gel composites and conduct later experiments. In addition, **Fig. 3.4** shows the relationship between the composition of charged iron ions and the content of FeOOH for DMAA + FeOOH gel composite. The figure suggests that the DMAA + FeOOH gel composite was able to obtain the similar content of FeOOH characteristic as DMAPAAQ + FeOOH gel composite.

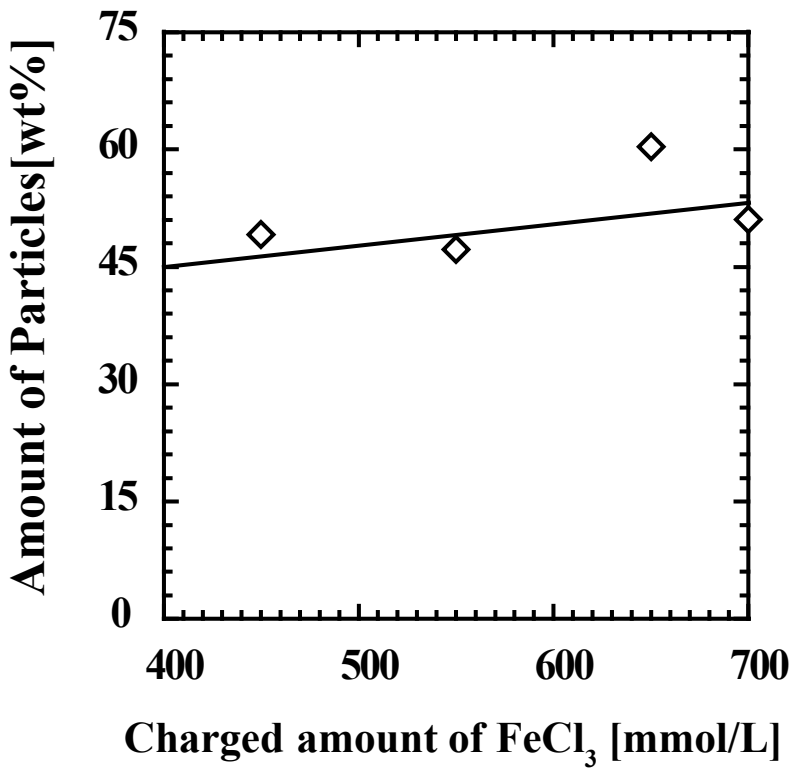

Figure 3.4. Thermogravimetric analysis to analyse the Content of FeOOH in DMAA+FeOOH gel composite.

3.3.3 Identification of FeOOH particles

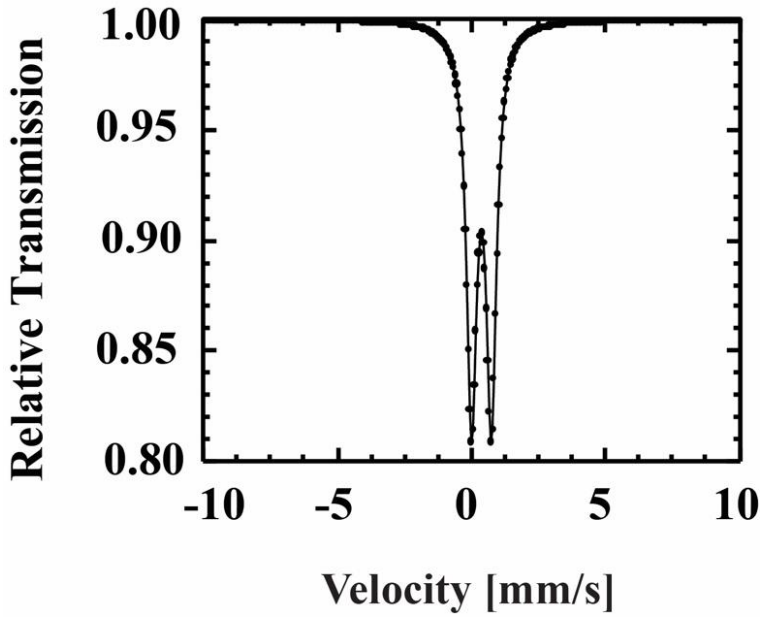

Figure 3.5. Mössbauer spectroscopy of DMAPAAQ+FeOOH gel composite.

Arsenic adsorption property varies depending on different types of FeOOH. Hence, I performed Mössbauer spectroscopy to identify the type of FeOOH within the gel composite.

So far, three different types of FeOOH particles such as α-FeOOH, β-FeOOH, γ-FeOOH have been observed (Wang et al., 2004). As shown in **Table. 3.2** and in the previous section titled 'Content of FeOOH in the gel composite', the gel composite was prepared with 700 mM/L of $FeCl_3$ and the highest content of FeOOH in the gel composite from TG analysis is 62.05 wt%. I experimented the type of FeOOH inside the structure of DMAPAAQ + FeOOH gel composite. The results of the Mössbauer spectroscopy of DMAPAAQ + FeOOH gel composite is shown in **Fig. 3.5.** In the figure, a quadrupole doublet was observed. After comparing this result with previous studies (e.g. (Morris et al., 1985; Takada et al., 1964)),

there is similarity between the peak of γ-FeOOH with the peak in the figure 3.5. Therefore, within the gel composite, FeOOH particles are γ-FeOOH.

This finding has a significant importance to rationale the high arsenic adsorption efficiency of the gel composite, DMAPAAQ + FeOOH. Repo et al.'s (2012) study suggests that γ-FeOOH can adsorb both As(III) and As(V) in high quantity(Repo et al., 2012). Therefore, the presence of γ-FeOOH is one of the reasons for the high capability of arsenic adsorption efficiency by DMAPAAQ + FeOOH gel composite as shown in the previous chapter.

3.3.4 Surface functional group characterization using FTIR spectroscopy

3.3.4.1 Effect of impregnation of FeOOH particles on gels and gel composites

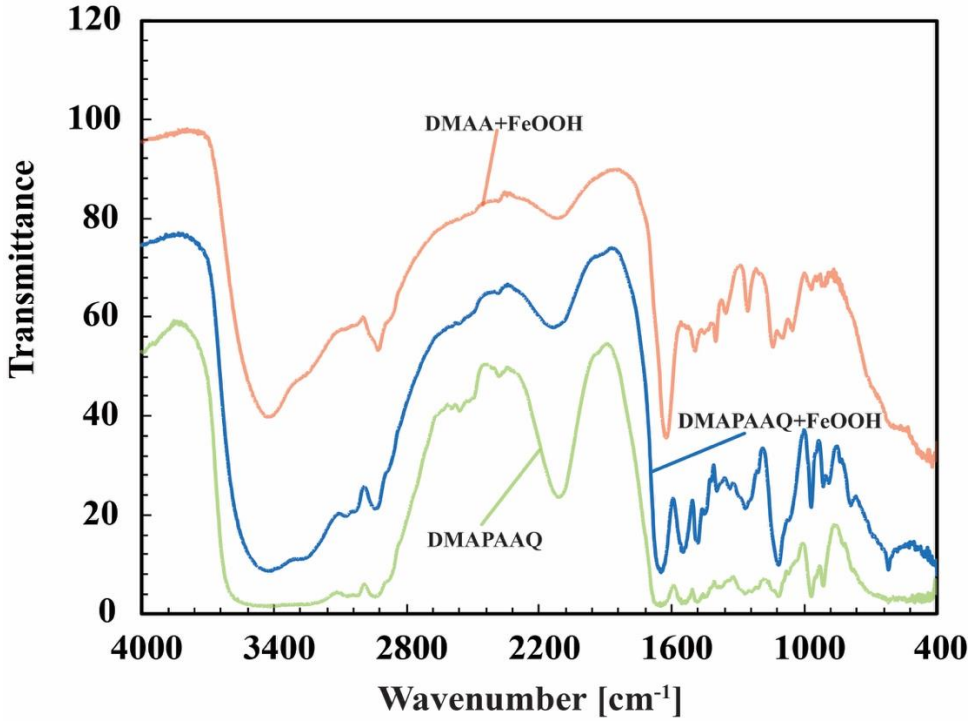

Figure 3.6. FTIR spectroscopy of DMAPAAQ gel (light green line), DMAPAAQ+FeOOH (blue line) and DMAA+FeOOH gel composite (pink line).

I compared the spectral peaks of the DMAPAAQ gel, DMAPAAQ + FeOOH and DMAA + FeOOH gel composites, to determine the difference in surface functional group characterization, before (light green line in **Fig. 3.6**) and after (blue line in **Fig. 3.6**) the impregnation of DMAPAAQ gel structure with FeOOH. In addition, the comparison of ionic and non-ionic gel composite characteristics were determined. The FTIR spectrum of non-ionic gel composite of DMAA+FeOOH was examined for the purpose of comparing ionic and non-ionic gel composite characteristics. As **Fig. 3.6** and **Table 3.2** shows, the FTIR spectrum of DMAPAAQ+FeOOH gel (blue line), the spectral bands at 3417, 3282, 3064, 2596, 2561, 2112, 1643, 1485, 1382, 1336, 1269 and 623 cm^{-1} were shifted to 3414, 3277,

3074, 2945, 2598, 2567, 2144, 1649, 1481, 1396, 1338, 1267 and 619 cm^{-1},respectively, after the FeOOH impregnation to DMAPAAQ gel. I ascribed this to the vibration of the Aliphatic primary amine N-H stretching, Alcohol O-H stretching, Carboxylic acid O-H stretching, Alkyne C≡C stretching, Alkene C=C stretching, Alkane C-H bending, Aldehyde C-H bending, and Aromatic ester C-O stretching groups. As shown in **Table 3.2**, these shifts contribute to the change in groups. In addition, the spectral peak at 914 cm^{-1} (Alkene C=C bending) disappeared and new peaks appeared at spectral band 889 (1,2,4-trisubstituted C-H bending) and 788 cm^{-1} (1,2,3-trisubstituted C-H bending). Spectral bands at 2522 (Carboxylic acid O-H stretching), 1116 (Secondary alcohol C-O stretching) and 968 cm^{-1} (Alkene C=C bending) remained the same for both DMAPAAQ gel and DMAPAAQ + FeOOH gel composite.

In the case of the non-cationic gel composite, DMAA + FeOOH, the spectral peaks appeared at wavelengths 3433 (Aliphatic primary amine N-H stretching), 2929 (Amine salt N-H stretching), 2123 (Alkyne C≡C stretching), 1625 (Alkene C=C stretching), 1494 and 1454 (Alkane C-H bending), 1400 (Aldehyde C-H bending), 1355 (Alcohol O-H bending), 1255 (Aromatic ester C- O stretching), 1141 (Tertiary alcohol C-O stretching), 1099 (Secondary alcohol C-O stretching), 968 and 906 cm^{-1} (Alkene C=C bending) .

The above analysis suggests that there are differences in surface functional characteristics after loading FeOOH in DMAPAAQ gel structure. Some of the groups found in DMAPAAQ+FeOOH gel composite are: strong alcoholic and carboxylic acid O-H stretching group, Primary amine N-H stretching group, alkane C-H bending, alkene C=C

stretching, aldehyde C-H bending, aromatic ester C-O stretching, and strong alkene C=C bending group. After the FeOOH impregnation in DMAPAAQ gel, 1,2,4- trisubstituted strong C-H bending group and alkyne C≡C stretching group were generated in the structure.

3.3.4.2 Effect of As (V) and As(III) adsorption on DMAPAAQ+FeOOH gel composites

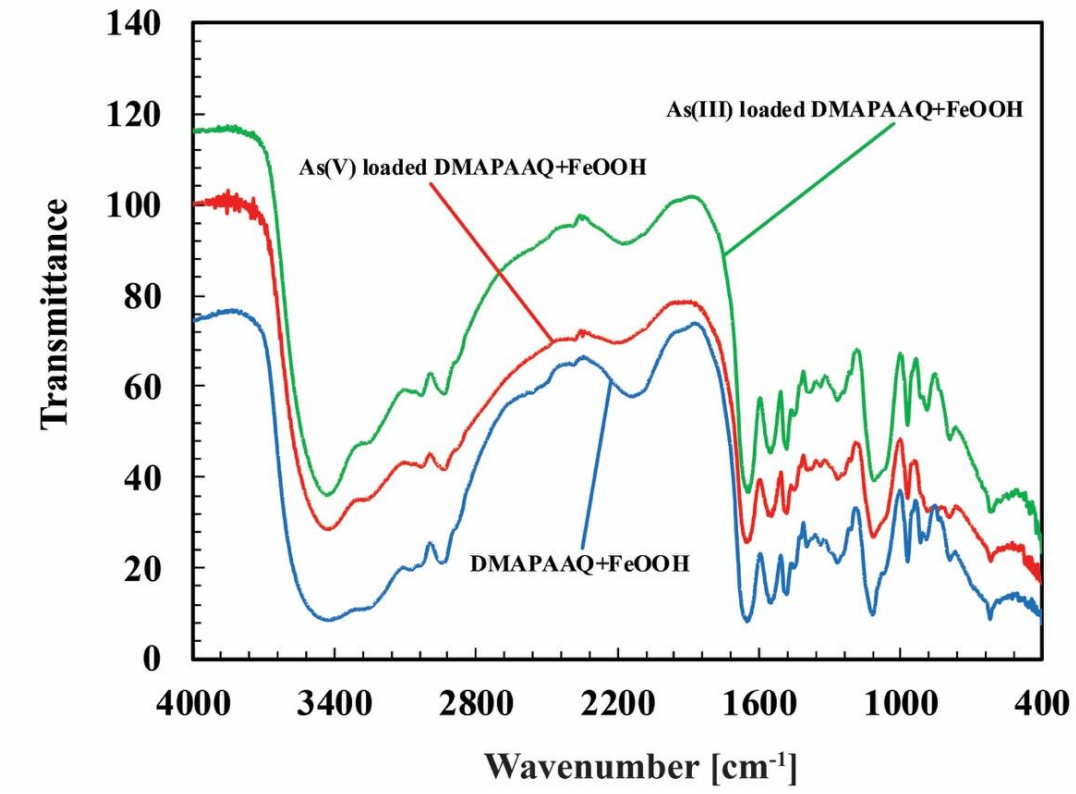

Figure 3.7. FTIR spectroscopy of DMAPAAQ+FeOOH gel composite (blue), As (III) loaded (Green line) and As (V) loaded DMAPAAQ+FeOOH gel composite (red line).

The FTIR spectra of As(III) and As(V) loaded DMAPAAQ+FeOOH gel composite revealed a shift in the position of some spectral peaks. **Fig. 3.7** and **Table 3.2** shows the FTIR

spectral bands of DMAPAAQ+FeOOH (blue line), As(III) loaded (green line) and As(V) loaded DMAPAAQ+FeOOH (red line) to determine the changes in surface functional groups in DMAPAAQ+FeOOH gel composite due to arsenic adsorption In the As(III) loaded DMAPAAQ+FeOOH gel composite (green line in **Fig. 3.7**), the spectral bands at 3414, 3074, 2945, 2144, 1396, 1267, 1116, 889 and 619 cm^{-1} were shifted to 3433, 3066, 2935, 2160, 1382, 1265, 1110, 885 and 615 cm^{-1}, respectively, after the As(III) impregnation of DMAPAAQ+FeOOH gel composite. I ascribed this to the vibration of the Aliphatic primary amine N-H stretching, Alcohol O-H stretching, Amine salt N-H stretching, Alkyne C≡C stretching, Aldehyde C-H bending, Aromatic ester C-O stretching, Secondary alcohol C-O stretching, and 1,2,4-trisubstituted C-H bending groups.

Similarly, in the As(V) loaded DMAPAAQ+FeOOH gel composite (red line in **Fig. 3.7**), the spectral bands at 3414, 2945, 2144, 1649, 1396, 1116, 889, 788 and 619 cm^{-1} were shifted to 3421, 2933, 2212, 1643, 1388, 1114, 885, 790 and 615 cm^{-1} respectively after the adsorption of DMAPAAQ + FeOOH gel with As(V). I ascribed this to the vibration of the Aliphatic primary amine N-H, Amine salt N-H stretching, Alkyne C≡C stretching, Alkene C=C stretching, Aldehyde C-H bending, Secondary alcohol C-O stretching, 1,2,4-trisubstituted C-H bending, and 1,2,3-trisubstituted C-H bending groups. New spectral peaks appeared at 2326 and 2347 cm^{-1} (Carbon di oxide O=C=O stretching).

In both the As(III) and As(V) loaded DMAPAAQ+FeOOH gel composites, the spectral peaks at 2598, 2567 and 2522 cm^{-1} (Carboxylic acid O-H stretching) disappeared. The spectral bands at 3277 (Alcohol O-H stretching), 1481 (Alkane C-H bending), 1338

(Alcohol O-H bending), 968 cm^{-1} (Alkene C=C bending) were the same for the DMAPAAQ+FeOOH gel composites, As(III) and As(V) loaded DMAPAAQ+FeOOH gel composites.

The analysis suggests that ion exchange and surface complexation reactions occurred in the gel composite. The shifts in the spectral bands denote that As(III) and As(V) changed the surface functional characteristics of DMAPAAQ+FeOOH gel composite, by being highly adsorbed in the structure of the gel composite. Some of the groups found in As(III) and As(V) stretching group were: Primary amine N-H stretching group, alkyne C≡C stretching, alkene C=C stretching, alkane C-H bending, aldehyde C-H bending, aromatic ester C-O stretching, secondary alcohol C-O stretching, strong alkene C=C bending. After the loading of As(V) in DMAPAAQ gel, carbon dioxide (O=C=O stretching) was generated in the gel structure.

Referring to the "Arsenic adsorption isotherm" section from the previous chapter, the maximum capability of adsorption of arsenic by DMAPAAQ+FeOOH was higher when compared with the other currently studied methods at neutral pH levels. The higher adsorption capability has strong correlation with the FTIR analysis because the N-H stretching groups shift due to the adsorption of both As(III) and As(V) to DMAPAAQ+FeOOH. Furthermore, a change (disappearance) was observed in O-H stretching groups after the impregnation of both As(III) and As(V) to DMAPAAQ+FeOOH. The arsenic adsorption mechanisms discussed in the previous chapter also supports the above hypothesis. Hence, the FTIR analysis can describe why DMAPAAQ+FeOOH has a higher

Q_{max} value (maximum adsorption capacity) than the other adsorbents recently studied(Safi et al., 2019a).

Table 3.2. FTIR spectroscopy peak analysis.

Wavelength	DMAA+ FeOOH	DMAPAAQ	DMAPAAQ+ FeOOH	As(III) loaded DMAPAAQ+FeOOH	As(V) loaded DMAPAAQ+FeOOH	Group	Compound Class	Strength
615								
619								
623								
788						C-H Bending	1,2,3-trisubstituted	Strong
790								
885						C-H Bending	1,2,4-trisubstituted	Strong
889								
906						C=C Bending	Alkene	Strong
914								
968								
1099						C-O Stretching	Secondary alcohol C-0	Strong
1110								
1114								
1116								
1141						C-O Stretching	Tertiary alcohol	Strong

1255						C-O Stretching	Aromatic ester	Strong
1265								
1267								
1269								
1336						O-H Bending	Alcohol	Medium
1338								
1355								
1382						C-H Bending	Aldehyde	Medium
1388								
1396								
1400								
1454						C-H Bending	Alkane	Medium
1481								
1485								
1494								
1625						C=C Stretching	Alkene	Medium
1643								
1649								
2112						C≡C Stretching	Alkyne	Weak
2123								
2144								
2160								

2212								
2326						O=C=O Stretching	Carbon di oxide	Strong
2347								
2522						O-H Stretching	Carboxylic acid	Strong, broad
2561								
2567								
2596								
2598								
2929						N-H Stretching	Amine salt	Strong, broad
2933								
2935								
2945								
3064						O-H Stretching	Alcohol	Weak, broad
3066								
3074								
3277							Alcohol	Strong, broad
3282								
3414						N-H Stretching	Aliphatic primary amine	Medium
3417								
3421								
3433								

3.3.5 X-Ray Photoelectron Spectroscopy (XPS) Analysis of Arsenic adsorption on DMAPAAQ+FeOOH gel

The surface of DMAPAAQ + FeOOH gel composite was examined using XPS to verify the presence of As(III) and As(V). Two different samples were analyzed with XPS. One sample consisted of DMAPAAQ + FeOOH gel adsorbed with 50 mg/L of As(III) solution (**Fig. 3.8 (a)**). And the other sample was DMAPAAQ + FeOOH gel adsorbed with 50 mg/L of As(V) solution (**Fig. 3.8 (b)**). The results of XPS analysis of both the samples are shown in **Fig. 3.8 (a)** and **(b)**. I found that the samples of DMAPAAQ + FeOOH gel reacted with arsenic in the presence of the As3d core level peak.

In the both figures of **Fig. 3.8**, the XPS of the As3d peaks indicate the presence of arsenic on the surface of DMAPAAQ + FeOOH gel composite. The XPS spectrum of As 3d confirmed the coexistence of As (III) and As (V) in the structure of the polymer gel composite. The As3d binding energies were 44.23 and 45.28 eV for samples reacted with As(III) and As(V), respectively.

As(III) binding energies are about 1 eV lower than that of As(V). Also, the shape of the peak notifies the presence of a single species contributor. When arsenic was adsorbed to cupric oxide nanoparticles, similar results were obtained. Martinson and Reddy (2009) reported that in such cases, adsorption of As(III) involves a process of oxidation prior to adsorption (Martinson and Reddy, 2009). In addition, similar findings were also reported

when Fe-Mn binary oxide adsorbent was used to adsorb arsenic (Zhang et al., 2007) and when arsenic was adsorbed by Zeolite supported nanoscale zero-valent iron (Li et al., 2018).

Therefore, the oxidation of As (III) to As (V) occurred in the adsorption process of arsenic by DMAPAAQ + FeOOH gel composite.

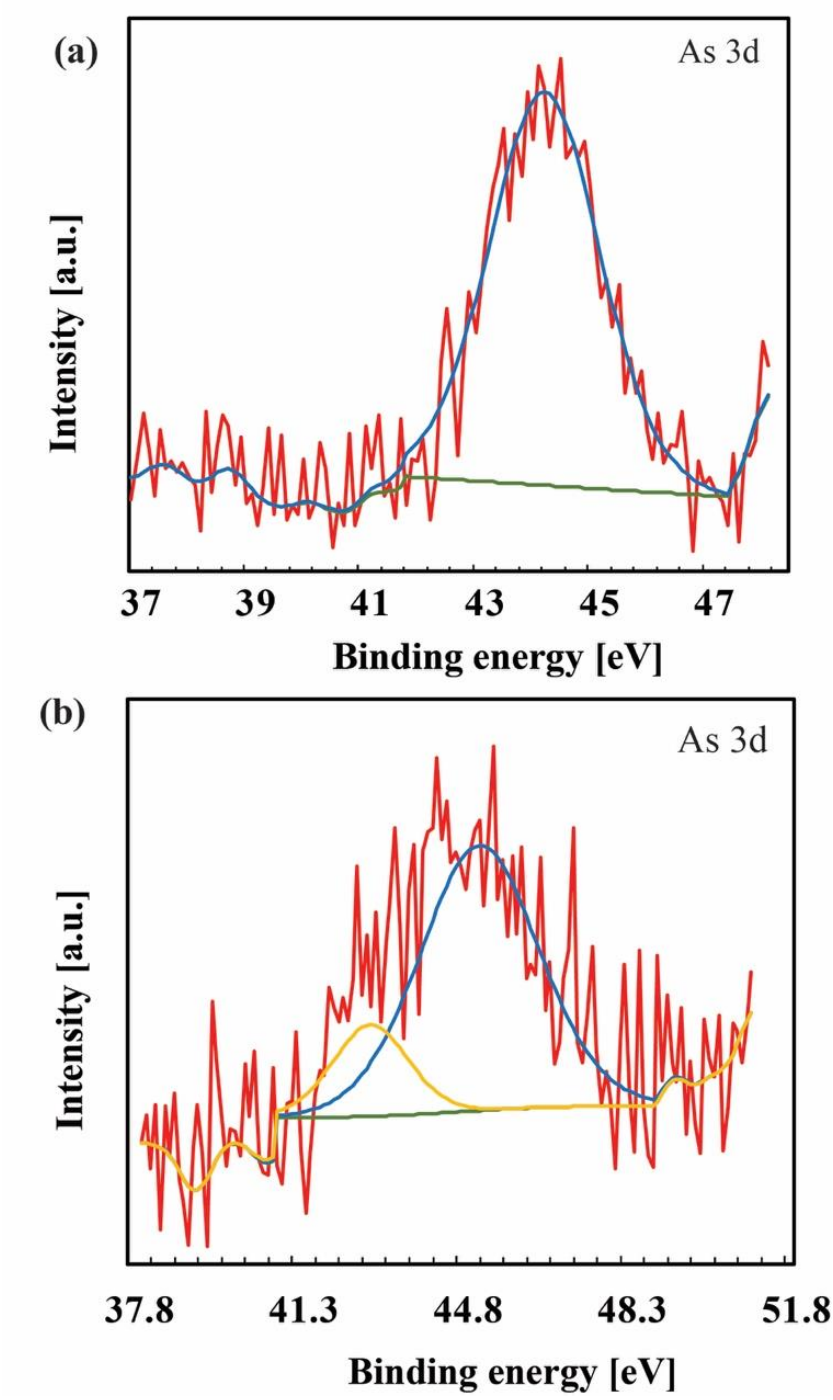

Figure 3.8. XPS at As3d peak of DMAPAAQ+FeOOH gel **(a)** reacted with As(III), **(b)** reacted with As(V).

3.4. Conclusion

In the DMAPAAQ+FeOOH gel composite, the presence of iron particles was confirmed from the TEM images. The results from the TG analysis showed that DMAPAAQ+FeOOH gel composite contained 62.05% FeOOH particles in the gel composite. The high efficiency compared to the other adsorbents in the chapter 2 may be because of the high content of FeOOH particles in the gel composite. The XRD analysis suggests that the polymer structure of the gel is amorphous. Mössbauer spectroscopy of DMAPAAQ+FeOOH gel composite suggests that the FeOOH particles present in the DMAPAAQ+FeOOH gel composite are γ-FeOOH, which aid in the adsorption of both As(III) and As(V). Therefore, γ-FeOOH contributed 64.4% of the adsorption of As(V) by DMAPAAQ + FeOOH gel composite. The adsorption amount of As(V) by the γ-FeOOH particles in the DMAPAAQ + FeOOH gel structure was 79.5 mg/g, which is almost 140% higher than that of the iron hydroxide powder(Safi et al., 2019a; Yanagita et al., 2013). Hence, it can be concluded that, γ-FeOOH particles enhanced the arsenic adsorption in the DMAPAAQ+FeOOH gel structure.

The FTIR analysis suggests that there were shifts in the surface functional groups due to the impregnation of FeOOH in the gel composite. In addition, shifts are apparent because of impregnation of As(III) and As(V) into DMAPAAQ+FeOOH gel composite. XPS analysis suggests that As(III) were oxidized to As(V) prior to being adsorbed by the DMAPAAQ + FeOOH gel composite.

There is further scope of research regarding the adsorption applications of As(III) to the gel composite, which will be discussed in the next chapter. This chapter contributes to the field by examining and discussing the characteristics of an effective adsorbent of arsenic and the positive effects on contaminated water. All the discussions in this chapter show that the gel composite, DMAPAAQ+FeOOH can solve the issue of arsenic contamination of groundwater not only by its high absorbance of arsenic, but also through its effective selectivity and regeneration.

References

Barakat, M.A.A., Sahiner, N., 2008. Cationic hydrogels for toxic arsenate removal from aqueous environment. Journal of Environmental Management 88, 955–961. https://doi.org/10.1016/j.jenvman.2007.05.003

Chaudhry, S.A., Ahmed, M., Siddiqui, S.I., Ahmed, S., 2016. Fe(III)–Sn(IV) mixed binary oxide-coated sand preparation and its use for the removal of As(III) and As(V) from water: Application of isotherm, kinetic and thermodynamics. Journal of Molecular Liquids 224, 431–441. https://doi.org/10.1016/J.MOLLIQ.2016.08.116

Chaudhry, S.A., Zaidi, Z., Siddiqui, S.I., 2017. Isotherm, kinetic and thermodynamics of arsenic adsorption onto Iron-Zirconium Binary Oxide-Coated Sand (IZBOCS): Modelling and process optimization. Journal of Molecular Liquids 229, 230–240. https://doi.org/10.1016/J.MOLLIQ.2016.12.048

Li, Z., Wang, L., Meng, J., Liu, X., Xu, J., Wang, F., Brookes, P., 2018. Zeolite-supported nanoscale zero-valent iron: New findings on simultaneous adsorption of Cd(II), Pb(II), and As(III) in aqueous solution and soil. Journal of Hazardous Materials 344, 1–11. https://doi.org/10.1016/j.jhazmat.2017.09.036

Lin, S., Yang, H., Na, Z., Lin, K., 2018. A novel biodegradable arsenic adsorbent by immobilization of iron oxyhydroxide (FeOOH) on the root powder of long-root Eichhornia crassipes. Chemosphere 192, 258–266. https://doi.org/10.1016/j.chemosphere.2017.10.163

Martinson, C.A., Reddy, K.J., 2009. Adsorption of arsenic(III) and arsenic(V) by cupric oxide nanoparticles. Journal of Colloid and Interface Science 336, 406–411. https://doi.org/10.1016/j.jcis.2009.04.075

Michler, G.H. (Ed.), 2008. Amorphous Polymers, in: Electron Microscopy of Polymers, Springer Laboratory. Springer Berlin Heidelberg, Berlin, Heidelberg, pp. 277–293. https://doi.org/10.1007/978-3-540-36352-1_16

Morris, R. V, Lauer, H. V, Lawson, C.A., Gibson, E.K., Nace, G.A., Stewart, C., 1985. Spectral and other physicochemical properties of submicron powders of hematite (α-Fe2O3), maghemite (γ-Fe2O3), magnetite (Fe3O4), goethite (α-FeOOH), and lepidocrocite (γ-FeOOH). Journal of Geophysical Research: Solid Earth 90, 3126–3144. https://doi.org/10.1029/JB090iB04p03126

Niazi, N.K., Bibi, I., Shahid, M., Ok, Y.S., Shaheen, S.M., Rinklebe, J., Wang, H., Murtaza, B., Islam, E., Farrakh Nawaz, M., Lüttge, A., 2018. Arsenic removal by Japanese oak wood biochar in aqueous solutions and well water: Investigating arsenic fate using integrated spectroscopic and microscopic techniques. Science of the Total Environment 621, 1642–1651. https://doi.org/10.1016/j.scitotenv.2017.10.063

Rehman, S. ur, Khan, A.R., Sahiner, M., Sengel, S.B., Aktas, N., Siddiq, M., Sahiner, N., 2017. Removal of arsenate and dichromate ions from different aqueous media by amine based p(TAEA-co-GDE) microgels. Journal of Environmental Management 197, 631–641. https://doi.org/10.1016/j.jenvman.2017.04.053

Repo, E., Mäkinen, M., Rengaraj, S., Natarajan, G., Bhatnagar, A., Sillanpää, M., 2012. Lepidocrocite and its heat-treated forms as effective arsenic adsorbents in aqueous medium. Chemical Engineering Journal 180, 159–169. https://doi.org/10.1016/j.cej.2011.11.030

Safi, S.R., Gotoh, T., Iizawa, T., Nakai, S., 2019a. Development and regeneration of composite of cationic gel and iron hydroxide for adsorbing arsenic from ground water. Chemosphere 217, 808–815. https://doi.org/10.1016/j.chemosphere.2018.11.050

Safi, S.R., Gotoh, T., Iizawa, T., Nakai, S., 2019b. Removal of Arsenic Using a Cationic Polymer Gel Impregnated with Iron Hydroxide. Journal of Visualized Experiments e59728. https://doi.org/10.3791/59728

Sahiner, N., Demirci, S., Sahiner, M., Yilmaz, S., Al-Lohedan, H., 2015. The use of superporous p(3-acrylamidopropyl)trimethyl ammonium chloride cryogels for removal of toxic arsenate anions. Journal of Environmental Management 152, 66–74. https://doi.org/10.1016/j.jenvman.2015.01.023

Takada, T., Kiyama, M., Bando, Y., Nakamura, T., Shiga, M., Shinjo, T., Yamamoto, N., Endoh, Y., Takaki, H., 1964. Mössbauer Study of α -, β- and γ-FeOOH. Journal of the Physical Society of Japan 19, 1744. https://doi.org/10.1143/JPSJ.19.1744

Tang, L., Feng, H., Tang, J., Zeng, G., Deng, Y., Wang, J., Liu, Y., Zhou, Y., 2017. Treatment of arsenic in acid wastewater and river sediment by Fe@Fe2O3 nanobunches: The effect of environmental

conditions and reaction mechanism. Water Research 117, 175–186. https://doi.org/10.1016/j.watres.2017.03.059

Wang, X., Chen, X., Gao, L., Zheng, H., Mingrong, J., Chenming, T., Tao, S., Zhang, Z., 2004. Synthesis of b-FeOOH and a-Fe2O3 nanorods and electrochemical properties of b-FeOOH. J. Mater. Chem. 14, 905–907. https://doi.org/10.1007/s13204-014-0395-1

Yanagita T., Jiang Y., Nakamura M., 2013. Arsenic Adsorption Properties of New Iron Hydroxide. Journal of Japan Society on Water Environment 36, 149–155. https://doi.org/10.2965/jswe.36.149

Zhang, G.-S., Qu, J.-H., Liu, H.-J., Liu, R.-P., Li, G.-T., 2007. Removal Mechanism of As(III) by a Novel Fe−Mn Binary Oxide Adsorbent: Oxidation and Sorption. Environ. Sci. Technol. 41, 4613–4619. https://doi.org/10.1021/es063010u

Chapter 4: Removal of As(III) using DMAPAAQ+FeOOH

4.1. Introduction

Arsenic is a toxic element. The followings are the most commonly found types of arsenic in the environment: 1. Arsenate, As(V) and 2. Arsenite, As(III). The most predominant arsenic species in groundwater is As(III), which has a toxicity of 25–60 times that of As(V) (Korte and Fernando, 1991). This chapter emphasizes on removal of As(III) from aqueous solutions using the polymer gel composite.

Some ion-imprinting polymers have been created and used in recent years due to their extraordinary ability to detect specific ions (Ashraf et al., 2011; Chang et al., 2011). Because of their unique cavity structure and specialized adsorption sites that are complementary to the target ions, ion imprinted polymers (IIPs) offer an unequaled advantage in selective adsorption and recovery of heavy metals (Fu et al., 2015; Rao et al., 2006). Imprinted polymer adsorbents of various types have been made and used to selectively remove heavy metal cations, such as Cu (Hoai et al., 2010), Cd (Zhu et al., 2017), Ni (Saraji and Yousefi, 2009), and Pb (Liu et al., 2011). However, arsenic species in natural waters generally exist as oxyanions ($H_2AsO_3^-$, $HAsO_3^{2-}$) rather than as metal cations. The charge-to-radius ratios of metal anions are 3–5 times lower than those of metal cations (Alizadeh et al., 2016), with functional monomers or ligands, this lowers the electrostatic impact, making it harder to generate particular recognition sites. Second, anions are difficult to dissolve in the nonpolar

imprinting chemicals often utilized. Metal anions are rarely used as templates in ion imprinting for the two reasons stated above (Fang et al., 2018)

In chapter 2, a composite of polymer gel, *N,N*-dimethylamino propylacrylamide, methyl chloride quaternary (DMAPAAQ), and Iron Hydroxide (FeOOH) was developed and it's mechanism to adsorb As(V) was elaborated. The maximum As(V) adsorption capacity by the gel was 123.4 mg/g, which is higher than the other adsorbents previously developed. The gel selectively adsorbed arsenic in the presence of Sulphate ($SO4^{2-}$) and Chloride (Cl^{-}) solutions. Also, the gel could be regenerated with 87.6% efficiency when the experiment was continued for eight consecutive days, with NaCl being used for desorption, instead of harmful NaOH (Safi et al., 2019a, 2019b).

In chapter 3, the causes of the high amount of adsorption of As(V) by DMAPAAQ+FeOOH gel was explained. In addition, the changes in the surface functional groups due to the adsorption of arsenic was examined. Also, characterization of the adsorbent, DMAPAAQ+FeOOH, was experimented. The content and type of FeOOH inside the gel composite was also examined and related with the reason behind high arsenic adsorption (Safi et al., 2019c).

Diverse processes have been developed for As(III) oxidation, such as chemical oxidants (chlorine, permanganate, etc.) (Sorlini and Gialdini, 2010) and advanced oxidation processes (AOPs) (UV/H_2O_2) (Sorlini et al., 2010), Fenton reaction (Hug and Leupin, 2003), UV/nitrite (Kim et al., 2014), UV/peroxydisulfate (Neppolian et al., 2008), and PMS (Wang et al., 2014). The major concern for conventional chemical oxidants (chlorine, chloramine

and ozone) is the potential generation of toxic byproducts, such as trihalomethane, nitrosoamine and bromate (Sharma and Sohn, 2009). The UV based AOPs require special reaction devices. Drawbacks of Fenton process are its strong pH-dependence and sludge generation. In contrast, PMS is a relatively benign oxidant because its end products (SO_4^{2-}) are normally inert and nonpolluting. Additionally, solid PMS is easier to handle compared to liquid or gas oxidants. However, the direct oxidation of As(III) by PMS is limited and time-consuming. Moreover, extra processes are required to remove the resulting As(V) and residual As(III).

Heterogeneous catalytic process coupling oxidation with adsorption will simplify the overall removal process (Kim et al., 2015; Önnby et al., 2014; Voegelin and Hug, 2003). Metal oxides are a major class of catalysts used in heterogeneous oxidation process (Lei et al., 2015). Meanwhile, they can work as efficient adsorbents for arsenic adsorption (Lata and Samadder, 2016; Wei et al., 2019).

In this chapter, specifically, To assure the elimination of As(III), a heterogeneous catalytic oxidation system may be built by combining iron oxides with cationic polymer gel. As(III) is harder to remove than As(V) (Deng et al., 2018). But the system integrating oxidation and adsorption will simplify the removal process. In the system, the γ-FeOOH particles are the predominant oxidant species for the oxidation of As(III). Because of possible synergistic effects, composite adsorbents of iron oxides coupled with other metal oxides were more effective for As removal than their separate oxides (Andjelkovic et al., 2014; Meng et al., 2018; Wei et al., 2018).

The later part of this chapter examined whether As(III) can be removed effectively at neutral pH levels by DMAPAAQ+FeOOH. In addition, the regeneration efficiency of DMAPAAQ+FeOOH gel in removing As(III) was compared to that of previously discussed (in chapter 2) 87.6% removal efficiency while removing As(V). Also, the selectivity of As(III) adsorption in the presence of sulphate and chloride was discussed.

4.2. Materials and Methods

4.2.1 Materials

The monomer, *N,N'*-Dimethylaminopropyl acrylamide, methyl chloride quaternary (DMAPAAQ) (75% in H_2O) was supplied by KJ Chemicals Corporation, Tokyo, Japan. The crosslinker, *N,N'*-methylene bisacrylamide (MBAA), and the As(III) source, sodium (meta)arsenite, were purchased from Sigma-Aldrich, St. Louis, MO, USA. The accelerator, sodium sulphite (Na_2SO_3), the arsenic(V) source, disodium hydrogen arsenate heptahydrate ($Na_2HAsO_4.7H_2O$), the adsorbents, activated charcoal and silica gel, and ferric chloride ($FeCl_3$) were purchased from Nacalai Tesque, Inc., Kyoto, Japan. Sodium hydroxide (NaOH) was purchased from Kishida Chemicals Corporation, Osaka, Japan. The monomer, *N,N'*-Dimethylacrylamide (DMAA) were purchased from TCI, Japan. The initiator, ammonium peroxodisulfate (APS) was purchased from Kanto Chemical Co. Inc., Tokyo, Japan.

4.2.2 Synthesis of the Polymer Gels and Composites

The polymer gels DMAPAAQ and DMAPAAQ + FeOOH were prepared by the free-radical polymerisation method described in chapter 2 and also in chapter 3. The amounts of the crosslinker, initiator, and accelerator were identical in the compositions of DMAPAAQ, DMAPAAQ + FeOOH, and DMAA + FeOOH. For the composites DMAPAAQ + FeOOH and DMAA + FeOOH, $FeCl_3$ and NaOH were added to impregnate the iron components in the polymer gel structure. The reason for adding NaOH was that NaOH reacted with $FeCl_3$

during the polymerisation. Consequently, the majority of the FeOOH particles were produced inside the gel structure.

4.2.3 Adsorption Experiment

To perform the As (III)-adsorption experiment, 20 mg of dried gel composite (DMAPAAQ + FeOOH) was added to 40 mL of As (III) solution in a small beaker and stirred at 120 rpm at 20 °C for 24 h. The experiments were conducted with solutions of higher As (III) concentrations to evaluate the maximum effectiveness of the adsorbents at the removal of As (III). I experimented at 20 °C to maintain natural conditions. Following this, a 35 mL sample was collected using a syringe. The amount of As(III) remaining in the solution was measured by inductively coupled plasma mass spectrometry (ICP-MS). The amount of As(III) adsorbed was measured using Equation (1).

$$Q = [(C_0 - C_v) * V]/m \quad 1)$$

where Q is the amount of As(III) adsorbed [mol/g], C_0 is the initial concentration [mol/L], C_v is the equilibrium concentration [mol/L], V is the volume of the solution [L], and m is the mass of the adsorbent [g].

To investigate the pH-sensitivity, 20 mg of dried DMAPAAQ + FeOOH were added to 40 mL of As(III) solution. Additionally, HCl and NaOH were added to the solution to obtain different pH values in the range of 2–11). The solution was subsequently placed in a

small beaker and stirred at 120 rpm at 20 °C for 24 h. Thereafter, 35 mL of the sample was collected using a syringe. The amount of As(III) remaining in the solution was measured using ICP-MS.

4.2.4 Fourier Transform Infrared Spectroscopy

FTIR spectroscopy (IR-Prestige 21, Shimadzu, Kyoto, Japan) was used to examine the changes in the surface functional groups of DMAPAAQ + FeOOH following the adsorption of As(III). The concentration of the As(III) solution, prepared using distilled water, was 50 mg/L. To adsorb As(III), 20 mg each of dried DMAPAAQ + FeOOH was immersed in a 50 mg/L As(III) solution for 24 h at 25 °C. Subsequently, the As(III)-loaded gel pieces were carefully separated from the solutions and dried in an oven at 50 °C for 24 h. FTIR spectra were recorded in the wavelength range of 400–4000 cm^{-1} for DMAPAAQ + FeOOH and it's respective Mn-loaded samples. Potassium bromide (KBr)-pellet technique was used for FTIR analysis.

4.2.5 pH sensitivity of DMAPAAQ+FeOOH gel composite

To perform the pH sensitivity experiment, 20 mg of dried DMAPAAQ+FeOOH gel composite was added in 40 mL of As(III) solution. Additionally, HCl and NaOH were added to the solution to obtain different pH values. The solution was then placed in a small beaker and was kept in the stirrer at 120 rpm rotation, at 20°C for 24 hours. Following this, 35 ml

sample was collected using a syringe. The remaining amount of arsenic present in the solution was measured by inductively coupled plasma mass spectrometry (ICP-MS).

4.2.6 Regeneration of DMAPAAQ+FeOOH gel composite for arsenic adsorption

To test the regeneration of the DMAPAAQ+FeOOH gel composite, the adsorption-desorption experiment was conducted repeatedly for eight days. The adsorption experiment was conducted using 25 mg/L As(III) solution. The details of the adsorption operation are the same which were described in the section 2.3. After the adsorption experiment, samples were collected for measuring the remaining As(III) in the water. The gels were separated and washed with deionized water five times so as to remove external As(III) from the gel surface. Following this, the gel was added to 0.5 M 40 mL NaCl solution to perform the desorption experiment under the same conditions as the adsorption experiment. Samples were collected in the same way as previously mentioned to measure desorbed arsenic in the NaCl solution. This adsorption-desorption cycle was performed for eight days.

4.2.7 Selectivity of arsenic adsorption

To evaluate the selective adsorption of As(III) by the gel composites, the adsorption experiments were conducted using 20mg dried adsorbent. The adsorbent was added to a 40 mL solution of 25 mg/L As(III) and different concentrations of Na_2SO_4 and NaCl. The solutions were then magnetically stirred for 24 hours at 20°C and 120 rpm. The samples were

collected using a syringe and the remaining amount of arsenic present in the solution was measured by inductively coupled plasma mass spectrometry (ICP-MS).

4.2.8 X-Ray Photoelectron Spectroscopy (XPS) Analysis

The XPS analysis was conducted using an ESCA 3400 Electron spectrometer by Kratos Analytical Ltd., UK. I grinded 0.2 mg of DMAPAAQ + FeOOH gel into fine powder and placed the powder into glass film designated for XRD experiment. About 20 mg of dried DMAPAAQ + FeOOH gel pieces were immersed in 50 mg/L As(III) solution. The solution was then placed in a shaker for almost 9 hours at 25°C and 120 rpm. The gels were then collected and dried in the oven at 70°C for 12 hours. After drying, the gels were grinded with a mortar into fine powder, which was used for the experiment.

4.3. Results and Discussion

4.3.1 Adsorption of As (III) using the cationic gel composite

Table 4.1. Adsorption isotherm parameters for the adsorption of As(III) on DMAPAAQ + FeOOH.

Isotherm Parameter			**As (III)**
	R^2		0.986
Langmuir model	Q_{max}, mg/g	mg/g	27.68
		mmol/g	0.37

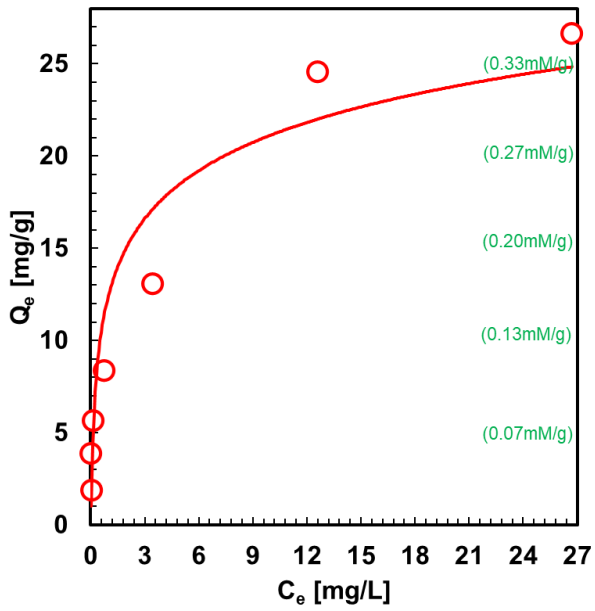

Figure 4.1. Amount of As (III) adsorbed by DMAPAAQ + FeOOH at different initial concentrations of As (III) solution.

Figure 4.1 shows that the amount of As(III) adsorption increased with increasing As(III). The plot of Langmuir model for As(III) are highlighted in **Table 4.1**. From the correlation coefficients (R^2), the experimental data for As(III) adsorption more accurately fitted the Langmuir model. It suggests that As(III) ions were adsorbed as a multilayer on the sorbent surface. This may reflect the irregular energy distribution on the adsorbent surface due to the presence of different groups (i.e., amide and $–N^+(CH_3)_3$ functionalities) with different activation energies (Constantin et al., 2013; Imyim et al., 2016). The highest capacity of adsorption of As(III) on DMAPAAQ+FeOOH was as high as 27.68 mg/g. Hence, the interaction between As(III) and the adsorbent is strong.

The adsorption amount of As(III) is lower than that of As(V) in chapter 2. In (Imyim et al., 2016)solution, As(III) exists primarily as H_3AsO_3 and, to a marginal extent, as $H_2AsO_3^-$ (Sharma and Sohn, 2009). Therefore, only weak adsorption was expected. (Imyim et al., 2016). Due to its nonionic nature, As(III) has a lesser affinity for the adsorbent than As(V) (Andjelkovic et al., 2015; Luo et al., 2016). In the case of As(V), adsorption occurred directly between the As(V) ion and the gel surface. But in the case of As(III) adsorption, the adsorption relies heavily on the surface hydroxyl groups (-OH) on metal oxide adsorbents (Wei et al., 2019). As a result, there was first the conversion of As(III) to As(V) through oxidation by γ-FeOOH and then adsorption of As(V) occurred by both the amino group of DMAPAQ and FeOOH particles.

4.3.2 X-Ray Photoelectron Spectroscopy (XPS) Analysis of As(III) adsorption on DMAPAAQ+FeOOH gel

The surface of DMAPAAQ + FeOOH gel composite was examined using XPS to verify the presence of As(III) following the adsorption process. The sample was analyzed with XPS. The sample consisted of DMAPAAQ + FeOOH gel adsorbed with 50 mg/L of As(III) solution (**Fig. 4.2**). The result of XPS analysis of the sample are shown in Fig. 4.2. It was found that the sample of DMAPAAQ + FeOOH gel reacted with As (III) in the presence of the As3d core level peak.

In Fig. 4.2, the XPS of the As3d peaks indicate the presence of arsenic on the surface of DMAPAAQ + FeOOH gel composite. The XPS spectrum of As 3d confirmed the

coexistence of As (III) in the structure of the polymer gel composite. The As3d binding energies was 44.23 eV for sample reacted with As(III).

The shape of the peak notifies the presence of a single species contributor. When arsenic was adsorbed to cupric oxide nanoparticles, similar results were obtained. Martinson and Reddy (2009) reported that in such cases, adsorption of As(III) involves a process of oxidation prior to adsorption (Martinson and Reddy, 2009). In addition, similar findings were also reported when Fe-Mn binary oxide adsorbent was used to adsorb arsenic (Zhang et al., 2007) and when arsenic was adsorbed by Zeolite supported nanoscale zero-valent iron (Li et al., 2018).

Therefore, the oxidation of As (III) to As (V) occurred in the adsorption process of arsenic by DMAPAAQ + FeOOH gel composite.

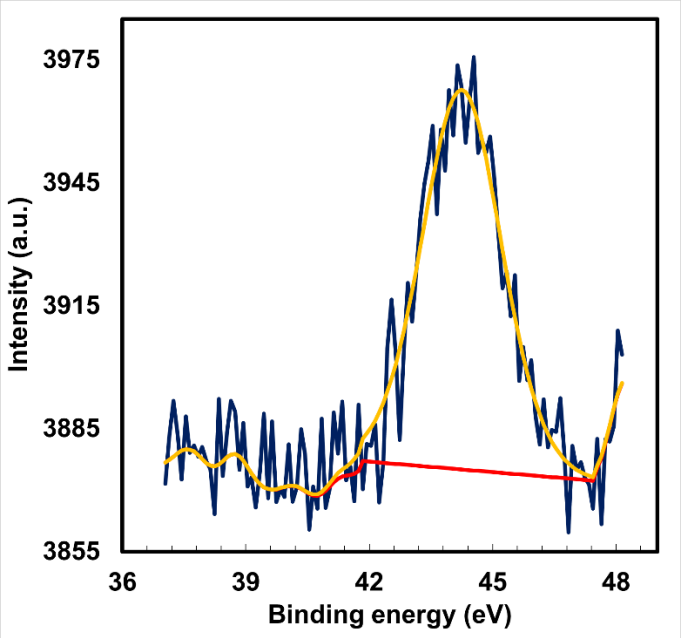

Figure 4.2. XPS Analysis of As(III) adsorption on DMAPAAQ+FeOOH gel .

4.3.3 Effect of pH

The pH sensitivity of DMAPAAQ+FeOOH gel composite was examined. The experiment was conducted with 25 mg/L of As(III) solution. Different concentration of HCl and NaOH was used along with the arsenic solution to obtain arsenic adsorption levels at different pH values. **Fig. 4.3** shows that, at low pH values, the amount of adsorption is lower, also at high pH values, the amount of adsorption is lower. Favourable adsorption of As (III) efficiency was achieved in the pH range from 4 to 9. At pH values between 4 and 9, the ionic attraction between negatively charged arsenic species and positively charged amino group of DMAPAAQ occurred more strongly (Imyim et al., 2016).

Results suggest that, at the neutral pH value, the highest amount of adsorption of arsenic was observed. As the pH values went from acidic to neutral gradually, the amount of arsenic adsorption increased. In real life conditions, where the pH of water is neutral (around 7), the adsorption capability of DMAPAAQ+FeOOH is highest.

Similar to the results in chapter 2, when the pH level was high, in the solution of As(III), in the form of anions, the electrostatic repulsion between OH^- and As(III) ions rises, resulting in a decrease in As(III) adsorption rate (Chi et al., 2021). As a result, at higher pH levels, adsorption did not occur. On the other hand, the protonation of the functional groups of the functional monomers of the polymer, which leads to a drop in coordination ability and the difficulty of complexing with the template ions, is blamed for the decrease in adsorption capacity at lower pH and such a situation was not favourable for As (III) removal (Chi et al., 2021; Goswami et al., 2012; Li et al., 2010). Therefore, adsorption amount of As (III) was low at low pH levels.

It is a significant finding because, as discussed previously in the “introduction” section, most of the polymer gels and other adsorbents fail to adsorb As(V) effectively at the neutral pH levels. Therefore, the remainder of the experiments were conducted with neutral pH values, taking into consideration real-life conditions of arsenic affected water.

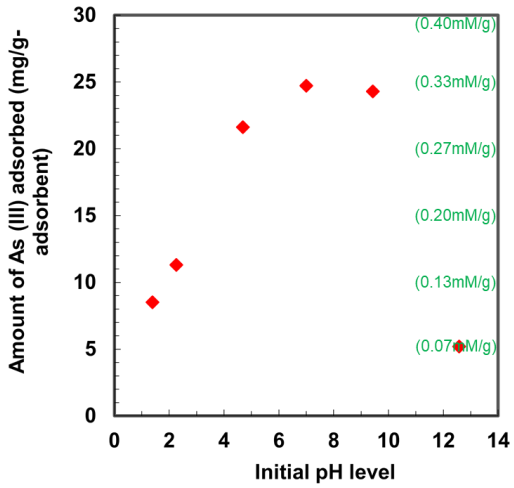

Figure 4.3. pH sensitivity analysis.

4.3.4 Surface Functional Group Characterisation Using FTIR Spectroscopy

The FTIR spectra of As(III) loaded DMAPAAQ+FeOOH gel composite revealed a shift in the position of some spectral peaks. **Fig. 4.4** and **Table 4.2** shows the FTIR spectral bands of DMAPAAQ+FeOOH (blue line) and As(III) loaded (red line) to determine the changes in surface functional groups in DMAPAAQ+FeOOH gel composite due to arsenic adsorption. In the As(III) loaded DMAPAAQ+FeOOH gel composite (red line in Fig. 4.4), the spectral bands at 3414, 3074, 2945, 2144, 1396, 1267, 1116, 889 and 619 cm^{-1} were shifted to 3433, 3066, 2935, 2160, 1382, 1265, 1110, 885 and 615 cm^{-1}, respectively, after the As(III) impregnation of DMAPAAQ+FeOOH gel composite. I ascribed this to the vibration of the Aliphatic primary amine N-H stretching, Alcohol O-H stretching, Amine salt N-H stretching, Alkyne C≡C stretching, Aldehyde C-H bending, Aromatic ester C-O stretching, Secondary alcohol C-O stretching, and 1,2,4-trisubstituted C-H bending groups.

In addition, the spectral peaks at 2598, 2567 and 2522 cm^{-1} (Carboxylic acid O-H stretching) disappeared. The spectral bands at 3277 (Alcohol O-H stretching), 1481 (Alkane C-H bending), 1338 (Alcohol O-H bending), 968 cm^{-1} (Alkene C=C bending) were the same for the DMAPAAQ+FeOOH gel composites and As(III) loaded DMAPAAQ+FeOOH gel composites.

The analysis suggests that ion exchange and surface complexation reactions occurred in the gel composite. The shifts in the spectral bands denote that As(III) changed the surface functional characteristics of DMAPAAQ+FeOOH gel composite, by being highly adsorbed in the structure of the gel composite. Some of the groups found in As(III) stretching group were: Primary amine N-H stretching group, alkyne C≡C stretching, alkene C=C stretching, alkane C-H bending, aldehyde C-H bending, aromatic ester C-O stretching, secondary alcohol C-O stretching, strong alkene C=C bending.

Referring to the "Arsenic adsorption isotherm" section from the previous chapter, the maximum capability of adsorption of arsenic by DMAPAAQ+FeOOH was higher when compared with the other currently studied methods at neutral pH levels. The higher adsorption capability has strong correlation with the FTIR analysis because the N-H stretching groups shift due to the adsorption of As(III) to DMAPAAQ+FeOOH. Furthermore, a change (disappearance) was observed in O-H stretching groups after the impregnation of As(III) to DMAPAAQ+FeOOH. The arsenic adsorption mechanisms discussed in the previous chapter also supports the above hypothesis.

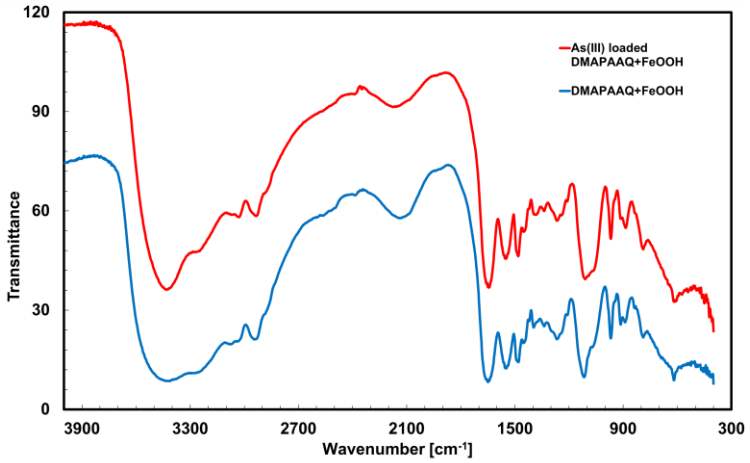

Figure 4.4. Comparative FTIR analysis of DMAPAAQ + FeOOH and As(III) loaded DMAPAAQ + FeOOH.

Table 4.2. FTIR spectroscopy peak analysis.

Wavelength	**DMAPAAQ+ FeOOH**	**As(III) loaded DMAPAAQ+FeOOH**	**Group**	**Compound Class**	**Strength**
615					
619					
623					
788			C-H Bending	1,2,3-trisubstituted	Strong
790					
885					Strong

889	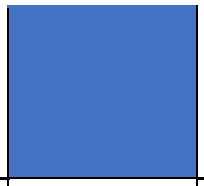		C-H Bending	1,2,4-trisubstituted	
906			C=C Bending	Alkene	Strong
914					
968					
1099			C-O Stretching	Secondary alcohol C-0	Strong
1110					
1114					
1116					
1141			C-O Stretching	Tertiary alcohol	Strong
1255			C-O Stretching	Aromatic ester	Strong
1265					
1267					
1269					
1336			O-H Bending	Alcohol	Medium
1338					

1355					
1382			C-H Bending	Aldehyde	Medium
1388					
1396					
1400					
1454			C-H Bending	Alkane	Medium
1481					
1485					
1494					
1625			C=C Stretching	Alkene	Medium
1643					
1649					
2112			C≡C Stretching	Alkyne	Weak
2123					
2144					
2160					

2212					
2326			O=C=O Stretching	Carbon di oxide	Strong
2347					
2522			O-H Stretching	Carboxylic acid	Strong, broad
2561					
2567					
2596					
2598					
2929			N-H Stretching	Amine salt	Strong, broad
2933					
2935					
2945					
3064			O-H Stretching	Alcohol	Weak, broad
3066					
3074					
3277				Alcohol	

3282					Strong, broad
3414			N-H Stretching	Aliphatic primary amine	Medium
3417					
3421					
3433					

4.3.5 Selective adsorption of As (III) by DMAPAAQ + FeOOH

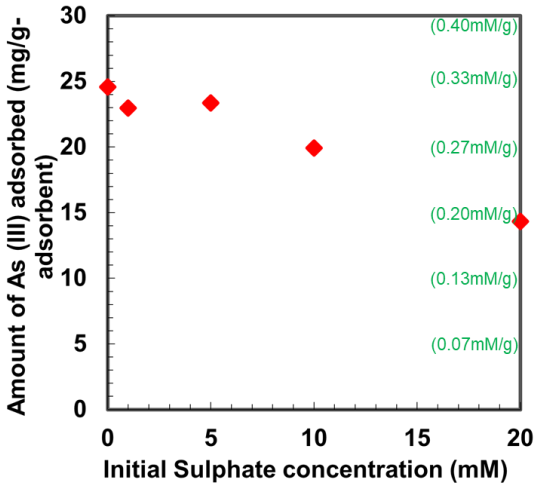

Figure 4.5. Sulphate selectivity.

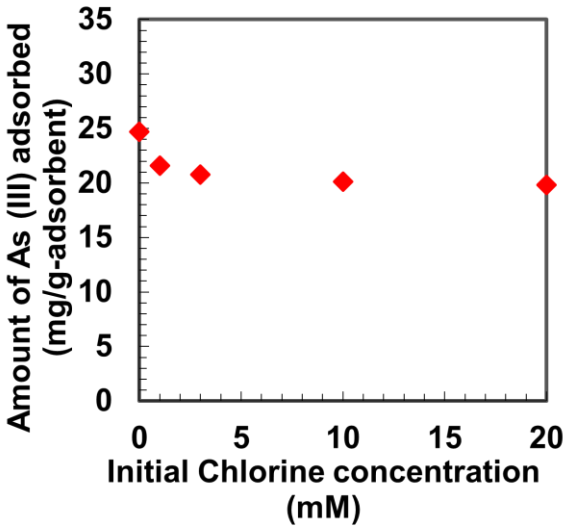

Figure 4.6. Chlorine selectivity.

The selectivity of As(III) adsorption was examined in the presence of Sulphate and Chloride ion. Besides arsenic, the groundwater contains various ions such as CO_3^{2-}, HCO_3^-, H_2CO_3, Cl^-, SO_4^{2-}, SO_3^{2-}, HS^- (Chaplin et al., 2006). According to the Hofmeister series, the ratio of the oscillator strengths from the methyl symmetric stretch and the methylene symmetric stretch of Sulphate ion ($SO4^{2-}$) was highest. Therefore, Sulphate ion ($SO4^{2-}$) has the ability to penetrate the headgroup region of the monolayer and can disrupt the hydrocarbon packing (Zhang and Cremer, 2006). In groundwater, concentration of Sulphate can be as high as 230 mg/L (Fawell et al., 2004). Therefore, I chose SO_4^{2-} ion to examine the selectivity of arsenic by our gel composite, because if DMAPAAQ+FeOOH can adsorb As(III) from the solution of mixture of As(III) and Na_2SO_4 effectively, then the presence of other ions will also not affect the capability of arsenic adsorption by the adsorbent. This experiment is important, because in real life, water does not only contain As(III), but also many other ions. The effect of SO_4^{2-} concentration on the adsorption of As(III) by DMAPAAQ+FeOOH is shown in **Fig. 4.5**. The results suggested that the adsorption amount decreased as the SO_4^{2-} increased in the solution. However, adsorption of As(III) could still be achieved when the concentration of SO_4^{2-} was as high as 20 mM.

In the case of amino group of DMAPAAQ+FeOOH, As(III) is adsorbed through ionic interaction with the amino group. When the initial sulfate ion concentration is increased, the sulfate ion acts as an anion, which inhibits the adsorption of As(III), causing the amount of arsenic adsorption to be decreased drastically, which was previously proved in chapter 2. On the other hand, the FeOOH particles help to retain the adsorption performance because the efficiency of the FeOOH particles in adsorbing As(III) do not get hampered by the presence

of sulphate ions. This is because the iron hydroxide can selectively adsorb arsenic by complex adsorption. Therefore, DMAPAAQ+FeOOH gel composite can selectively adsorb As(III) from water.

Hence, while considering the combination of the amino group and particles of FeOOH in the DMAPAAQ+FeOOH gel composite, though the adsorption amount of As(III) slightly reduced if compared to no sulphate presence with the solution of 20 mM of sulphate, but the adsorption of As(III) could be occurred mainly due to the presence of high content of FeOOH.

The effect of Cl^- concentration on the adsorption of As(III) by DMAPAAQ+FeOOH is also examined and is shown in **Fig. 4.6**. The results suggested that the adsorption amount decreased slightly when the Cl^- concentration was increased from 0 to 3 mM. However for the later concentrations of Cl^- upto 20 mM, the adsorption amount remained constant.

As(III) is adsorbed through ionic interaction with the amino group. When the initial chloride ion concentration is increased, the chloride ion acts as an anion, which inhibits the adsorption of As(III) by the amino group, causing the amount of arsenic adsorption to be decreased slightly. Although, the amino group of DMAPAAQ + FeOOH exchanges As(III) ion with Cl^- , the FeOOH particles do not exchange the same. Hence, the FeOOH particles continue adsorbing As(III), not Cl^-. Therefore, the FeOOH particles help to retain the adsorption performance because the efficiency of the FeOOH particles in adsorbing As(III) do not get hampered by the presence of Cl^- ions. Therefore, the selectivity of adsorption of arsenic by DMAPAAQ + FeOOH could be achieved, when Cl^- was added with As(III)

solution. This finding in important because, the groundwater contain Cl^- ion. This is because the iron hydroxide can selectively adsorb arsenic by complex adsorption. Therefore, DMAPAAQ+FeOOH gel composite can selectively adsorb As(III) from water and is a better adsorbent than DMAPAAQ gel.

4.3.6 Regeneration of DMAPAAQ+FeOOH gel composite

Regeneration is an important characteristic for an adsorbent because it helps to reduce cost, increase the usability, make the adsorbent eco-friendly and ensures easy handling (Rehman et al., 2016). As a result, industrial manufacturing of the adsorbent is possible. **Fig. 4.7** shows the regeneration of DMAPAAQ+FeOOH gel composite. The adsorption of As(III) is performed in 25 mg/L solution and the desorption of arsenic is performed in 0.5 mol/L NaCl solution. The adsorption-desorption process was continued for eight consecutive days.

The efficiency of the regeneration process was calculated using the data of the amount of adsorption of arsenic by DMAPAAQ+FeOOH gel composite on day 1 and day 7. It was found that the efficiency of the regeneration process is 48.7%. The reduction of the efficiency of the regeneration process can be attributed because of two reasons. One reason is the loss of adsorption sites. Some amino groups of DMAPAAQ and also the FeOOH, in DMAPAAQ+FeOOH gel composite, did not desorb the adsorbed arsenic ions effectively in the NaCl solution during the desorption process. A similar trend was also observed while adsorbing As(V) on biochar (He et al., 2018) and also As(V) regeneration by DMAPAAQ+FeOOH in chapter 2.

Another reason behind the regeneration efficiency of As(III) is lower than that of As(V) in chapter 2 because in the case of As(V), adsorption occurred directly between the As(V) ion and the gel surface. But in the case of As(III) adsorption, there was first the conversion of As(III) to As(V) through oxidation and then adsorption of As(V) occurred. It is highly likely that the remaining amount of As in the gel after the desorption process is As(III), which did not oxidize during the previous adsorption cycle. Hence, in the following adsorption cycle, besides the amount of As(III) in the solution, the previously retained As(III) inside the gel structure adds up. Which caused the reduction in efficincy of regeneration of As(III) after each cycle of adsorption. However, the 48.7% of regeneration efficiency proves that the gel composite can be reused a few times, which ensures cost reduction.

One of the significant contributions of our research is the use of NaCl for the desorption process for As(III) desorption. Although, NaOH is most widely used for the desorption process, but considering its harmfulness, I experimented the desorption process with NaCl, instead of NaOH. As shown in the Fig. 4.7, the gel composite was successfully regenerated when the adsorption-desorption experimentation was continued for eight consecutive days.

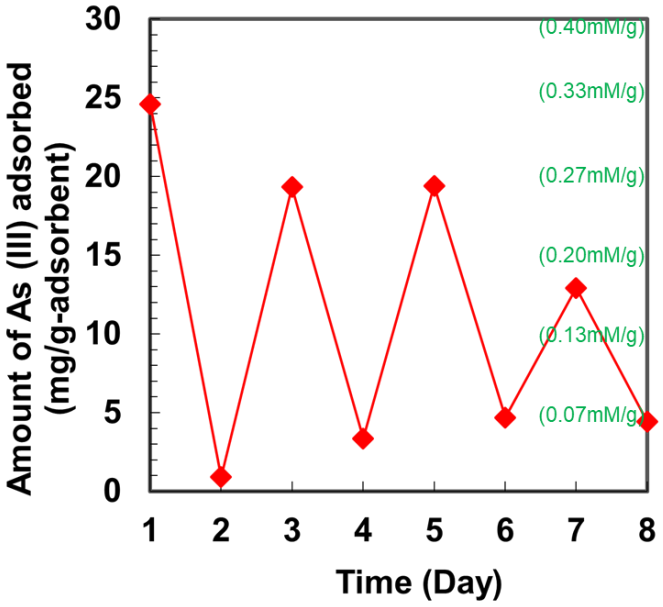

Figure 4.7. Regeneration experiment.

4.4. Conclusions

The pH sensitivity of the gel composite was investigated, and it was discovered that the gel can adsorbs a highest quantity of As(III) at neutral pH levels.

The DMAPAAQ+FeOOH arsenic adsorption isotherm resembles the Langmuir isotherm very well. At neutral pH levels, the maximum adsorption capacity of the DMAPAAQ+FeOOH gel composite (27.68 mg/g) was computed.

The DMAPAAQ+FeOOH gel composite's adsorption mechanism was also described. As(III) was converted to As(V) through oxidation and was then adsorbed on the gel surface by both the amino group and FeOOH particles. In addition, the results indicated that in the presence of Sulphate and Chloride ion, the DMAPAAQ+FeOOH gel composite preferentially adsorbs As(III). As a result, even if other ions are present, the gel composite may preferentially adsorb As(III) from groundwater. As(III) selectivity is provided by the FeOOH in the DMAPAAQ+FeOOH gel composite.

Furthermore, because the gel composite can be renewed, it is both cost-effective and environmentally beneficial. The regeneration experiment was carried out for eight days in a row with an efficiency of 48.7 percent. I investigated the regeneration process in a different way, using NaCl instead of the potentially hazardous NaOH for As(III) desorption. Finally, unlike other techniques now in use, DMAPAAQ+FeOOH does not require any extra separation steps, resulting in easy gel handling and a straightforward adsorption procedure.

In the next chapter, the removal efficiency of Mn by DMAPAAQ+FeOOH will be discussed. Also, the simultaneous removal of As(III), As(V) and Mn will be examined.

References

Alizadeh, T., Sabzi, R.E., Alizadeh, H., 2016. Synthesis of nano-sized cyanide ion-imprinted polymer via non-covalent approach and its use for the fabrication of a CN−-selective carbon nanotube impregnated carbon paste electrode. Talanta 147, 90–97. https://doi.org/10.1016/j.talanta.2015.09.043

Andjelkovic, I., Stankovic, D., Nesic, J., Krstic, J., Vulic, P., Manojlovic, D., Roglic, G., 2014. Fe Doped TiO2 Prepared by Microwave-Assisted Hydrothermal Process for Removal of As(III) and As(V) from Water. Ind. Eng. Chem. Res. 53, 10841–10848. https://doi.org/10.1021/ie500849r

Andjelkovic, I., Tran, D.N.H., Kabiri, S., Azari, S., Markovic, M., Losic, D., 2015. Graphene Aerogels Decorated with α-FeOOH Nanoparticles for Efficient Adsorption of Arsenic from Contaminated Waters. ACS Appl. Mater. Interfaces 7, 9758–9766. https://doi.org/10.1021/acsami.5b01624

Ashraf, S., Cluley, A., Mercado, C., Mueller, A., 2011. Imprinted polymers for the removal of heavy metal ions from water. Water Science and Technology 64, 1325–1332. https://doi.org/10.2166/wst.2011.423

Chang, L., Wu, S., Chen, S., Li, X., 2011. Preparation of graphene oxide–molecularly imprinted polymer composites via atom transfer radical polymerization. J Mater Sci 46, 2024–2029. https://doi.org/10.1007/s10853-010-5033-z

Chi, Z., Zhu, Y., Liu, W., Huang, H., Li, H., 2021. Selective removal of As(III) using magnetic graphene oxide ion-imprinted polymer in porous media: Potential effect of external magnetic field. Journal of Environmental Chemical Engineering 9, 105671. https://doi.org/10.1016/j.jece.2021.105671

Constantin, M., Asmarandei, I., Harabagiu, V., Ghimici, L., Ascenzi, P., Fundueanu, G., 2013. Removal of anionic dyes from aqueous solutions by an ion-exchanger based on pullulan microspheres. Carbohydrate Polymers 91, 74–84. https://doi.org/10.1016/j.carbpol.2012.08.005

Fang, L., Min, X., Kang, R., Yu, H., Pavlostathis, S.G., Luo, X., 2018. Development of an anion imprinted polymer for high and selective removal of arsenite from wastewater. Science of The Total Environment 639, 110–117. https://doi.org/10.1016/j.scitotenv.2018.05.103

Fu, J., Chen, L., Li, J., Zhang, Z., 2015. Current status and challenges of ion imprinting. J. Mater. Chem. A 3, 13598–13627. https://doi.org/10.1039/C5TA02421H

Goswami, A., Raul, P.K., Purkait, M.K., 2012. Arsenic adsorption using copper (II) oxide nanoparticles. Chemical Engineering Research and Design 90, 1387–1396. https://doi.org/10.1016/j.cherd.2011.12.006

He, R., Peng, Z., Lyu, H., Huang, H., Nan, Q., Tang, J., 2018. Synthesis and characterization of an iron-impregnated biochar for aqueous arsenic removal. Science of The Total Environment 612, 1177–1186. https://doi.org/10.1016/j.scitotenv.2017.09.016

Hoai, N.T., Yoo, D.-K., Kim, D., 2010. Batch and column separation characteristics of copper-imprinted porous polymer micro-beads synthesized by a direct imprinting method. Journal of Hazardous Materials 173, 462–467. https://doi.org/10.1016/j.jhazmat.2009.08.107

Hug, S.J., Leupin, O., 2003. Iron-Catalyzed Oxidation of Arsenic(III) by Oxygen and by Hydrogen Peroxide: pH-Dependent Formation of Oxidants in the Fenton Reaction. Environ. Sci. Technol. 37, 2734–2742. https://doi.org/10.1021/es026208x

Imyim, A., Sirithaweesit, T., Ruangpornvisuti, V., 2016. Arsenite and arsenate removal from wastewater using cationic polymer-modified waste tyre rubber. Journal of Environmental Management 166, 574–578. https://doi.org/10.1016/j.jenvman.2015.11.005

Kim, D., Bokare, A.D., Koo, M. suk, Choi, W., 2015. Heterogeneous Catalytic Oxidation of As(III) on Nonferrous Metal Oxides in the Presence of H2O2. Environ. Sci. Technol. 49, 3506–3513. https://doi.org/10.1021/es5056897

Kim, D., Lee, J., Ryu, J., Kim, K., Choi, W., 2014. Arsenite Oxidation Initiated by the UV Photolysis of Nitrite and Nitrate. Environ. Sci. Technol. 48, 4030–4037. https://doi.org/10.1021/es500001q

Korte, N.E., Fernando, Q., 1991. A review of arsenic (III) in groundwater. Critical Reviews in Environmental Control 21, 1–39. https://doi.org/10.1080/10643389109388408

Lata, S., Samadder, S.R., 2016. Removal of arsenic from water using nano adsorbents and challenges: A review. Journal of Environmental Management 166, 387–406. https://doi.org/10.1016/j.jenvman.2015.10.039

Lei, Y., Chen, C.-S., Tu, Y.-J., Huang, Y.-H., Zhang, H., 2015. Heterogeneous Degradation of Organic Pollutants by Persulfate Activated by CuO-Fe3O4: Mechanism, Stability, and Effects of pH and Bicarbonate Ions. Environ. Sci. Technol. 49, 6838–6845. https://doi.org/10.1021/acs.est.5b00623

Li, Y., Li, X., Dong, C., Qi, J., Han, X., 2010. A graphene oxide-based molecularly imprinted polymer platform for detecting endocrine disrupting chemicals. Carbon 48, 3427–3433. https://doi.org/10.1016/j.carbon.2010.05.038

Li, Z., Wang, L., Meng, J., Liu, X., Xu, J., Wang, F., Brookes, P., 2018. Zeolite-supported nanoscale zero-valent iron: New findings on simultaneous adsorption of Cd(II), Pb(II), and As(III) in aqueous solution and soil. Journal of Hazardous Materials 344, 1–11. https://doi.org/10.1016/j.jhazmat.2017.09.036

Liu, H., Yang, F., Zheng, Y., Kang, J., Qu, J., Chen, J.P., 2011. Improvement of metal adsorption onto chitosan/Sargassum sp. composite sorbent by an innovative ion-imprint technology. Water Research 45, 145–154. https://doi.org/10.1016/j.watres.2010.08.017

Luo, J., Luo, X., Hu, C., Crittenden, J.C., Qu, J., 2016. Zirconia (ZrO2) Embedded in Carbon Nanowires via Electrospinning for Efficient Arsenic Removal from Water Combined with DFT Studies. ACS Appl. Mater. Interfaces 8, 18912–18921. https://doi.org/10.1021/acsami.6b06046

Martinson, C.A., Reddy, K.J., 2009. Adsorption of arsenic(III) and arsenic(V) by cupric oxide nanoparticles. Journal of Colloid and Interface Science 336, 406–411. https://doi.org/10.1016/j.jcis.2009.04.075

Meng, C., Mao, Q., Luo, L., Zhang, J., Wei, J., Yang, Y., Tan, M., Peng, Q., Tang, L., Zhou, Y., 2018. Performance and mechanism of As(III) removal from water using Fe-Al bimetallic material. Separation and Purification Technology 191, 314–321. https://doi.org/10.1016/j.seppur.2017.09.051

Neppolian, B., Celik, E., Choi, H., 2008. Photochemical Oxidation of Arsenic(III) to Arsenic(V) using Peroxydisulfate Ions as an Oxidizing Agent. Environ. Sci. Technol. 42, 6179–6184. https://doi.org/10.1021/es800180f

Önnby, L., Kumar, P.S., Sigfridsson, K.G.V., Wendt, O.F., Carlson, S., Kirsebom, H., 2014. Improved arsenic(III) adsorption by Al2O3 nanoparticles and H2O2: Evidence of oxidation to arsenic(V) from

X-ray absorption spectroscopy. Chemosphere 113, 151–157. https://doi.org/10.1016/j.chemosphere.2014.04.097

Rao, T.P., Kala, R., Daniel, S., 2006. Metal ion-imprinted polymers—Novel materials for selective recognition of inorganics. Analytica Chimica Acta 578, 105–116. https://doi.org/10.1016/j.aca.2006.06.065

Rehman, S. ur, Siddiq, M., Al-Lohedan, H., Aktas, N., Sahiner, M., Demirci, S., Sahiner, N., 2016. Fast removal of high quantities of toxic arsenate via cationic p(APTMACl) microgels. Journal of Environmental Management 166, 217–226. https://doi.org/10.1016/j.jenvman.2015.10.026

Safi, S.R., Gotoh, T., Iizawa, T., Nakai, S., 2019a. Development and regeneration of composite of cationic gel and iron hydroxide for adsorbing arsenic from ground water. Chemosphere 217, 808–815. https://doi.org/10.1016/j.chemosphere.2018.11.050

Safi, S.R., Gotoh, T., Iizawa, T., Nakai, S., 2019b. Removal of Arsenic Using a Cationic Polymer Gel Impregnated with Iron Hydroxide. Journal of Visualized Experiments e59728. https://doi.org/10.3791/59728

Safi, S.R., Senmoto, K., Gotoh, T., Iizawa, T., Nakai, S., 2019c. The effect of γ-FeOOH on enhancing arsenic adsorption from groundwater with DMAPAAQ + FeOOH gel composite. Scientific Reports 9, 11909. https://doi.org/10.1038/s41598-019-48233-x

Saraji, M., Yousefi, H., 2009. Selective solid-phase extraction of Ni(II) by an ion-imprinted polymer from water samples. Journal of Hazardous Materials 167, 1152–1157. https://doi.org/10.1016/j.jhazmat.2009.01.111

Sharma, V.K., Sohn, M., 2009. Aquatic arsenic: Toxicity, speciation, transformations, and remediation. Environment International 35, 743–759. https://doi.org/10.1016/j.envint.2009.01.005

Sorlini, S., Gialdini, F., 2010. Conventional oxidation treatments for the removal of arsenic with chlorine dioxide, hypochlorite, potassium permanganate and monochloramine. Water Research, Groundwater Arsenic: From Genesis to Sustainable Remediation 44, 5653–5659. https://doi.org/10.1016/j.watres.2010.06.032

Sorlini, S., Gialdini, F., Stefan, M., 2010. Arsenic oxidation by UV radiation combined with hydrogen peroxide. Water Science and Technology 61, 339–344. https://doi.org/10.2166/wst.2010.799

Voegelin, A., Hug, S.J., 2003. Catalyzed Oxidation of Arsenic(III) by Hydrogen Peroxide on the Surface of Ferrihydrite: An in Situ ATR-FTIR Study. Environ. Sci. Technol. 37, 972–978. https://doi.org/10.1021/es025845k

Wang, Z., Bush, R.T., Sullivan, L.A., Chen, C., Liu, J., 2014. Selective Oxidation of Arsenite by Peroxymonosulfate with High Utilization Efficiency of Oxidant. Environ. Sci. Technol. 48, 3978–3985. https://doi.org/10.1021/es405143u

Wei, Y., Liu, C., Luo, S., Ma, J., Zhang, Y., Feng, H., Yin, K., He, Q., 2018. Deep oxidation and removal of arsenite in groundwater by rationally positioning oxidation and adsorption sites in binary Fe-Cu oxide/TiO2. Chemical Engineering Journal 354, 825–834. https://doi.org/10.1016/j.cej.2018.08.101

Wei, Y., Liu, H., Liu, C., Luo, S., Liu, Y., Yu, X., Ma, J., Yin, K., Feng, H., 2019. Fast and efficient removal of As(III) from water by CuFe2O4 with peroxymonosulfate: Effects of oxidation and adsorption. Water Research 150, 182–190. https://doi.org/10.1016/j.watres.2018.11.069

Zhang, G.-S., Qu, J.-H., Liu, H.-J., Liu, R.-P., Li, G.-T., 2007. Removal Mechanism of As(III) by a Novel Fe−Mn Binary Oxide Adsorbent: Oxidation and Sorption. Environ. Sci. Technol. 41, 4613–4619. https://doi.org/10.1021/es063010u

Zhu, F., Li, L., Xing, J., 2017. Selective adsorption behavior of Cd(II) ion imprinted polymers synthesized by microwave-assisted inverse emulsion polymerization: Adsorption performance and mechanism. Journal of Hazardous Materials 321, 103–110. https://doi.org/10.1016/j.jhazmat.2016.09.012

Chapter 5: Simultaneous Removal of Arsenic and Manganese from Synthetic Aqueous Solutions Using Polymer Gel Composites

5.1. Introduction

The objective of this chapter is to effectively remove two of the most harmful elements in groundwater, arsenic and manganese, simultaneously and under natural water conditions. Following arsenic (As), Mn is one of the most commonly-found contaminants in most rivers and groundwater in Bangladesh (Sarkar et al., 2019). In addition, As and Mn are among the most critical pollutants of drinking water in the South African region (Verlicchi and Grillini, 2019). The coexistence of As and Mn in groundwater has been reported earlier (Bora et al., 2017). Therefore, the simultaneous removal of As and Mn needs to be studied.

Many studies have been conducted on the removal of As and a few have focused on the removal of Mn. However, studies on simultaneous removal of As and Mn are rare because it is difficult to remove anionic and cationic components using a single adsorbent. Although As and Mn have been removed separately or exclusively (Budinova et al., 2009; Pires et al., 2015), their simultaneous adsorption has not been conducted to date. Two previous studies have reported the removal of As, Mn, and Fe (Bora et al., 2017; Yang et al., 2014) and one study developed a treatment system using coagulation and filtration for the simultaneous removal of As and Mn (Waste, 2010). Although these three studies claimed to remove As, they removed only one oxidation state of arsenic, arsenite (As(III)). In these studies, As(III)

was oxidised by the coexisting MnO_2, resulting in the removal of As(III) and Mn from the initial solution. Furthermore, the influence of the precipitate formed due to the coexistence of As(III) and Mn on the removal efficiencies of the methods has not been investigated using response surface methodology (RSM), microorganisms in a biofilter and the sedimentation-filtration treatment process (Waste, 2010). Furthermore, in solutions containing arsenate (As(V)) and As(III), the extent of simultaneous removal of As and Mn would differ, because As(V) is not oxidised by MnO_2. Furthermore, no studies were found on the simultaneous removal of Mn and total As. Finally, the changes in the surface functional groups were not investigated using Fourier transform infrared (FTIR) spectroscopy, and the adsorption mechanisms were not confirmed in the aforementioned works. Therefore, I have conducted a pioneering study on the simultaneous removal of total As and Mn using a single polymer-based adsorbent, without requiring additional separation processes.

It has been reported that γ-FeOOH effectively removes Mn (Sung and Morgan, 1981). However, the efficient removal of Mn was achieved at a high pH. Furthermore, the performance of γ-FeOOH at removing Mn from water under natural conditions was not evaluated. The impregnation of Fe in adsorbents such as pumice increased the adsorption of Mn by approximately 14 times (Çifçi and Meriç, 2017). Polymer-based adsorbents are effective at removing As in both of its oxidation states (Ociński, 2019; Rahim and Mas Haris, 2015). However, there is no prior study on using polymer-based adsorbents to adsorb Mn. Therefore, I investigated the Mn removal efficiency of an Fe-impregnated cationic polymer gel.

In this chapter, I investigated the adsorptive removal of Mn using my previously-developed gel, DMAPAAQ + FeOOH . Additionally, I compared the Mn removal efficiency of DMAPAAQ + FeOOH gel to that of the non-ionic gel, *N,N'*-Dimethylacrylamide (DMAA) and non-ionic gel composite (DMAA + FeOOH). Finally, I conducted a simultaneous adsorption of As and Mn. Furthermore, I investigated the pH-sensitivity of the Mn adsorption, and used FTIR spectroscopy to examine whether Mn adheres to the surface functional group of the gel composite. Although various factors such as pH and temperature have significant effects on the removal of Mn (Kan et al., 2013), I conducted my experiments while maintaining natural conditions.

5.2. Materials and Methods

5.2.1 Materials

The monomer, *N,N'*-Dimethylaminopropyl acrylamide, methyl chloride quaternary (DMAPAAQ) (75% in H_2O) was supplied by KJ Chemicals Corporation, Tokyo, Japan. The crosslinker, *N,N'*-methylene bisacrylamide (MBAA), and the As(III) source, sodium (meta)arsenite, were purchased from Sigma-Aldrich, St. Louis, MO, USA. The accelerator, sodium sulphite (Na_2SO_3), the manganese source, manganese sulphate pentahydrate $MnSO_4.5H_2O$, the arsenic(V) source, disodium hydrogen arsenate heptahydrate ($Na_2HAsO_4.7H_20$), the adsorbents, activated charcoal and silica gel, and ferric chloride ($FeCl_3$) were purchased from Nacalai Tesque, Inc., Kyoto, Japan. Sodium hydroxide (NaOH) was purchased from Kishida Chemicals Corporation, Osaka, Japan. The monomer, *N,N'*-Dimethylacrylamide (DMAA) and 2-acrylamido 2-methyl propane sulfonic acid (AMPS) were purchased from TCI, Japan. The initiator, ammonium peroxodisulfate (APS) was purchased from Kanto Chemical Co. Inc., Tokyo, Japan.

5.2.2 Synthesis of the Polymer Gels and Composites

The polymer gels DMAPAAQ and DMAPAAQ + FeOOH were prepared by the free-radical polymerisation method described in the previous chapters. The amounts of the crosslinker, initiator, and accelerator were identical in the compositions of DMAPAAQ, DMAPAAQ + FeOOH, and DMAA + FeOOH. For the composites DMAPAAQ + FeOOH and DMAA + FeOOH, $FeCl_3$ and NaOH were added to impregnate the iron components in

the polymer gel structure . The reason for adding NaOH was that NaOH reacted with $FeCl_3$ during the polymerisation. Consequently, the majority of the FeOOH particles were produced inside the gel structure.

5.2.3 Adsorption Experiment

To perform the Mn-adsorption experiment, 20 mg of dried gel composite (γ-FeOOH, DMAPAAQ, DMAPAAQ + FeOOH, DMAA, activated charcoal, silica gel, and DMAA + FeOOH) was added to 40 mL of Mn or As solution in a small beaker and stirred at 200 rpm at 20 °C for 24 h. I conducted my experiments with solutions of higher Mn concentrations to evaluate the maximum effectiveness of the adsorbents at the removal of Mn. The detailed compositions of DMAPAAQ, DMAPAAQ + FeOOH, DMAA and DMAA + FeOOH are described in the previous chapters. As activated charcoal and silica gel are effective adsorbents, I used them to examine their adsorptive effectiveness and compared them with my results. Although the removal of Mn increases significantly with increase in temperature (Kan et al., 2013), I experimented at 20 °C to maintain natural conditions. Following this, a 30 mL sample was collected using a syringe. The amount of Mn remaining in the solution was measured by inductively coupled plasma mass spectrometry (ICP-MS). The amount of Mn adsorbed was measured using Equation (5.1).

$$Q = [(C_0 - C_v) * V]/m \quad (5.1)$$

where Q is the amount of Mn adsorbed [mol/g], C_0 is the initial concentration [mol/L], C_v is the equilibrium concentration [mol/L], V is the volume of the solution [L], and m is the mass of the adsorbent [g].

To investigate the pH-sensitivity, 20 mg of dried DMAPAAQ + FeOOH, activated charcoal, and silica gel were added to 40 mL of Mn solution. Additionally, HCl and NaOH were added to the solution to obtain different pH values in the range of 2–11). The solution was subsequently placed in a small beaker and stirred at 120 rpm at 20 °C for 24 h. Thereafter, 35 mL of the sample was collected using a syringe. The amount of arsenic remaining in the solution was measured using ICP-MS.

5.2.4 Fourier Transform Infrared Spectroscopy

FTIR spectroscopy (IR-Prestige 21, Shimadzu, Kyoto, Japan) was used to examine the changes in the surface functional groups of DMAPAAQ + FeOOH, DMAPAAQ, and γ-FeOOH following the adsorption of Mn. The concentration of the Mn solution, prepared using distilled water, was 500 mg/L. To adsorb Mn, 20 mg each of dried DMAPAAQ + FeOOH, DMAPAAQ, and γ-FeOOH were immersed in a 500 mg/L Mn solution for 24 h at 25 °C. Subsequently, the Mn-loaded gel pieces were carefully separated from the solutions and dried in an oven at 50 °C for 24 h. FTIR spectra were recorded in the wavelength range of 400–4000 cm^{-1} for DMAPAAQ, DMAPAAQ + FeOOH, γ-FeOOH, and their respective Mn-loaded samples. Potassium bromide (KBr)-pellet technique was used for FTIR analysis.

5.3. Results and Discussion

5.3.1 Adsorption of Mn Using the Cationic Gel and its Composite

To examine the efficiency of Mn removal using the cationic gel and cationic gel composite, I experimented with the amount of adsorption of Mn using the DMAPAAQ + FeOOH and DMAPAAQ gels. **Figure 5.1** shows that the amount adsorbed increased with the increase in the concentration of the Mn solution when DMAPAAQ + FeOOH was used. An identical trend was noted for DMAPAAQ. However, the adsorption amount of Mn was higher for DMAPAAQ + FeOOH than for DMAPAAQ at initial $MnSO_4$ concentrations higher than 25 mg/L. The maximum amounts of Mn adsorbed by DMAPAAQ and DMAPAAQ + FeOOH were 13.32 and 39.02 mg/g, respectively. DMAPAAQ achieved its maximum adsorption amount of Mn following impregnation with γ-FeOOH particles. The DMAPAAQ + FeOOH gel composite contained 62.1% (*w*/*w*) of γ-FeOOH in its gel structure (Safi et al., 2019b), which increased its Mn adsorption capacity.

Table 5.1 shows that the adsorption of Mn using DMAPAAQ + FeOOH gel follows the Langmuir isotherm closely, with an R^2 of 0.92. Equation (5.2) shows the Langmuir model equation.

$$C_e/Q_e = 1/(K_b\, Q_{max}) + C_e/Q_{max} \quad (5.2)$$

where C_e is the concentration of adsorbate solution (mg/L) after adsorption equilibrium, Q_e is the adsorption capacity of the sample (mg/g dry adsorbent), K_b is the adsorption coefficient (L/mg), and Q_{max} is the maximum adsorption amount

(mg/g).Therefore, ionic or covalent chemical bonds were formed between the adsorbent (DMAPAAQ + FeOOH) and the adsorbate (Mn) ("Langmuir Adsorption - an overview | ScienceDirect Topics," n.d.). The adsorption sites provided by the particles of γ-FeOOH, in the structure of DMAPAAQ + FeOOH, form ionic bonds with Mn ions. Moreover, the amino groups of the DMAPAAQ polymer, in the structure of DMAPAAQ + FeOOH, bind with As ions. Hence, monolayer adsorption occurs in the structure of the gel composite, and multilayer adsorption was not possible.

Table 5.1. Adsorption isotherm parameters for the adsorption of Mn and As on DMAPAAQ + FeOOH.

Isotherm Parameter			**Mn**	**As**
Langmuir model	R^2		0.92	0.997
	Q_{max}	mg/g	39.02	123.4
		mmol/g	0.52	1.63

On the other hand, in the case of DMAPAAQ gel, the methyl groups adhering to the amino group in the structure of DMAPAAQ bind with sulphate through ionic interactions. Sulphate ions additionally bind with Mn^{2+}. Consequently, the cationic gel, DMAPAAQ, can adsorb Mn, despite Mn being a cation.

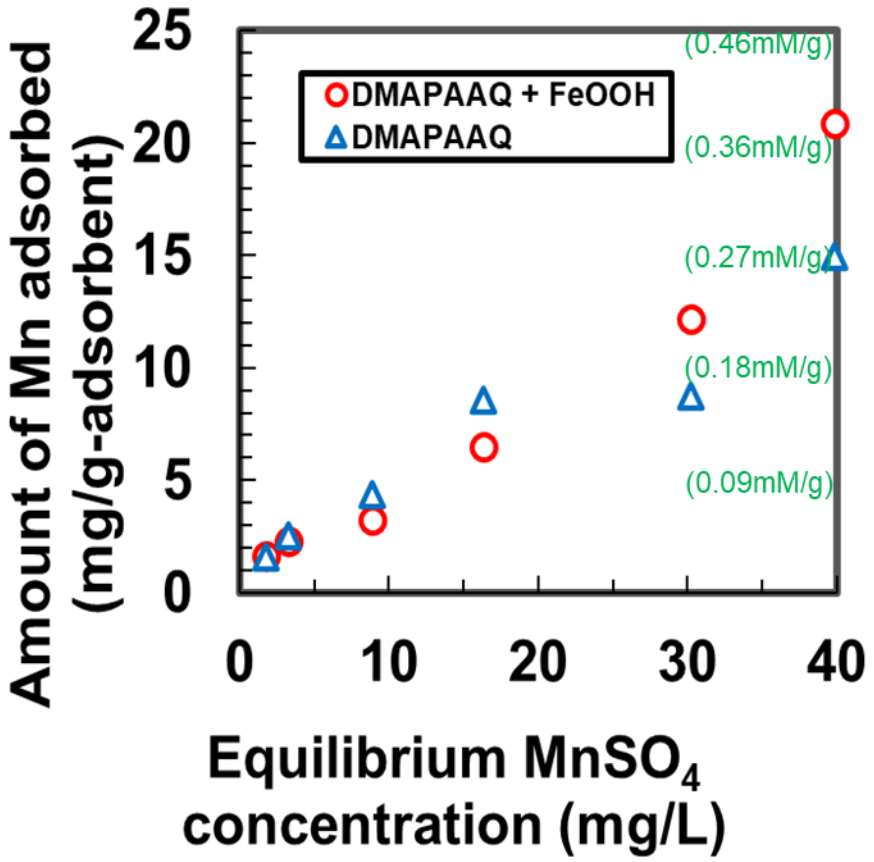

Figure 5.1. Amount of Mn adsorbed by DMAPAAQ and DMAPAAQ + FeOOH at different initial concentrations of $MnSO_4$.

5.3.2 Comparative Adsorption of Mn

To further understand how γ-FeOOH increased the adsorption and to evaluate the advantage of the cationic gels over non-ionic gels, I experimented with the amount of Mn adsorbed using the non-cationic gel composite, DMAA + FeOOH, DMAA, and γ-FeOOH. **Figure 5.2** shows that in the adsorption of Mn by the DMAA gel was nearly zero, which occurred because there was no bonding between the adsorption sites of the gel and the Mn

ions. The amount of Mn adsorbed by DMAA + FeOOH was marginally higher than that of DMAA. Since DMAA cannot adsorb Mn, I infer that the impregnated FeOOH particles contributed to the adsorption of Mn by DMAA + FeOOH by bonding with Mn ions. However, γ-FeOOH achieved significant adsorption of Mn, which increased with the increase in the initial concentration of the $MnSO_4$ solution.

The thermogravimetric analysis of DMAA + FeOOH suggests that the fraction of FeOOH in the gel was 51.3% (*w*/*w*). The adsorbed amounts of Mn by DMAA + FeOOH, γ-FeOOH, and DMAA gel were 0.78, 2.4, and 0 mg/g, respectively, when the concentration of $MnSO_4$ was 26 mg/L. Therefore, the 51.3% (*w*/*w*) of γ-FeOOH particles were the sole contributor to DMAA + FeOOH being able to adsorb Mn. Similarly, γ-FeOOH particles improved the amount of adsorption of Mn in DMAPAAQ + FeOOH because I observed an increase in the Mn adsorption from 14.96 to 20.89 mg/g when DMAPAAQ was impregnated with γ-FeOOH. The presence of γ-FeOOH particles in the polymer structure helped remove contaminants because the latter adhered to the polymer binding sites (Safi et al., 2019b). However, at concentrations of Mn lower than 25 mg/L, the effectiveness of γ-FeOOH at improving the Mn adsorption amount was lower for DMAPAAQ + FeOOH and DMAA + FeOOH. At Mn concentrations lower than 25 mg/L, the Mn components did not strongly adhere to the adsorption sites of the polymer structure. Therefore, the removal of Mn under natural water conditions was possible when the cationic and non-ionic gels were impregnated with γ-FeOOH.

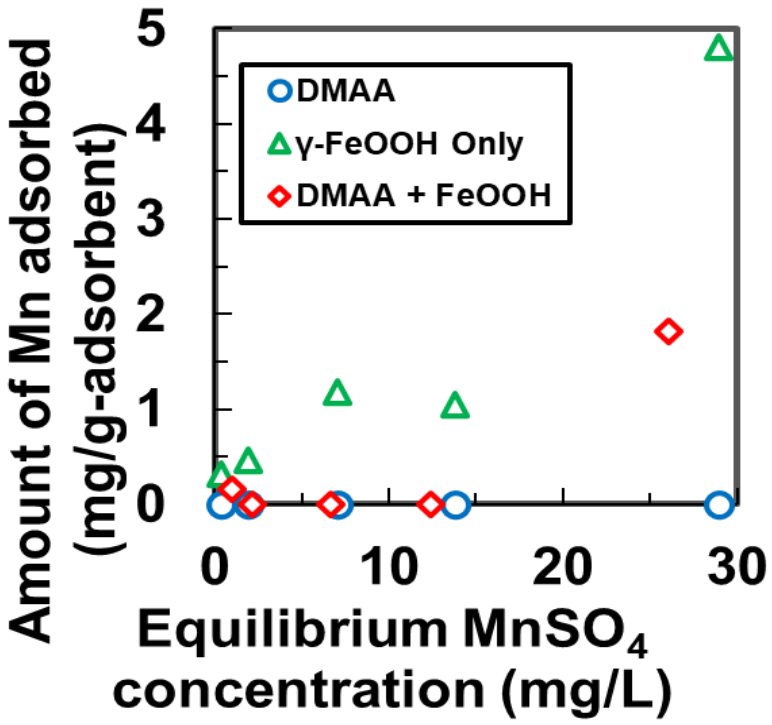

Figure 5.2. Amount of Mn adsorbed by DMAA, γ-FeOOH, and DMAA + FeOOH at different initial $MnSO_4$ concentrations.

5.3.3 Simultaneous Adsorption of Mn and As

Previously, γ-FeOOH was proven to be effective at separately removing As [13,20,21] and Mn (Sung and Morgan, 1981) discretely. However, the effectiveness of γ-FeOOH at simultaneously removing As and Mn has not been studied earlier. Additionally, the simultaneous removal of cations and anions by a single adsorbent has not been achieved previously. I examined the adsorption of Mn in the presence of As(V) and As(III) solutions (**Figure 5.3**), and the adsorption of As(V) and As(III) in the presence of Mn solution using DMAPAAQ + FeOOH (**Figure 5.4**).

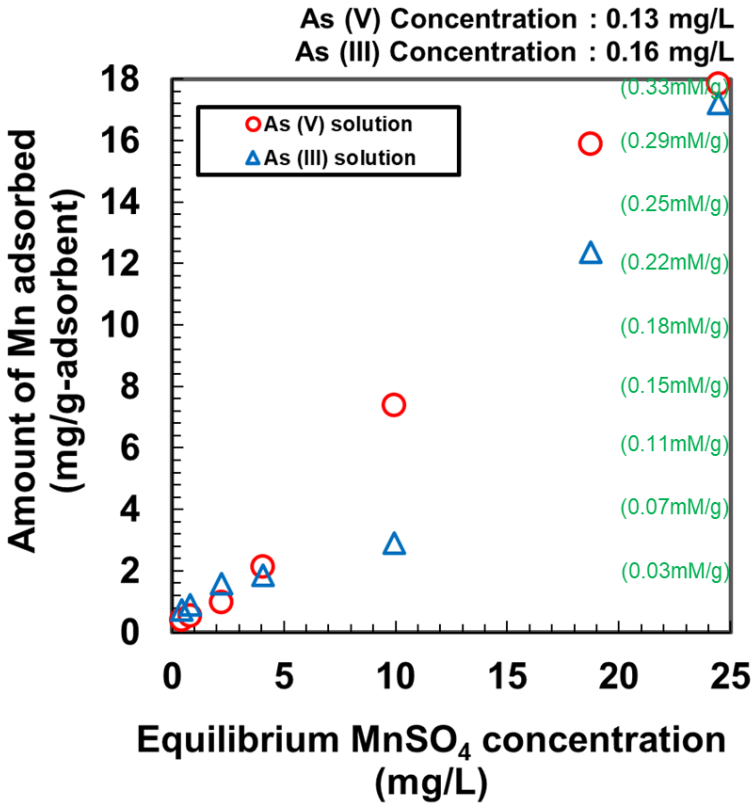

Figure 5.3. Adsorption of Mn by DMAPAAQ + FeOOH in the presence of As(III) and As(V) solutions.

In **Figure 5.3**, the adsorption of Mn from the solution of As(V) and As(III) is examined. The adsorbent was DMAPAAQ + FeOOH. The concentrations of As(III) and As(V) solutions were 0.16 and 0.13 mg/L, respectively. I conducted my experiments at low As concentrations because precipitation occurred at high As concentrations. Consequently, the actual amounts of Mn or As adsorbed could not be ascertained. However, at the As concentrations at which I conducted my experiment, no precipitation occurred. **Figure 5.3** shows that the adsorption of Mn was nearly unaffected by the presence of As (**Figure 5.1**).

A negligible increase in the adsorption of Mn in **Figure 5.3** can be observed due to the forming of precipitation.

Figure 5.4 shows that the amounts of As(V) and As(III) adsorbed remained nearly constant despite the presence of Mn in the solution. **Figure 5.4** suggests that when the initial concentration of $MnSO_4$ was lower, the amount of adsorption of As(V) was similar to that from the samples where the initial amount of $MnSO_4$ was higher. A similar phenomenon was observed when the adsorption of As(III) was studied in the presence of increasing Mn concentrations. The amount of As(III) adsorbed remained nearly constant despite the variation in the concentration of the Mn solution.

The two aforementioned observations from **Figures 5.3** and **5.4** suggest that the simultaneous adsorption of Mn and As by DMAPAAQ + FeOOH gel was achieved because As and Mn did not compete to adhere to the adsorption sites, which could accommodate both species simultaneously. The As ion was exchanged with the amino group in the polymer structure of DMAPAAQ, whereas Mn was connected to γ-FeOOH. An earlier report suggests that As can be adsorbed onto Mn but is subsequently re-adsorbed by Fe particles [22]. Hence, the adsorption sites provided by the γ-FeOOH particles in DMAPAAQ + FeOOH (which is 62.05% *w*/*w*) can adsorb As and Mn simultaneously.

The removal of As(V) was higher than that of As(III) at the initial $MnSO_4$ concentrations of 7.56 and 9.95 mg/L. Similar to the result of Yang et al.'s (2014) study, As (III) was removed in high amount simultaneously with Mn solution as manganese oxides oxidize As(III) to As(V) and then As(V) can be adsorbed on iron and manganese oxides as

well as the amino group of the gel composite to get removed from the water. (Yang et al., 2014). At neutral pH, adsorption processes are ineffective on uncharged forms of As(III) [24], because As(III) cannot be ionised at neural pH. In contrast, As(V) is ionised at pH 7. These results prove that As and Mn can be effectively removed by DMAPAAQ + FeOOH.

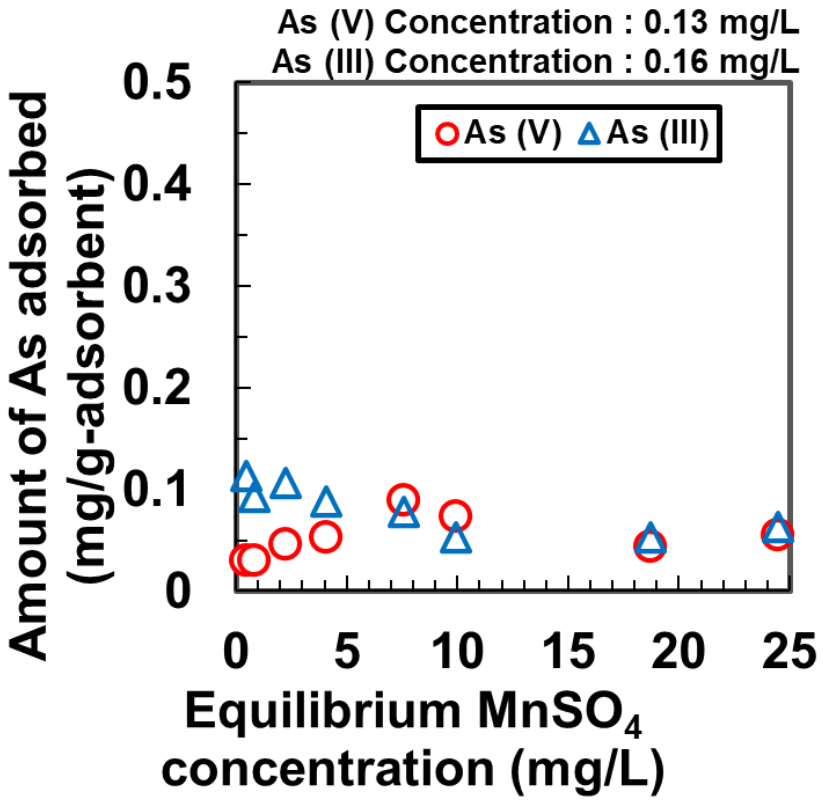

Figure 5.4. Adsorption of As(III) and As(V) by DMAPAAQ + FeOOH at different concentrations of Mn.

5.3.4 Surface Functional Group Characterisation Using FTIR Spectroscopy

5.3.4.1 FTIR Spectra of DMAPAAQ + FeOOH Gel Composite Following Mn Adsorption

I compared the spectral peaks of the DMAPAAQ + FeOOH composites to determine the difference in the surface functional groups, before (blue line in **Figure 5.5 (a)**) and after (red line in **Figure 5.5 (a)**) the adsorption of Mn by the gel. As shown in **Figure 5.5 (a)** and **Table 5.2**, in the FTIR spectrum of DMAPAAQ + FeOOH gel (blue line), there were shifts in the spectral bands, attributed to the vibrations of the alcohol O-H stretching, primary amine N-H stretching, aliphatic primary amine N-H stretching, secondary amine N-H amine stretching, and amine salt N-H stretching, respectively, following the adsorption of Mn by the DMAPAAQ + FeOOH gel composite. These shifts occurred due to the change in groups. In addition, the spectral peaks attributed to primary amine N-H stretching disappeared, and new peaks attributed to alcohol O-H stretching appeared in the spectral bands. The spectral bands attributed to secondary amine N-H stretching, alcohol O-H stretching, alkane C-H stretching, carbon dioxide O=C=O stretching, carboxylic acid C=O stretching, nitro compound N-O stretching and alkane C-H bending remained unchanged for DMAPAAQ + FeOOH.

5.3.4.2 FTIR Spectra of DMAPAAQ Gel Following Mn Adsorption

The FTIR spectrum of DMAPAAQ was examined to compare the effect of γ-FeOOH on the adsorption of Mn. As **Figure 5.5 (b)** and **Table 5.2** show, in the FTIR spectrum of DMAPAAQ (red line), there were shifts in the spectral bands following the adsorption of Mn by the DMAPAAQ gel, ascribed to the vibrations of alcohol O-H stretching, primary amine

N-H stretching, aliphatic primary amine N-H stretching, alcohol O-H stretching and amine C-N stretching, respectively. These shifts occurred due to the change in groups. In addition, the spectral peaks ascribed to alcohol O-H stretching and carboxylic acid C=O stretching disappeared, and new peaks appeared in the spectral bands ascribed to primary amine N-H stretching, alcohol O-H stretching and vinyl/phenyl ester C=O stretching. The spectral bands ascribed to secondary amine N-H stretching, alcohol O-H stretching, nitro compound N-H stretching, and alkane C-H bending remained unchanged for the DMAPAAQ gel.

5.3.4.3 FTIR Spectra of DMAA + FeOOH Gel Composite Following Mn Adsorption

The FTIR spectrum of the non-ionic gel composite of DMAA + FeOOH gel composite was examined to compare the characteristics of the ionic and non-ionic gel composites. As shown in **Figure 5.5 (c)** and **Table 5.2**, in the FTIR spectrum of DMAA + FeOOH (purple line), there was shift in the spectral band ascribed to the vibration of the alcohol O-H stretching following the adsorption of Mn by DMAA + FeOOH. This shift occurred because the group was altered. In addition, the spectral peaks ascribed to alcohol O-H stretching and alkane C-H stretching disappeared, and new peaks ascribed to alcohol O-H stretching, primary amine N-H stretching, aliphatic primary amine N-H stretching, and primary amide C=O stretching appeared in the spectral bands. The spectral bands ascribed to aliphatic primary amine N-H stretching, secondary amine N-H stretching, alcohol O-H stretching, alkyne C≡C Stretching, vinyl/phenyl ester C=O stretching, carboxylic acid C=O stretching, and alkane C-H bending remained unchanged for DMAA + FeOOH.

Table 5.2. FTIR spectroscopy peak analysis.

Wavelength	DMAPAAQ + FeOOH	DMAPAAQ + FeOOH + Mn	DMAPAAQ	DMAPAAQ + Mn	γ-FeOOH	γ-FeOOH + Mn	Group	Compound Class	Appearance
1209							C-N stretching	amine	medium
1211									
1458							C-H bending	alkane	medium
1508							N-O stretching	nitro compound	strong
1541									
1693							C=O stretching	primary amide	strong
1753							C=O stretching	carboxylic acid	strong
1764							C=O stretching	vinyl/phenyl ester	strong
1774									
2139							C≡C Stretching	alkyne	weak
2347							O=C=O stretching	carbon dioxide	strong
2387									
2954							N-H stretching	amine salt	strong, broad
2956									
3047							C-H stretching	alkane	medium
3051									
3234							O-H stretching	alcohol	strong, broad
3255									
3273									
3275									
3294									

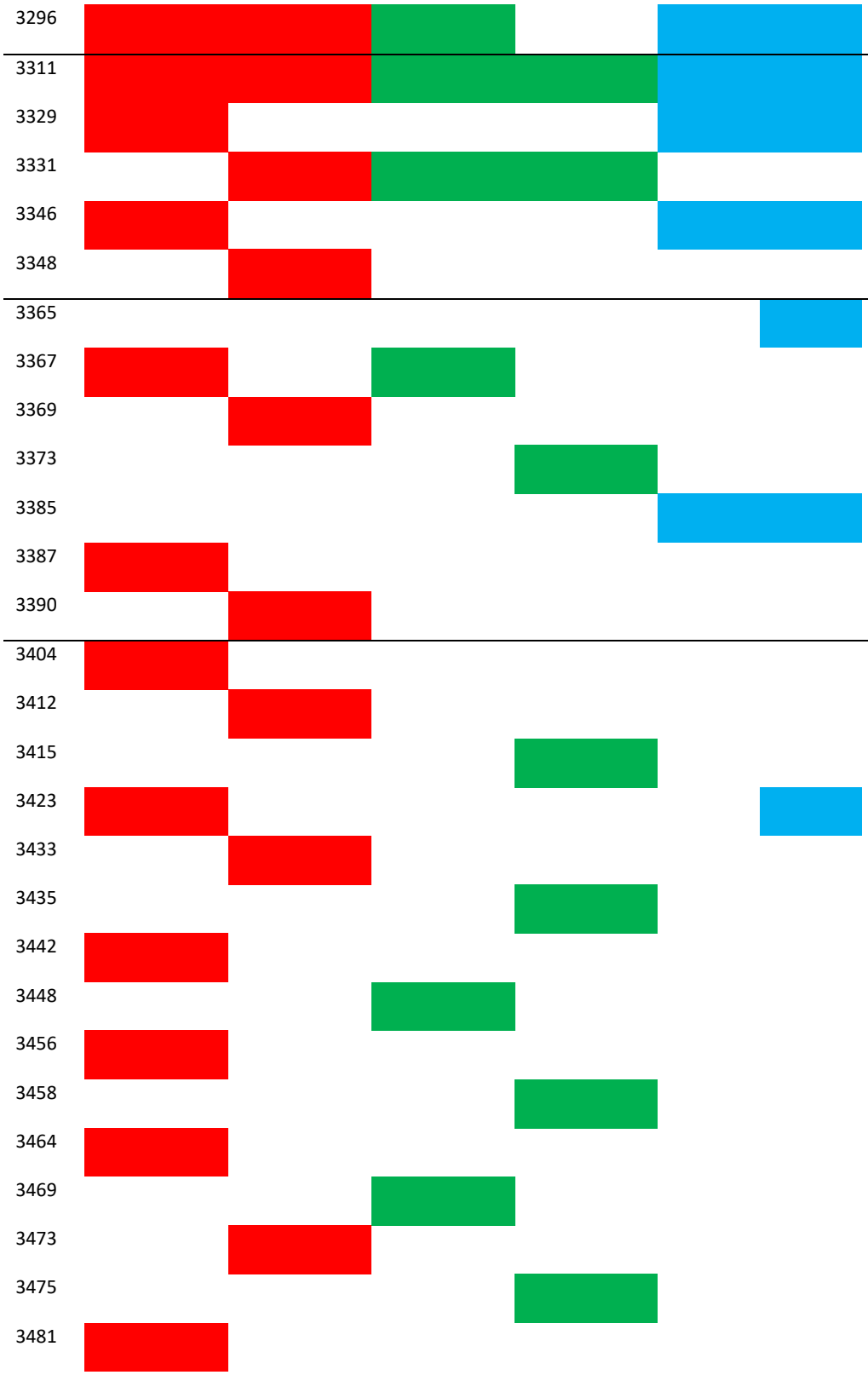

N-H stretching	secondary amine	medium
N-H stretching	aliphatic primary amine	medium
N-H stretching	primary amine	medium

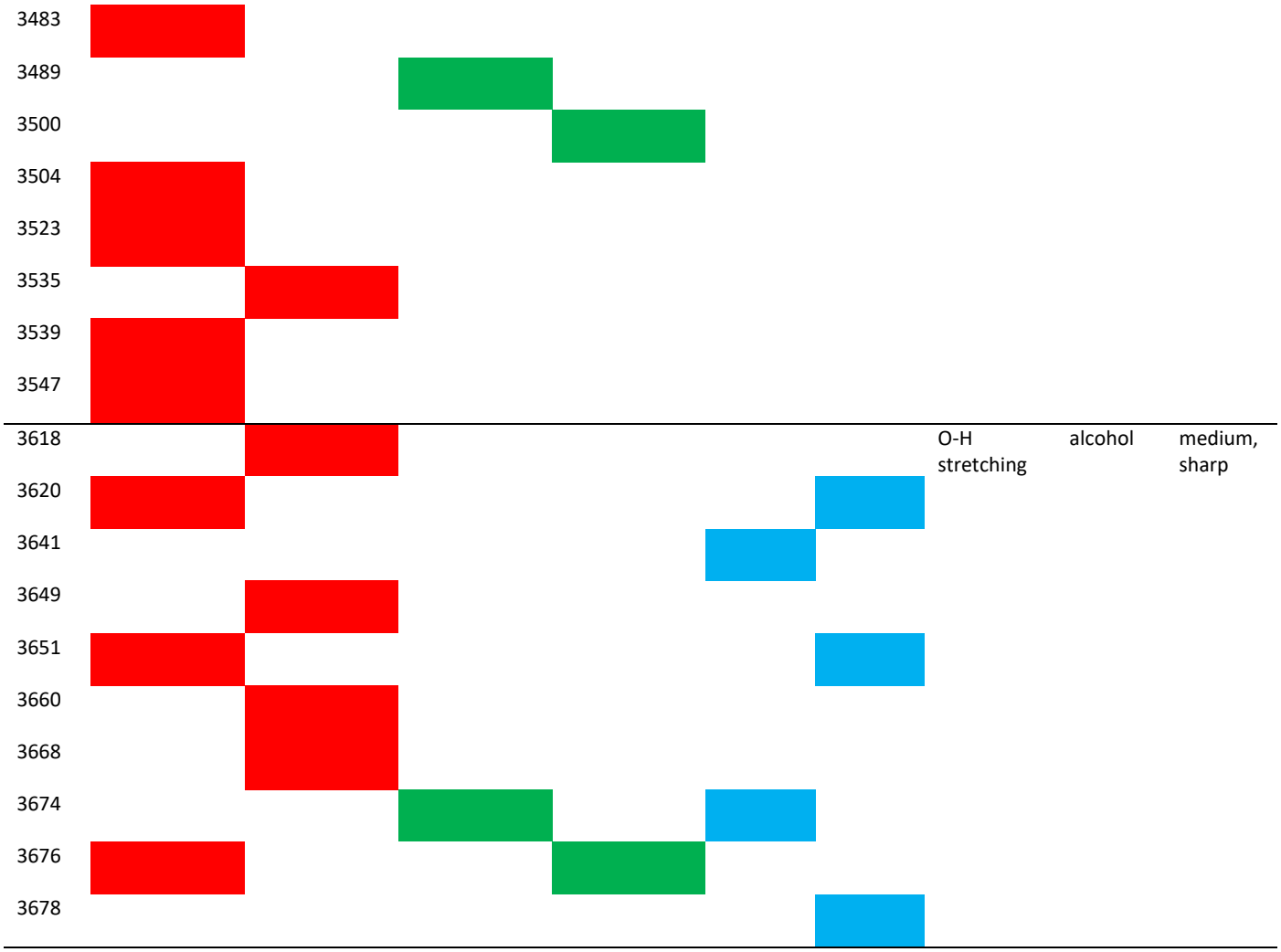

The above analysis suggests that the surface functional characteristics are altered following the loading of Mn into DMAPAAQ + FeOOH, DMAPAAQ gel and γ-FeOOH structure. Changes in the surface functional characteristics have also been reported when As(III) and As(V) were adsorbed by DMAPAAQ + FeOOH (Safi et al., 2019a). In addition, the cationic and non-ionic gel composites showed differences in the changes to the surface

functional groups. These results prove that Mn was successfully adsorbed on the surface functional groups of the cationic gel, cationic gel composite, and anionic gel composite.

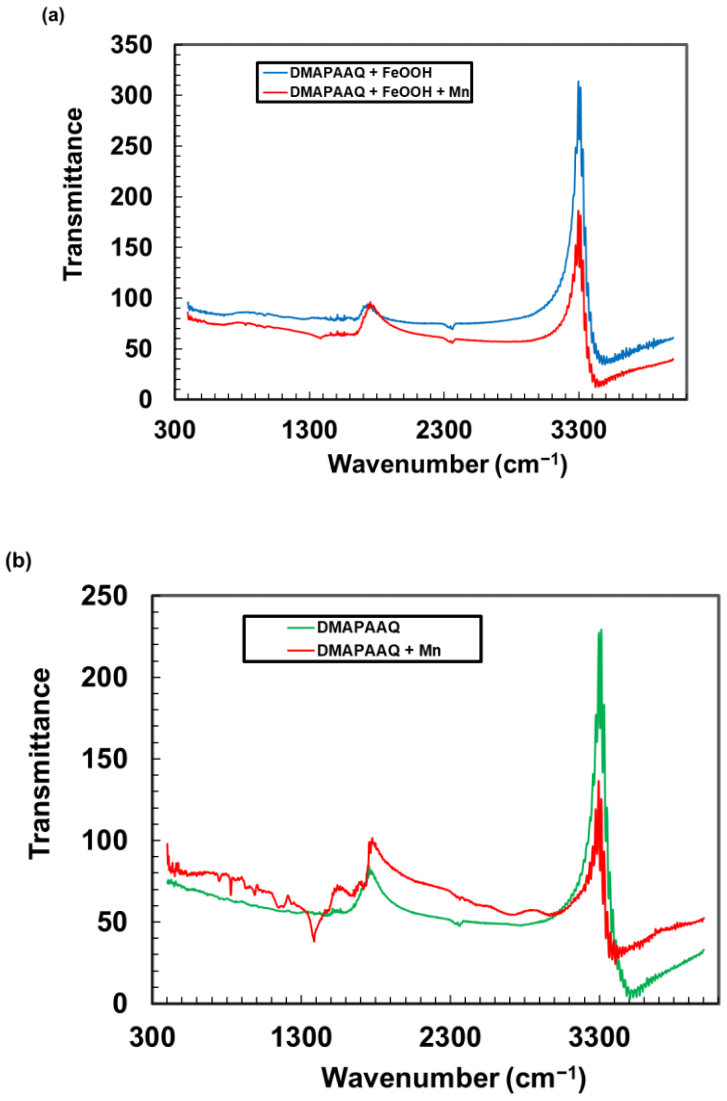

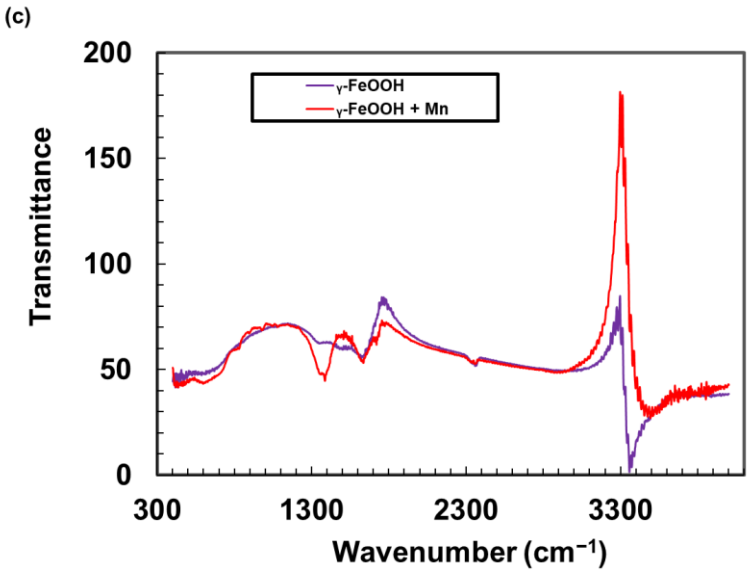

Figure 5.5. Comparative FTIR analysis of (a) DMAPAAQ + FeOOH and Mn-loaded DMAPAAQ + FeOOH, (b) DMAPAAQ and Mn-loaded DMAPAAQ, and (c) γ-FeOOH and Mn-loaded γ-FeOOH.

5.3.5 Effect of Experimental Parameters on the Adsorption of Mn by DMAPAAQ + FeOOH

The pH-sensitivity of Mn adsorption by DMAPAAQ + FeOOH was investigated using an Mn solution of 33.05 mg/L concentration. Different concentrations of HCl and NaOH were used in combination with the Mn solution to ascertain the arsenic adsorption levels at different pH. The samples were prepared by immersing 0.2 g of DMAPAAQ + FeOOH in various solutions having different pH ranging from 2 to 9. In all the samples, the initial concentration of Mn was 33.05 mg/L. The adsorption was performed at 20 °C under stirring at 194 rpm. Samples were collected following 24 h of adsorption. **Figure 5.6** shows that the amount of adsorption increased slightly in the case of DMAPAAQ + FeOOH between pH 2 and 7. This increase in the adsorption of Mn was attributed to the surface of

the DMAPAAQ + FeOOH gel composite becoming adsorption-friendly, which favoured the adsorption of the positively charged Mn (Dawodu and Akpomie, 2014). The extent of adsorption was maximum at neutral pH, and it reduced as the pH of the solution increased. This might be attributed to the partial hydrolysis of Mn(II) ions with increasing pH, resulting in the formation of complexes with OH^-, such as $Mn(OH)^+$, $Mn(OH)^2$, $Mn_2(OH)^{3+}$, Mn_2OH^{3+}, and $Mn(OH)_4^{2-}$ species in solution (Smith, Robert M. and Martell, Arthur E., 1976). I surmise that Mn-hydroxyl species may participate in the adsorption and/or precipitation onto the adsorbent structure (Budinova et al., 2009). Zeolites have been reported to exhibit similar behaviour (Hui et al., 2005).

However, the amount of adsorption diminished at high pH. At higher pH levels, precipitation occurs because of the oxidation of Mn(II) (Greenwood and Earnshaw, 1984). A similar observation was reported when Mn was adsorbed by natural zeolitic tuff from the Vranjska Banja deposit in Serbia (Rajic et al., 2009).

In addition, Budinova et al. (2009) (Budinova et al., 2009) reported similar observations when Mn was adsorbed by bean pod carbon. The effect of pH on the removal of Mn(II) using bean pod carbon showed that the removal of manganese ionic species remained constant between pH 2.75 and 6.

This is a significant finding because, as discussed previously in the ‘Introduction’ section, most polymer gels and other adsorbents fail to adsorb Mn effectively at neutral pH. The maximum adsorption of Mn was obtained at pH 7.02 for DMAPAAQ+ FeOOH.

Therefore, the remainder of the experiments were conducted at neutral pH, considering the real-life conditions of Mn-affected water.

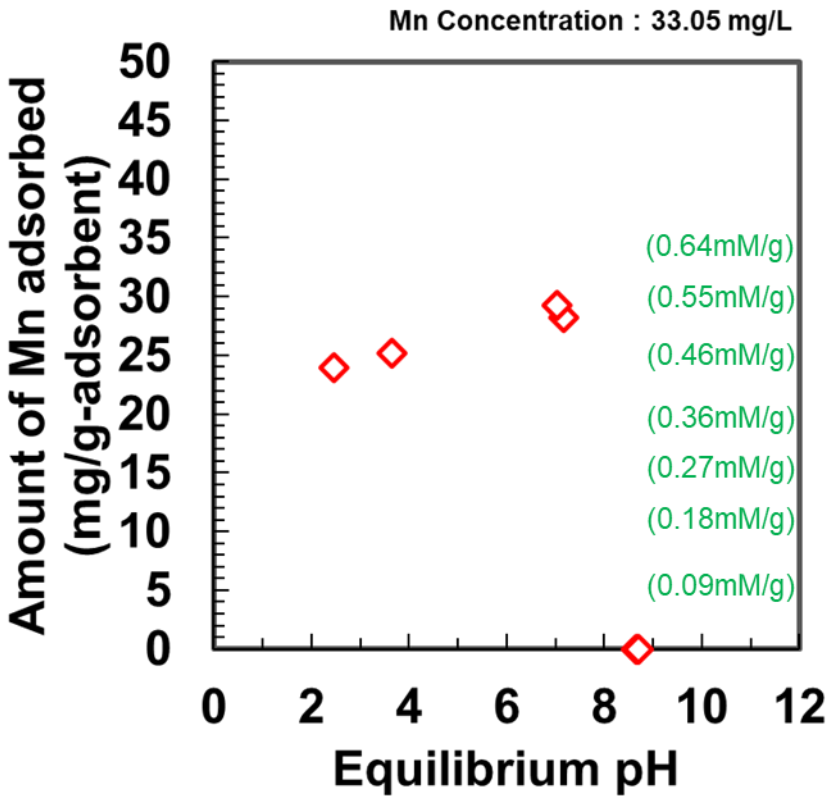

Figure 5.6. Effect of pH on the adsorption of Mn by DMAPAAQ + FeOOH gel.

5.3.6 Comparison to the Adsorption of Mn Using Other Adsorbents

I investigated the adsorptive removal of Mn using other adsorbents such as silica gel and activated charcoal. The samples were prepared by immersing 0.2 g of activated charcoal and silica gel in 40 mL of Mn solutions of different concentrations including 1, 2, 5, 10, 20, 25, and 40 mg/L. The adsorption was performed at 20 °C under stirring at 194 rpm. Following

24 h of adsorption, the samples were collected. The results shown in **Figure 5.7** indicate that Mn was sparingly adsorbed by these two gels, and that the adsorption followed the Langmuir adsorption isotherm. At neutral pH, the maximum adsorption by the silica gel and activated charcoal were 6.89 and 10.82 mg/L, respectively, which are lower than that by DMAPAAQ + FeOOH at initial concentrations of Mn higher than 15 mg/L. Compared to the adsorption sites provided by activated charcoal and silica gel, the presence of γ-FeOOH in the structure of DMAPAAQ + FeOOH made the adsorption sites more favourable for Mn to adhere to and be adsorbed.

In addition, other adsorbents previously studied for the removal of Mn had less maximum adsorption capacity than that of DMAPAAQ + FeOOH. The maximum adsorption amount of Mn by the other adsorbents, for instance, granular activated carbon (Jusoh et al., 2005), clinoptilolite from Turkey (Erdem et al., 2004), quartz (Kroik et al., 1999), marble (Kroik et al., 1999), dolomite (Kroik et al., 1999), Na-montmorillonite (Abollino et al., 2003), clinoptilolite-Fe oxide (Doula, 2006), tannic acid immobilised activated carbon (Üçer et al., 2006), natural sepiolite (Kocaoba, 2009), natural zeolite (NZ) (Ates, 2014), and activated carbon from bean pods waste (Budinova et al., 2009) were 2.54, 4.22, 0.06, 1.20, 2.21, 3.22, 27.12, 1.73, 0.25, 7.68, and 23.4 mg/g, respectively. Although these maximum adsorption amount values followed different experimental conditions and no experimental relation between them existed, these adsorbents only represent the Mn retention tendency by the respective adsorbents.

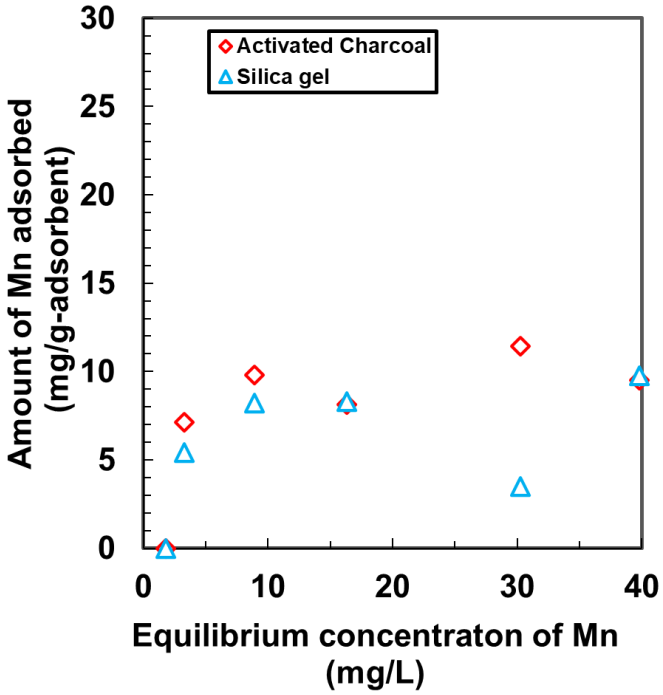

Figure 5.7. Adsorption of Mn by activated charcoal and silica gel.

5.4. Conclusions

In summary, Mn was effectively removed by the DMAPAAQ gel, DMAPAAQ + FeOOH gel composite, DMAA + FeOOH gel composite, activated charcoal, silica gel, and γ-FeOOH at natural water conditions. The highest amount of Mn adsorption was achieved by DMAPAAQ + FeOOH at 39.02 mg/g. This occurred because the presence of γ-FeOOH in the polymer structure of DMAPAAQ + FeOOH helped to increase its efficiency at removing Mn, similar to how γ-FeOOH improved the Mn-adsorption performance of DMAA + FeOOH. Therefore, the DMAPAAQ + FeOOH gel removes Mn more effectively than the abovementioned adsorbents.

This was a pioneering study on the simultaneous adsorption of As and Mn. I concluded that As and Mn can be removed simultaneously using DMAPAAQ + FeOOH without impacting the removal performance, because As was attached to the amino group in the polymer structure of DMAPAAQ as AsO_7^- and Mn was attached to γ-FeOOH. The uptake of As(V) was greater than that of As(III) because As(III) cannot be ionised at neutral pH, though As(V) can. Additionally, pH had no effect on the adsorption of Mn by DMAPAAQ + FeOOH at neutral and acidic pH. The maximum adsorption of Mn by DMAPAAQ + FeOOH was attained at pH 7.02, which is an important finding for the practical implementation of the adsorbent in removing Mn. Finally, the FTIR results prove that Mn was successfully attached to the surface functional groups of DMAPAAQ + FeOOH. No other work on the removal of Mn has performed FTIR analysis to date.

References

Abollino, O., Aceto, M., Malandrino, M., Sarzanini, C., Mentasti, E., 2003. Adsorption of heavy metals on Na-montmorillonite. Effect of pH and organic substances. Water Research 37, 1619–1627. https://doi.org/10.1016/S0043-1354(02)00524-9

Ates, A., 2014. Role of modification of natural zeolite in removal of manganese from aqueous solutions. Powder Technology 264, 86–95. https://doi.org/10.1016/j.powtec.2014.05.023

Bissen, M., Frimmel, F.H., 2003. Arsenic — a Review. Part I: Occurrence, Toxicity, Speciation, Mobility. Acta hydrochimica et hydrobiologica 31, 9–18. https://doi.org/10.1002/aheh.200390025

Bora, A.J., Mohan, R., Dutta, R.K., 2017. Simultaneous removal of arsenic, iron and manganese from groundwater by oxidation-coagulation-adsorption at optimized pH. Water Supply 18, 60–70. https://doi.org/10.2166/ws.2017.092

Budinova, T., Savova, D., B.Tsyntsarski, Ania, C.O., Cabal, B., Parra, J.B., Petrov, N., 2009. Biomass waste-derived activated carbon for the removal of arsenic and manganese ions from aqueous solutions. Applied Surface Science 255, 4650–4657. https://doi.org/10.1016/j.apsusc.2008.12.013

Çifçi, D.İ., Meriç, S., 2017. Manganese adsorption by iron impregnated pumice composite. Colloids and Surfaces A: Physicochemical and Engineering Aspects 522, 279–286. https://doi.org/10.1016/j.colsurfa.2017.03.004

Dawodu, F.A., Akpomie, K.G., 2014. Simultaneous adsorption of Ni(II) and Mn(II) ions from aqueous solution unto a Nigerian kaolinite clay. Journal of Materials Research and Technology 3, 129–141. https://doi.org/10.1016/j.jmrt.2014.03.002

Doula, M.K., 2006. Removal of Mn2+ ions from drinking water by using Clinoptilolite and a Clinoptilolite–Fe oxide system. Water Research 40, 3167–3176. https://doi.org/10.1016/j.watres.2006.07.013

Erdem, E., Karapinar, N., Donat, R., 2004. The removal of heavy metal cations by natural zeolites. Journal of Colloid and Interface Science 280, 309–314. https://doi.org/10.1016/j.jcis.2004.08.028

Greenwood, N.N., Earnshaw, A., 1984. Manganese, Chemistry of the elements. Pergamon Press, Oxford.

Hui, K.S., Chao, C.Y.H., Kot, S.C., 2005. Removal of mixed heavy metal ions in wastewater by zeolite 4A and residual products from recycled coal fly ash. Journal of Hazardous Materials 127, 89–101. https://doi.org/10.1016/j.jhazmat.2005.06.027

Jusoh, A.B., Cheng, W.H., Low, W.M., Nora'aini, A., Megat Mohd Noor, M.J., 2005. Study on the removal of iron and manganese in groundwater by granular activated carbon. Desalination, Desalination and the Environment 182, 347–353. https://doi.org/10.1016/j.desal.2005.03.022

Kan, C.-C., Aganon, M.C., Futalan, C.M., Dalida, M.L.P., 2013. Adsorption of Mn2+ from aqueous solution using Fe and Mn oxide-coated sand. Journal of Environmental Sciences 25, 1483–1491. https://doi.org/10.1016/S1001-0742(12)60188-0

Kocaoba, S., 2009. Adsorption of Cd(II), Cr(III) and Mn(II) on natural sepiolite. Desalination 244, 24–30. https://doi.org/10.1016/j.desal.2008.04.033

Kroik, A.A., Shramko, O.N., Belous, N.V., 1999. Sewage cleaning with applying of natural sorbents. Chemistry of Technology and Water 21, 310.

Langmuir Adsorption - an overview | ScienceDirect Topics [WWW Document], n.d. URL https://www.sciencedirect.com/topics/engineering/langmuir-adsorption (accessed 10.20.20).

Ociński, D., 2019. Optimization of hybrid polymer preparation by ex situ embedding of waste Fe/Mn oxides into chitosan matrix as an effective As(III) and As(V) sorbent. Environ Sci Pollut Res 26, 26026–26038. https://doi.org/10.1007/s11356-019-05856-x

Pires, V.G.R., Lima, D.R.S., Aquino, S.F., Libânio, M., Pires, V.G.R., Lima, D.R.S., Aquino, S.F., Libânio, M., 2015. EVALUATING ARSENIC AND MANGANESE REMOVAL FROM WATER BY CHLORINE OXIDATION FOLLOWED BY CLARIFICATION. Brazilian Journal of Chemical Engineering 32, 409–419. https://doi.org/10.1590/0104-6632.20150322s00003564

Rahim, M., Mas Haris, M.R.H., 2015. Application of biopolymer composites in arsenic removal from aqueous medium: A review. Journal of Radiation Research and Applied Sciences 8, 255–263. https://doi.org/10.1016/j.jrras.2015.03.001

Rajic, N., Stojakovic, D., Jevtic, S., Zabukovec Logar, N., Kovac, J., Kaucic, V., 2009. Removal of aqueous manganese using the natural zeolitic tuff from the Vranjska Banja deposit in Serbia. Journal of Hazardous Materials 172, 1450–1457. https://doi.org/10.1016/j.jhazmat.2009.08.011

Safi, S.R., Gotoh, T., Iizawa, T., Nakai, S., 2019a. Development and regeneration of composite of cationic gel and iron hydroxide for adsorbing arsenic from ground water. Chemosphere 217, 808–815. https://doi.org/10.1016/j.chemosphere.2018.11.050

Safi, S.R., Senmoto, K., Gotoh, T., Iizawa, T., Nakai, S., 2019b. The effect of γ-FeOOH on enhancing arsenic adsorption from groundwater with DMAPAAQ + FeOOH gel composite. Scientific Reports 9, 11909. https://doi.org/10.1038/s41598-019-48233-x

Sarkar, A.M., Rahman, A.K.M.L., Samad, A., Bhowmick, A.C., Islam, J.B., 2019. Surface and Ground Water Pollution in Bangladesh: A Review. 1 6, 47–69. https://doi.org/10.20448/journal.506.2019.61.47.69

Smith, Robert M., Martell, Arthur E., 1976. Critical Stability Constants, Inorganic Complexes, vol. 4. Springer Science+Business Media New York, p. 5.

Sung, W., Morgan, J.J., 1981. Oxidative removal of Mn(II) from solution catalysed by the γ-FeOOH (lepidocrocite) surface. Geochimica et Cosmochimica Acta 45, 2377–2383. https://doi.org/10.1016/0016-7037(81)90091-0

Üçer, A., Uyanik, A., Aygün, Ş.F., 2006. Adsorption of Cu(II), Cd(II), Zn(II), Mn(II) and Fe(III) ions by tannic acid immobilised activated carbon. Separation and Purification Technology 47, 113–118. https://doi.org/10.1016/j.seppur.2005.06.012

Verlicchi, P., Grillini, V., 2019. Surface and Groundwater Quality in South African Area—Analysis of the Most Critical Pollutants for Drinking Purposes. Proceedings 48, 3. https://doi.org/10.3390/ECWS-4-06430

Waste, T.O.C. of the 14th I.C. on T. and M., 2010. Tailings and Mine Waste 2010. CRC Press.

Yang, L., Li, X., Chu, Z., Ren, Y., Zhang, J., 2014. Distribution and genetic diversity of the microorganisms in the biofilter for the simultaneous removal of arsenic, iron and manganese from simulated groundwater. Bioresource Technology 156, 384–388. https://doi.org/10.1016/j.biortech.2014.01.067

Zhu, N., Yan, T., Qiao, J., Cao, H., 2016. Adsorption of arsenic, phosphorus and chromium by bismuth impregnated biochar: Adsorption mechanism and depleted adsorbent utilization. Chemosphere 164, 32–40. https://doi.org/10.1016/j.chemosphere.2016.08.036

Chapter 6: Conclusion

Chapter 1 introduced the major contaminants in groundwater which are increasingly becoming threat to the existence of human beings. One of the most ubiquitous and toxic components in water is arsenic. The effects of arsenic on human health was discussed. The sources and processes from which arsenic originates and is carried through was also discussed. Following this, the removal technologies that was used by the other researchers was enumerated. Polymer gels are increasingly becoming popular in treating arsenic were then conferred. A novel cationic gel composite was then introduced. Later, another threatening component in water, manganese, was introduced and it was discussed why it is a global aquatic threat. The current removal technologies and the research gaps were then discussed. Lastly, the objectives of this dissertation was explained.

Chapter 2 concludes that a composite of cationic gel and FeOOH using an unconventional preparation method to maximize the content of FeOOH in the gel composite could be prepared. The examination of the pH sensitivity of the gel composite was conducted and the gel could adsorb As(V) in high amount at neutral pH levels. The adsorption reaction kinetics suggest that the gel can reach equilibrium adsorption at 24 hours. The reaction rate of adsorption by the DMAPAAQ+FeOOH gel composite matches with pseudo 2^{nd} order kinetic model. The arsenic adsorption isotherm of DMAPAAQ+FeOOH matched well with Langmuir isotherm. The maximum adsorption capacity of DMAPAAQ+FeOOH gel composite was calculated (1.63mmol/g) and compared with the other previously studied adsorbents at neutral pH levels. DMAPAAQ+FeOOH gel composite showed better arsenic

adsorption capacity than the other adsorbents. The adsorption mechanism of DMAPAAQ+FeOOH gel composite was also analyzed and discussed. As(V) could be adsorbed by both the amino group of DMAPAAQ and FeOOH particles inside the DMAPAAQ+FeOOH gel composite and their ratio of adsorption of arsenic was 35.6% and 64.4%, respectively. Also, the results showed that DMAPAAQ+FeOOH gel composite selectively adsorbed arsenic in the presence of Sulphate ion. Hence, the gel composite can adsorb As(V) selectively from the groundwater even if other ions are present. The FeOOH in DMAPAAQ+FeOOH gel composite provided the selectivity of arsenic. In addition, the gel composite is cost effective and ecofriendly as it could be regenerated. The regeneration experiment was conducted for eight consecutive days with 87.6% efficiency. The regeneration process was examined differently, as NaCl was used instead of harmful NaOH for desorption of As(V). Finally, unlike the currently used methods, DMAPAAQ+FeOOH does not require any additional separation process, which results in an easy handling of the gel and a simplistic adsorption process.

Chapter 3 summarizes that the presence of iron particles was confirmed in the DMAPAAQ+FeOOH gel structure. The DMAPAAQ+FeOOH gel composite contained 62.05% FeOOH particles in the gel composite. The high efficiency in adsorbing arsenic is attributed to the high content of FeOOH particles in the gel composite. The polymer structure of the gel was amorphous. The FeOOH particles present in the DMAPAAQ+FeOOH gel composite were γ-FeOOH, which aided in the adsorption of both As(III) and As(V). Therefore, γ-FeOOH contributed 64.4% of the adsorption of As(V) by DMAPAAQ + FeOOH gel composite. The adsorption amount of As(V) by the γ-FeOOH particles in the

DMAPAAQ + FeOOH gel structure was 79.5 mg/g. Hence, γ-FeOOH particles enhanced the arsenic adsorption in the DMAPAAQ+FeOOH gel structure. In addition, there were shifts in the surface functional groups due to the impregnation of FeOOH in the gel composite. The shifts were apparent because of impregnation of As(III) and As(V) into DMAPAAQ+FeOOH gel composite. Lastly, As(III) were oxidized to As(V) prior to being adsorbed by the DMAPAAQ + FeOOH gel composite.

Chapter 4 finalizes that DMAPAAQ+FeOOH gel composite could adsorb highest quantity of As(III) at neutral pH levels. The As(III) adsorption isotherm resembles the Langmuir isotherm very well. At neutral pH levels, the maximum adsorption capacity of the DMAPAAQ+FeOOH gel composite (27.68 mg/g) was computed. The DMAPAAQ+FeOOH gel composite's adsorption mechanism was also described. As(III) was converted to As(V) through oxidation and was then adsorbed on the gel surface by both the amino group and FeOOH particles. In addition, the DMAPAAQ+FeOOH gel composite preferentially adsorbed As(III) even though there was presence of sulphate and chloride ion in the solutions. The As(III) selectivity was provided by the FeOOH in the DMAPAAQ+FeOOH gel composite. Furthermore, the regeneration experiment was carried out for eight days in a row with an efficiency of 48.7 percent. The regeneration process was conducted in a different way, using NaCl instead of the potentially hazardous NaOH for As(III) desorption. Finally, unlike other techniques now in use, DMAPAAQ+FeOOH does not require any extra separation steps, resulting in easy gel handling and a straightforward adsorption procedure.

To sum up the **Chapter 5,** Mn was effectively removed by the DMAPAAQ gel, DMAPAAQ + FeOOH gel composite, DMAA + FeOOH gel composite, activated charcoal, silica gel, and γ-FeOOH at natural water conditions. The highest amount of Mn adsorption was achieved by DMAPAAQ + FeOOH at 39.02 mg/g. This occurred because the presence of γ-FeOOH in the polymer structure of DMAPAAQ + FeOOH helped to increase its efficiency at removing Mn, similar to how γ-FeOOH improved the Mn-adsorption performance of DMAA + FeOOH. Therefore, the DMAPAAQ + FeOOH gel removes Mn more effectively than the abovementioned adsorbents. Also, it was concluded that As and Mn can be removed simultaneously using DMAPAAQ + FeOOH without impacting the removal performance, because As was attached to the amino group in the polymer structure of DMAPAAQ as AsO_7^- and Mn was attached to γ-FeOOH. The uptake of As(V) was greater than that of As(III) because As(III) cannot be ionised at neutral pH, though As(V) can. Additionally, pH had no effect on the adsorption of Mn by DMAPAAQ + FeOOH at neutral and acidic pH. The maximum adsorption of Mn by DMAPAAQ + FeOOH was attained at pH 7.02. Finally, Mn was successfully attached to the surface functional groups of DMAPAAQ + FeOOH.

In conclusion, this dissertation introduced the most suitable technique to adsorb two of the most notorious components from water, As and Mn. Besides providing the best adsorption performances, the adsorbent that this dissertation introduced provided better selective adsorption, recyclability and best performances at the natural water conditions for arsenic. Also, for Mn, the adsorbent, DMAPAAQ+FeOOH gel composite, provided high adsorption performance at neutral pH levels and also provided recyclability. Finally, the gel

composite could remove As and Mn simultaneously at neutral pH levels. Therefore, this dissertation provided a solution to solve the problem of removal of two of the most harmful components from water.

List of Achievements

Journal articles

1. **Safi S.R.**; Gotoh T., 2021, Simultaneous Removal of Arsenic and Manganese from Synthetic Aqueous Solutions Using Polymer Gel Composites. Nanomaterials, 11(4), 1032. (Chapter 5)

2. **Safi S.R.**, Senmoto K., Gotoh T., Iizawa T., Nakai S., 2019, The effect of γ-FeOOH on enhancing arsenic adsorption from groundwater with DMAPAAQ + FeOOH gel composite, Scientific Reports, 9, 11909. (Chapter 3)

3. **Safi S.R**, Gotoh T., 2021, Removal of Manganese Using Polymer Gel Composites. Materials Proceedings, 4(1):68. (Chapter 5)

4. **Safi S.R.**, Gotoh T., Iizawa T., Nakai S., 2019, Development and regeneration of composite of cationic gel and iron hydroxide for adsorbing arsenic from ground water, Chemosphere, 217, 808-815. (Chapter 2)

5. **Safi S.R.**, Gotoh, T., Iizawa, T., Nakai, S., 2019, Removal of Arsenic Using a Cationic Polymer Gel Impregnated with Iron Hydroxide. J. Vis. Exp., 148, e59728. (Chapter 2)

6. **Safi S.R.**, Nakata, T., Hara, S., Gotoh, T., Iizawa, T., Nakai, S., 2020, Synthesis, phase-transition behaviour, and oil adsorption performance of porous poly(oligo(ethylene glycol) alkyl ether acrylate) gels, Polymers, 12, 1405.

Conferences

1. Syed Ragib Safi, Takehiko Gotoh, Removal of Manganese using Polymer gel composites, The 2nd International Online-Conference on nanomaterials by MDPI, November 15-30, 2020. (Chapter 5)

2. Syed Ragib Safi, Takehiko Gotoh, Satoshi Nakai, Adsorption of Arsenite by Polymer gel impregnated with Iron hydroxide, Poster presentation at the 9th International Colloids Conference by Elsevier, Barcelona, Spain, June 16-19, 2019. (Chapter 4)

3. Syed Ragib Safi, Takehiko Gotoh, Satoshi Nakai, Effective removal of arsenate from groundwater by polymer gel impregnated with iron hydroxide, The 18th Asian Pacific Confederation of Chemical Engineering Congress (APCChE), Sapporo, Japan, September 23-29, 2019. (Chapter 2, Chapter 3)

4. Syed Ragib Safi, Takehiko Gotoh, Satoshi Nakai, Adsorption of arsenite by polymer gel impregnated with iron hydroxide, The 18th Asian Pacific Confederation of Chemical Engineering Congress (APCChE), Sapporo, Japan, September 23-29, 2019. (Chapter 4)

5. Syed Ragib Safi, Takehiko Gotoh, Takashi Iizawa, Satoshi Nakai, Development and Characteristics of a Composite of Cationic Gel and Iron hydroxide to Adsorb Arsenic from Groundwater, The Water and Environment Technology Conference, Ehime, Japan, July 14-15, 2018. (Chapter 2)

6. Syed Ragib Safi, Takehiko Gotoh, Takashi Iizawa, Satoshi Nakai, Development and Characteristics of a Composite of Cationic Gel and Iron hydroxide to Adsorb Arsenic from Groundwater, The 12th SPSJ International Polymer Conference, Hiroshima, Japan, December 4-7, 2018. (Chapter 2)

7. Syed Ragib Safi, Takehiko Gotoh, Takashi Iizawa, Satoshi Nakai, Preparation of composite of cationic gel and iron hydroxide for adsorbing arsenic from ground water, IWA-Aspire Conference, Malaysia, September 11-14, 2017. (Chapter 2)

8. Syed Ragib Safi, Takehiko Gotoh, Takashi Iizawa, Satoshi Nakai, Preparation and regeneration of composite of cationic gel and iron hydroxide for adsorbing arsenic, SCEJ 49th Autumn meeting, Nagoya, Japan, September 20-22, 2017. (Chapter 2)

9. Syed Ragib Safi, Takehiko Gotoh, Takashi Iizawa, Satoshi Nakai, Preparation of Composite of Cationic gel and Iron Hydroxide for Adsorbing Arsenic, 分離技術会年会, May 26-27, 2017. (Chapter 2)

Awards

1. 東洋エンジニアリング株式会社賞, 分離技術会年会, 2017
2. 学生賞, 分離技術会年会, 2017
3. 学生奨励賞河村祐治記念賞, 中国地区化学エ学懸話会, 2019

4. 中国四国支部支部長賞, 日本化学会, 2019
5. Excellent Poster Award, 18th Asian Pacific Confederation of Chemical Engineering Congress (APCChE) 2019, 2019